Mathematics of Reflection Seismology

William W. Symes*

August 2, 1998

Contents

*The Rice Inversion Project, Department of Computational and Applied Mathematics, Rice University, Houston TX 77251-1892

Note to the Reader

These notes will form a chapter in the forthcoming volume *Mathematical Frontiers in Reflection Seismology*, to be published by SIAM and SEG. The references to other chapters ("Chapter XXX") pertain to this book.

Acknowlegement

This work was partially supported by the National Science Foundation, the Office of Naval Research, the Air Force Office of Scientific Research, the Texas Geophysical Parallel Computation Project, the Schlumberger Foundation, IBM, and The Rice Inversion Project. TRIP Sponsors for 1995 are Advance Geophysical, Amerada Hess, Amoco Production Co., Conoco Inc., Cray Research Inc., Discovery Bay, Exxon Production Research Co., Interactive Network Technologies, and Mobil Research and Development Corp.

Present and past members of TRIP have helped me in my understanding of this subject. Their efforts yielded the software environment without which the examples in these notes would never have seen the light of day. Especially heartfelt thanks are due to Kidane Araya, Joakim Blanch, Michel Kern, Alain Sei, Quang-Huy Tran, and Roelof Versteeg.

I also wish to express my appreciation to Prof. Guy Chavent, whose invitations to give short courses on inverse problems in wave propagation at INRIA/Rocquencourt in 1990 and 1995 led to both the original version of these notes and to the current revision.

1 Introduction and Overview

This chapter develops mathematical concepts and tools underlying techniques for estimation of material structures from observations of *reflected waves*. These techniques belong in some sense to the theory of inverse problems for partial differential equations, but many of them have their origins outside of modern mathematics. Most of the ideas developed in this chapter arose first in the seismology, particularly in that branch devoted to exploration for petroleum. Therefore I shall take viewpoint and terminology from exploration seismology. A principal goal of this chapter is to provide a natural "Courant—Hilbert" setting for these ideas and terms, which play a very important role in the following chapters.

The most powerful idea in the subject as it stands today is that of *scale separation* coupled with linearization, and most of the chapter will concern its mathematical consequences. The second section describes briefly the reflection seismic experiment and the typical characteristics of its data. The principal task of theory is the explanation of these characteristics through a physical model, and the principal characteristic to be explained is the presence of *reflections*: space-time coherent oscillatory signals. The simplest theory offering a hope of such explanation is linear acoustics, presented in the next section. The fourth section introduces scale separation and linearization. The separation of the wavelength and medium scales permits great simplification in the description of solutions of the wave equation, through geometric acoustics. This high frequency asymptotic approximation, a second layer of perturbation theory, is developed in section 5. It explains the use of the term "wave propagation" to describe physical models defined by hyperbolic systems of partial differential equations. It also clarifies the meaning of *traveltime*, and the possible use of time-of-arrival as data for an inverse problem. Chapter XXX by Bube and Langan discusses one of the most imporant settings for the resulting *transmission tomography* problem.

Section 6 is central: it combines linearization and high frequency asymptotics to arrive at a description of the linearized wavefield which contains candidates for the all-important reflections. The simplest instance of this approximation occurs when both the reference medium parameters and their perturbations depend only on one of the space variables, namely depth, thus modeling flat-lying sedimentary strata undisturbed by tectonic processes. The approximation then reduces to the so-called *convolutional model*. This model is the subject of Chapter XXX by Robinson, and has been enormously influential in the development of seismic data processing. Section 7 extracts the geometrical ("kinematic") consequences of the approximation, which predicts a definite relation between the arrival times of reflected waves, on the one hand, and the reference (smooth) velocity distribution on the other. This relation leads to the possibility that the velocity could be deduced, or at least constrained, by the arrival times. This *reflection tomography* problem is the subject of Chapter XXX by Bube and Langan.

Another way to view the result of the approximation described in section 6 is as an *oscillatory integral* expression for the *scattering operator* mapping the parameter perturbations to the seismogram perturbation. This operator belongs to a special class of oscillatory integrals known as *Fourier Integral Operators*, a calculus for which was developed by Hörmander and others in the 1970's. This is hardly surprising, as these operators generalize expressions

known much earlier for solutions of various problems for the wave equation.

The calculus includes a construction of approximate inverses, or *parametrices*, in appropriate circumstances. In sections 8 through 10 I follow BEYLKIN, 1985 in deriving a *generalized Radon transform* expression for a parametrix of the scattering operator. A key step in this construction is the proof the the *normal operator* (i.e. the scattering operator followed by its adjoint) is a *pseudodifferential operator*, and the explicit computation of its symbol, carried out in section 8. Section 9 presents two constructions of the adjoint scattering operator, as a generalized Radon transform and *via* the solution of an adjoint boundary value problem. The theory of Fourier integral operators shows that the output of the adjoint, however computed, weighted or not, has high frequency signal strength concentrated in the same places as the parameter perturbations: thus the adjoint output *images* the parameter perturbations. As the high frequency filtered plots of both seismogram and parameter perturbations look very similar, but with signal strength in different places, the adjoint was dubbed early on a *migration operator* in exploration seismology. The "migration" is thus of high frequency signal components to their correct locations in the model of the Earth's subsurface. The two adjoint computation methods explained in section 9 are examples of so called Kirchhoff migration, on the one hand, and finite difference migration, on the other.

The parametrix may be viewed as a weighted adjoint as well. Accordingly, its application is often termed "migration/inversion" or "true amplitude migration". It is also called high frequency asymptotic inversion. The construction of the generalized Radon transform representation of the parametrix is reviewed in section 10.

Section 10 also discusses various shortcomings of migration and/or high frequency asymptotic inversion. Chief of these is that the results can be reliable only if the background medium, most especially the background velocity, about which the linearization is done, is essentially correct. Tomography, ie. traveltime inversion, provides one avenue of velocity estimation. Another approach is to view the background velocity as part of the model which is to be estimated as the solution of an inverse problem. Linearization itself is suspect: the linearized or perturbational seismogram does not explain *multiple reflections*, and these (nonlinear) signal components are present in both synthetic and field data. Other shortcomings involve the source of acoustic energy, which in reality does not have arbitrarily high frequency content (so throws the use of high frequency asymptotics somewhat into doubt) and is not generally *a priori* better known than is the subsurface. Several of these issues are discussed in Chapter XXX by Stolt and Weglein. In general the problems outlined in Section 10 remain open, and provide many opportunities for further research.

The material in this Chapter is a distillation of work reported in the literature by others; almost none of it is original. I am especially indebted to Gregory Beylkin, Norman Bleistein, Robert Burridge, Guy Chavent, Patrick Lailly, Rakesh, and Albert Tarantola, from whose papers I have taken the essential ideas. A reading list for study of this subject should include at least BAMBERGER et al., 1979, BEYLKIN, 1985, BEYLKIN and BURRIDGE, 1990, BLEISTEIN, 1987, RAKESH, 1988, KOLB et al., 1986, LAILLY, 1983, TARANTOLA, 1984, and TARANTOLA, 1986.

2 The Nature of Seismic Reflection Data

Figure 1 presents the result of a single seismic experiment in the North Sea. A ship has towed a noise-making device, in this case an array of *air guns*, which has released supersonically expanding bubbles of compressed air into the water. These in turn generated acoustic waves which propagated through the water and into the layers of rock in the subsurface. The ship also towed a cable full of special microphones, called hydrophones. Each hydrophone (or actually group) generated output voltage as the result of pressure fluctuations. Some of these pressure fluctuations were echoes, or *reflected waves*, from subsurface boundaries or other changes in rock mechanics met by the wave as it propagated. The analog—summed output voltage for each hydrophone group was digitized and recorded as a time series. These time series are the content of Figure 1.

The plotting method is typical of this subject, and will appear throughout this volume. Time increases downwards; the time unit is milliseconds (ms). Each vertical line or *trace* represents the time varying signal recorded by a single receiver (hydrophone group). The horizontal coordinate *for* each line represents amplitude of the recorded signal (voltage, in principle). The horizontal coordinate *between* the lines represents distance from the boat or source array, in this case increasing from right to left.

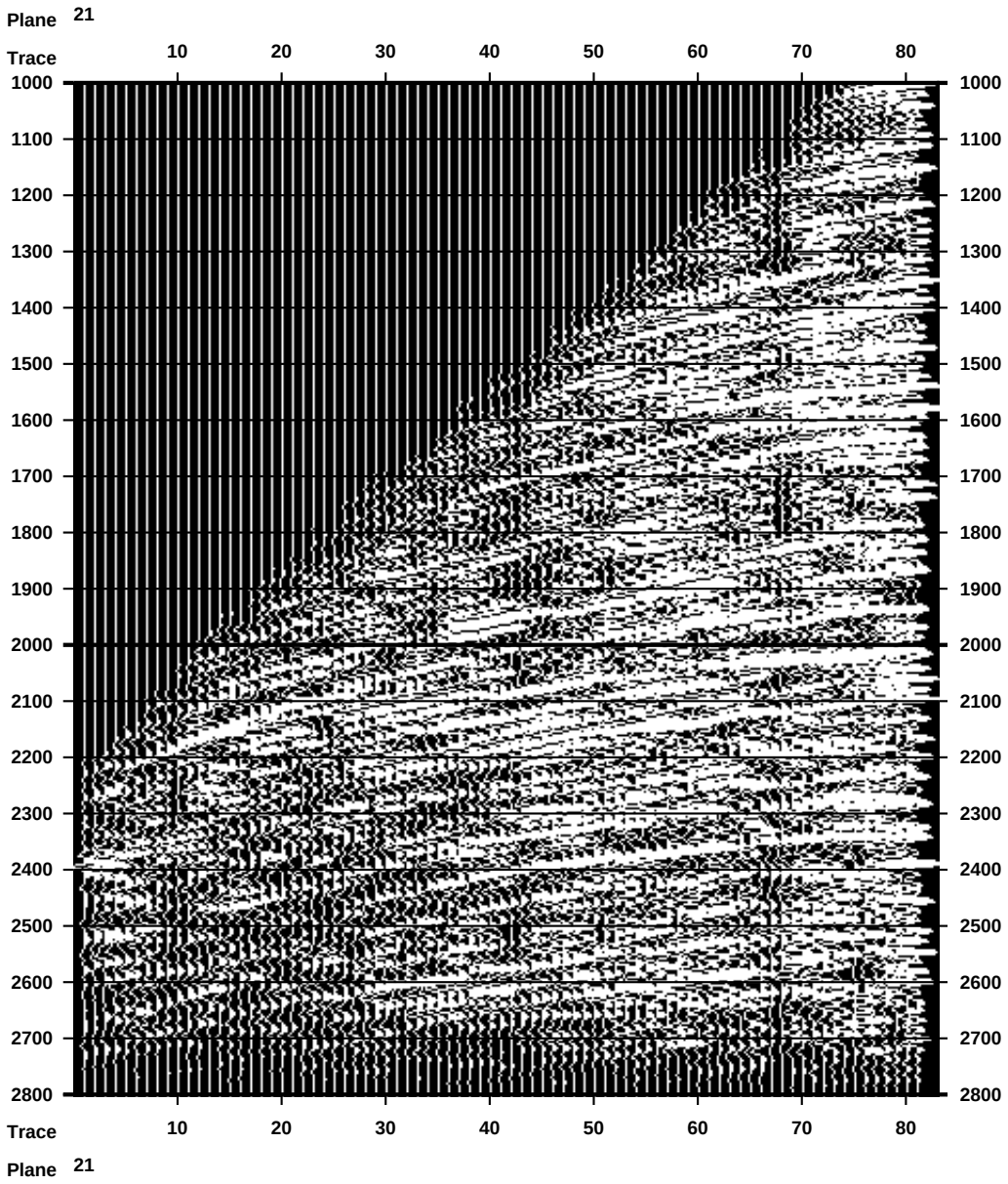

FIGURE 1: Shot record (single experiment data) from seismic data set acquired in the North Sea. Time sample rate is 4 ms, total time of recording was 3 s. Hydrophone group spacing is 25 m. Closest offset (distance from source to receiver) is 262 m, far offset is 2262 m. Tow depth of source array was 10 m, depth of hydrophone cable was 6 m. The author gratefully acknowledges Mobil Research and Development Corp. for provision of this data and permission for its use.

The variations in amplitude are evidently oscillatory. The plot has been filled with black ink in each excursion of the amplitude to the right of the axis in each trace. This device brings out another characteristic of the data: the presence of *space time coherent signals*, known as *reflections*. Evidently certain signal components occur at certain times on each trace, and as one moves away from the boat the time of occurence becomes later in a systematic way. It is natural to think that this time represents distance traveled by the wave, and a large part of this chapter will be devoted to providing a detailed physical justification for this idea, through a mathematical model of wave propagation and reflection.

Not all of the data is displayed in Figure 1. Sample values have been replaced by zeroes above a line sloping down to the left. The reason for this cutoff or *mute* is that part of the data above this line represents a different physical regime and has a different scale, as will be explained to some extent below.

This single seismic experiment produced 120 traces, each with 750 samples, representing 3 s of recorded data. (For other dimensional information see the figure caption.) However the data set from which Figure 1 was extracted contained more than 1000 such experiments. The ship steamed along a line, and conducted one experiment (a "shot") every ten seconds or so. The data collectively represents the influence of the subsurface of the earth to roughly 3 km, over a narrow swath roughly 25 km long through the North Sea. The total volume of data is roughly 750 Mb.

Moreover this is a small data set. The geometry of acquisition (ship sailing in a single line towing one cable) is termed "2D" in the current seismic literature. Almost all contemporary acquisition is in "3D" mode, which in practice means (at least) a ship towing up to a dozen cables steaming successivly along many parallel lines. Data volumes of hundreds of Gbytes or even Tbytes are not unusual.

Evidently data processing methods of considerable efficiency are required to extract from this vast quantity of data useful information about the subsurface. This book presents a number of tools and concepts derived from physical models of seismic wave propagation, which may be (and have been) used to design effective data processing methods. I hope also that this and the following chapters clarify the assumptions upon which current understanding and methods rest, along with their shortcomings, so as to delineate some of the many open questions and research opportunities.

The crucial data feature, which any successful model of reflection seismology must predict, is the presence of reflections. I turn now to the simplest physical setting in which such a prediction seems possible.

3 Acoustic Model of Reflection

Linear acoustics models small-amplitude transient deformations of fluids and gases, i.e. sound waves. This chapter will analyse linear acoustic models in one, two, and three space dimensions: while the real world is obviously three dimensional, a great deal of data processing is based on two-dimensional models for various reasons, and much intuition and most rigorous mathematics concern one-dimensional models.

The (small amplitude) excess pressure field $p(x,t)(x \in \mathbb{R}^n, t \in \mathbb{R})$ resulting from a source of acoustic energy $F(x,t)$ (the divergence of a body force field) satisfies

$$\frac{1}{\rho(x)c^2(x)}\frac{\partial^2 p}{\partial t^2}(x,t) - \nabla \cdot \frac{1}{\rho(x)}\nabla p(x,t) = F(x,t) \tag{1}$$

where $\rho(x)$ is the density at equilibrium and $c(x)$ the sound velocity, both functions of spatial location.

Assume that the fluid is in its equilibrium state (of zero excess pressure) for large negative time, which is possible provided that the source $F(x,t)$ is causal:

$$\left.\begin{array}{rcl} F(x,t) & \equiv & 0 \\ p(x,t) & \equiv & 0 \end{array}\right\} t << 0 \; .$$

Physical boundaries, e.g. the ocean surface, in principle imply boundary conditions as well, but we will ignore these. Thus the various fields are defined in $\mathbb{R}^n$ or $\mathbb{R}^{n+1}$, $n = 1,2,3$. The complications arising from boundary conditions are important in the design of data processing software, but do not alter the general principles presented below.

The (ideal "inverse") problem to be solved is:

> Given recordings $p(x_r,t_r)$ of the excess pressure field at a number of receiver locations x_r and times t_r, and for a number of sources $F(x,t)$, estimate the coefficients $\rho(x)$ and $c(x)$.

The papers in this volume present partial solutions to this problem.

Besides the modeling assumptions stated above, we make a number of further simplifying assumptions which are satisfied approximately by the field configurations of reflection seismology and sometimes by the laboratory configurations of ultrasonic NDE.

The *reflection* or backscattering configuration separates sources and receivers (x_s and x_r) from the region of unknown parameters by a hyperplane. That is, assume that the coefficients are known on one side of a datum plane $\{x_n =: z = z_d\}$:

$$\left.\begin{array}{rcl} \rho(x) & = & \rho_0(x) \\ c(x) & = & c_0(x) \end{array}\right\} z \leq z_d \; .$$

Whenever convenient we will also assume ρ_0, c_0 constant for $z \leq z_d$. In any case the coefficients are unknown only for $z > z_d$.

We also assume that the source has point support. This assumption results in a reasonable approximation when the spatial extent of the source is much smaller than a typical wavelength. We further make the somewhat less realistic restrictions that the sources used be identical, and that the source radiation pattern be *isotropic*. Real-world sources are often variable and distinctly anisotropic, but again the additional complications arising from source anisotropy do not seriously impair our conclusions. Thus a typical source will have the form

$$F(x,t) = f(t)\delta(x - x_s)$$

where x_s is the (point) source location and $f(t)$ is the *source time function* — a transient temporal signal. Note that some of the time-invariant physics of the measurement process may be "hidden" in the source time function $f(t)$ by virtue of the convolution theorem and source-receiver reciprocity. Since the wave motion measured by reflection seismology and ultrasonic NDE experiments really is transient — the material returns to its initial state after some time — it is easy to see that the mean of f, i.e. its dc component, vanishes. For other reasons having to do with the physics of sound generation and reception, effective sources have little energy in a band near zero Hertz as well. Also, the resolution, within which material inhomogeneities can be detected from reflected waves, depends on the frequency content of the acoustic field, and therefore of the source. All of these factors conspire to make prototypical effective sources $f(t)$ *oscillatory*, with a peak frequency corresponding to a wavelength of perhaps 1% of the duration of a typical record.

The frequency content of acoustic signals is also limited above, principally because at sufficiently high frequencies acoustic body waves in real materials are strongly attenuated. Thus, the acoustic model is a reasonable approximation only in a limited frequency band.

The *reflection configuration* places all sources and receivers on the known-medium side of the datum plane:

$$\begin{aligned} x_{s,n} &= z_s \leq z_d \\ x_{r,n} &= z_r \leq z_d \ . \end{aligned}$$

As indicated by the notation, we assume for simplicity only that the n^{th} coordinate of source position vectors (i.e. z_s) is the same for all placements of the source, and similarly for receiver positions. We also assume that the time interval of the pressure measurement is the same for all receivers. We denote by X_{sr} the set of source and receiver positions, which are in reality discrete but which we will occasionally idealize as continuous. We will ignore the issue of temporal sampling, and also the details of the pressure-measurement process — i.e. we regard the pressure as being measured directly, at the receiver points. Thus the data set for the problem studied here has the form

$$\{p(x_s, x_r, t) : (x_s, x_r) \in X_{s,r} \ , \quad 0 \leq t \leq T\} \ .$$

4 Linearization

Even with all the simplifying assumptions outlined above, the possibility of recovery of $\rho(x)$ and $c(x)$ from such data sets is poorly understood. In part, this is because the relation between the coefficients ρ and c and the solution of p of the pressure equation is nonlinear (even though the equation itself is linear!). The greatest progress in practical methods for wave imaging has relied on linearization of the $\rho, c \mapsto p$ relation. Accordingly, most of these notes will concern the structure of this linearized problem.

Heuristic, physical reasoning, computational experience, and the few available mathematical results all point to the following conclusion: the $\rho, c \mapsto \rho$ relation is well-approximated by its formal linearization $\rho + \delta\rho, c + \delta c \mapsto p + \delta p$ (described explicitly below) so long as

(1) the reference coefficients ρ, c are slowly-varying (smooth) relative to a typical data wavelength;

(2) the perturbations $\delta\rho$, δc are oscillatory ("rough").

Refinement of these rather vague criteria is an open research problem. As we shall see, the import of (1)–(2) is that the reference velocity c determines the kinematics of the perturbational wavefield δp, whereas $\delta\rho$ and δc determine the dynamics. Also, the smoothness of ρ and c will justify extensive use of high-frequency asymptotics. Together, these two techniques — linearization and brutally consistent reliance on asymptotics — will enable us to obtain decisive insight into the imaging problem, and to reproduce the essential content of conventional data processing methodology in a mathematically consistent way.

The formal linearization is obtained by applying regular perturbation to the pressure equation 1. We obtain that the formal perturbation field δp satisfies

$$\frac{1}{\rho c^2}\frac{\partial^2 \delta p}{\partial t^2} - \nabla\cdot\frac{1}{\rho}\nabla\delta p = \frac{2\delta c}{\rho c^3}\frac{\partial^2 p}{\partial t^2} - \frac{1}{\rho}\nabla\frac{\delta\rho}{\rho}\cdot\nabla p \qquad (2)$$
$$\delta p \equiv 0\ ,\quad t << 0$$

Evidently δp, so defined, is indeed linear in $\delta\rho$, δc. It will emerge that δp depends quite nonlinearly on the reference velocity c, so the problem has been only partly linearized. This observation is at the heart of velocity analysis, which means roughly the determination of the background medium (ρ, c) — which is of course also unknown in $\{z > z_d\}$, even if we accept the linearized field representation $p + \delta p$! Velocity analysis is mentioned briefly in Section 7.

Note that the assumption of the reflection configuration implies that $\delta\rho, \delta c \equiv 0$ for $z \leq z_d$.

Mathematical results on the accuracy of linearization, i.e. on the differentiability of the map $\rho, c \mapsto p$, are quite skimpy. Using techniques introduced by LIONS, 1972 and used in analysis of 1D inverse scattering problems by BAMBERGER et al., 1982, FERNANDEZ-BERDAGUER et al., 1993 have shown that this mapping is Fréchet differentiable in the L^2 sense, provided that the source wavelet $f(t)$ has several derivatives in L^∞. This quite general result does not address the scale separation phenomenon noted above. In effect, this approach shows that solutions to the wave equation exist, but does not explain why they act like waves.

Lewis and the author (LEWIS and SYMES, 1991) showed that for the 1D version of this problem, and for $f = \delta, \rho \equiv 1$, one has the estimate

$$\|p_2 - p_1 - \delta p\|_{L^2(\Omega)} \leq K_2\|\delta c\|_{L^2([0,D])}\|\delta c\|_{H^2([0,D])} + K_3\|\delta c\|^2_{L^2([0,D])}.$$

Here p_i corresponds to c_i, $i = 1, 2$, δp to $\delta c = c_2 - c_1$, $R \subset \mathbf{R}^2$ is a bounded domain interior to the forward light cone, $[0, D]$ is a suffiently large interval, and K_j depends on $\|c_1\|_{H^j[0,D]}$. This estimate is optimal. On the other hand, along bounded sequences $\{\delta c_n\} \subset H^2([0, D])$ which *oscillate*, i.e. tend to zero in $L^2([0, D])$, the linearization error tends to zero, even though generally $c_2 = c_1 + \delta c \to \infty$ in $H^3([0, D])$. This estimate thus quantifies the anomalous smoothness of the $\rho, c \mapsto p$ mapping for oscillatory perturbation of smooth ρ, c, at least in the 1D case.

Nothing like this estimate is known currently for several dimensional problems. Nonetheless massive numerical evidence supports the hypothesis that something similar is true, at least if the reference medium is smooth enough to support geometric optics. Figure 2 shows a comparison between seismograms calculated for a smooth velocity distribution c (part a), for an oscillatory perturbation thereof $c+\delta c$ (part b), and for the linearized seismogram (part c). The seismogram plots show samples of $p(x_s, x_r, t)$ for fixed source position x_s, a variety of receiver positions x_r, and an interval of time t, in typical seismic display as in Figure 1. Plots of the reference velocity c,the velocity perturbation δc, and the source time function $f(t)$ appear in Figure 3. In this example the density ρ is constant and unperturbed ($\delta\rho \equiv 0$). The numerical algorithm used to solve (approximately) the (two dimensional) wave equation to produce these and other figures in this chapter is a centered finite difference scheme of order two in time and four in space. The author has taken care to verify the accuracy of the computed solution by varying the grid size.

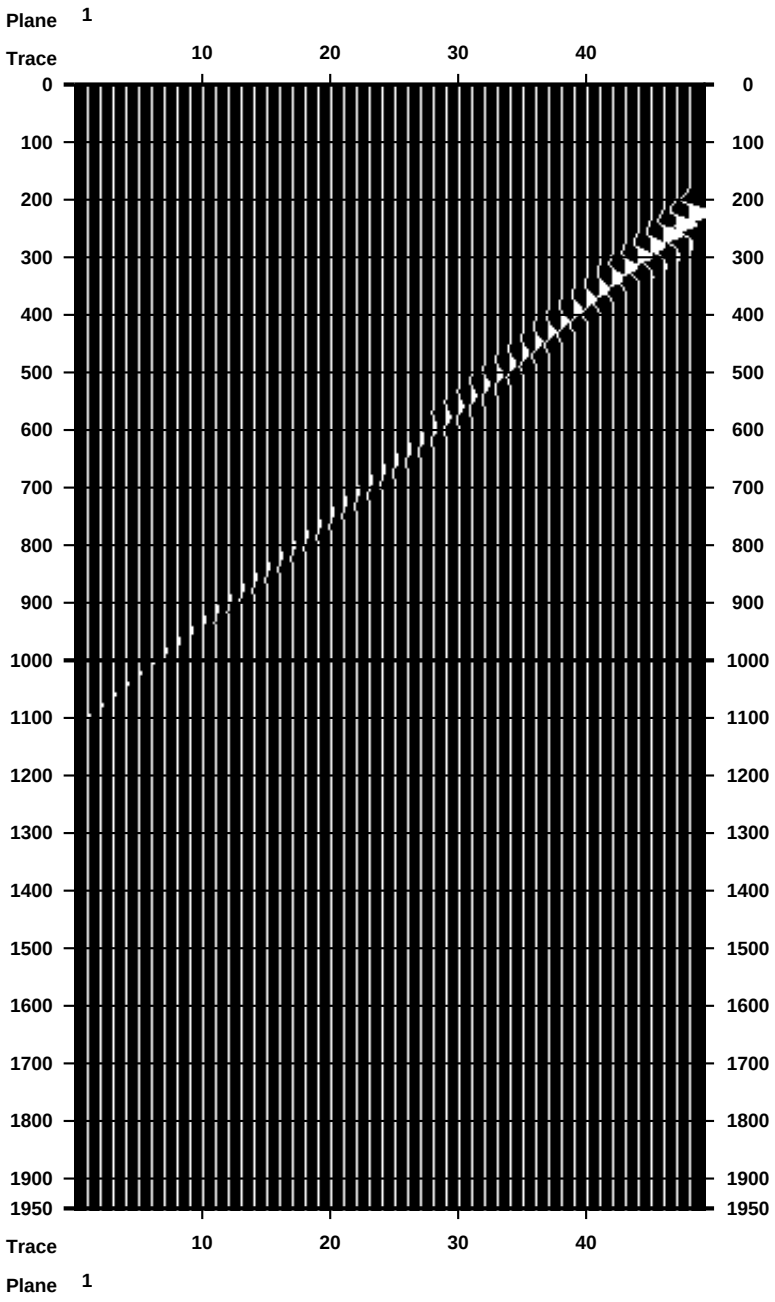

FIGURE 2(A): Seismogram (single experiment data) from simulation. Smooth velocity (Figure 3(a)), 15 Hz Ricker source (Figure 3(c)). Source-receiver offsets vary from 150 m to 1800 m at 25 m intervals.

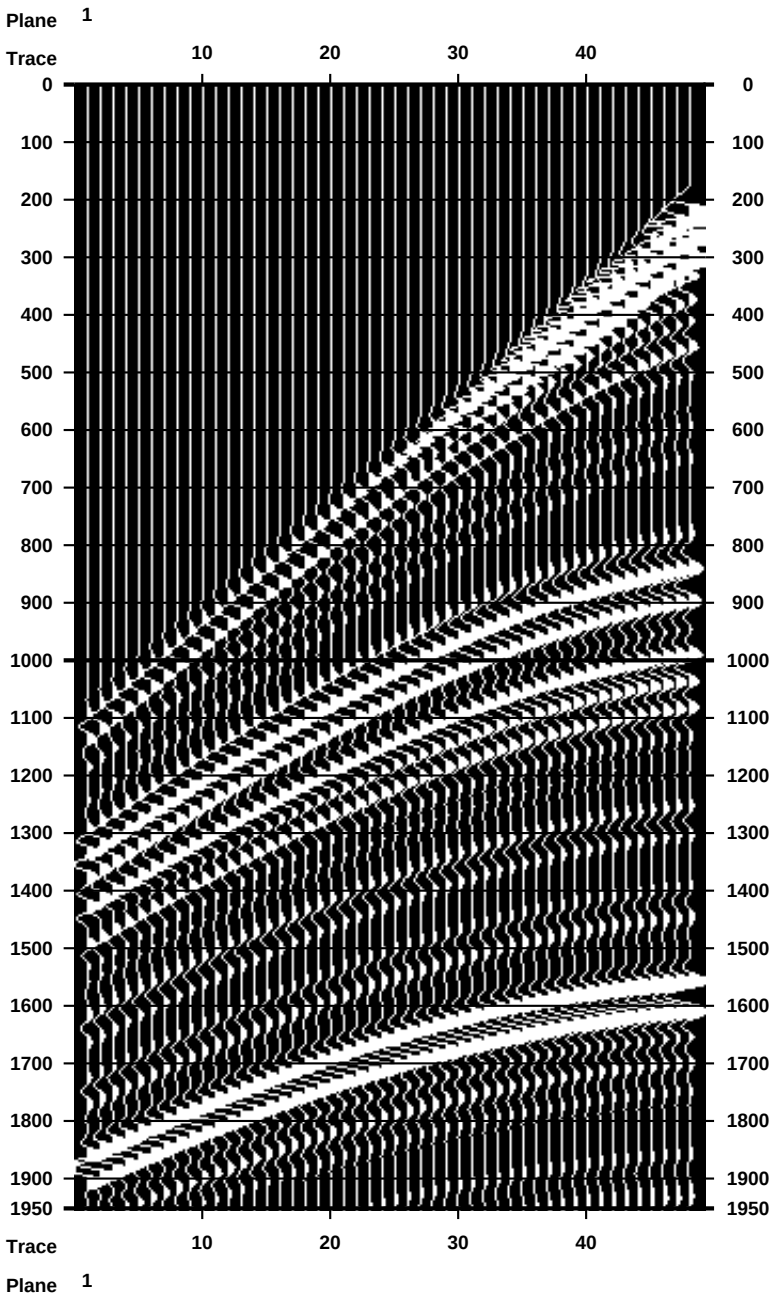

FIGURE 2(B): Seismogram for rough velocity (sum of Figure 3(a) and Figure 3(b)).

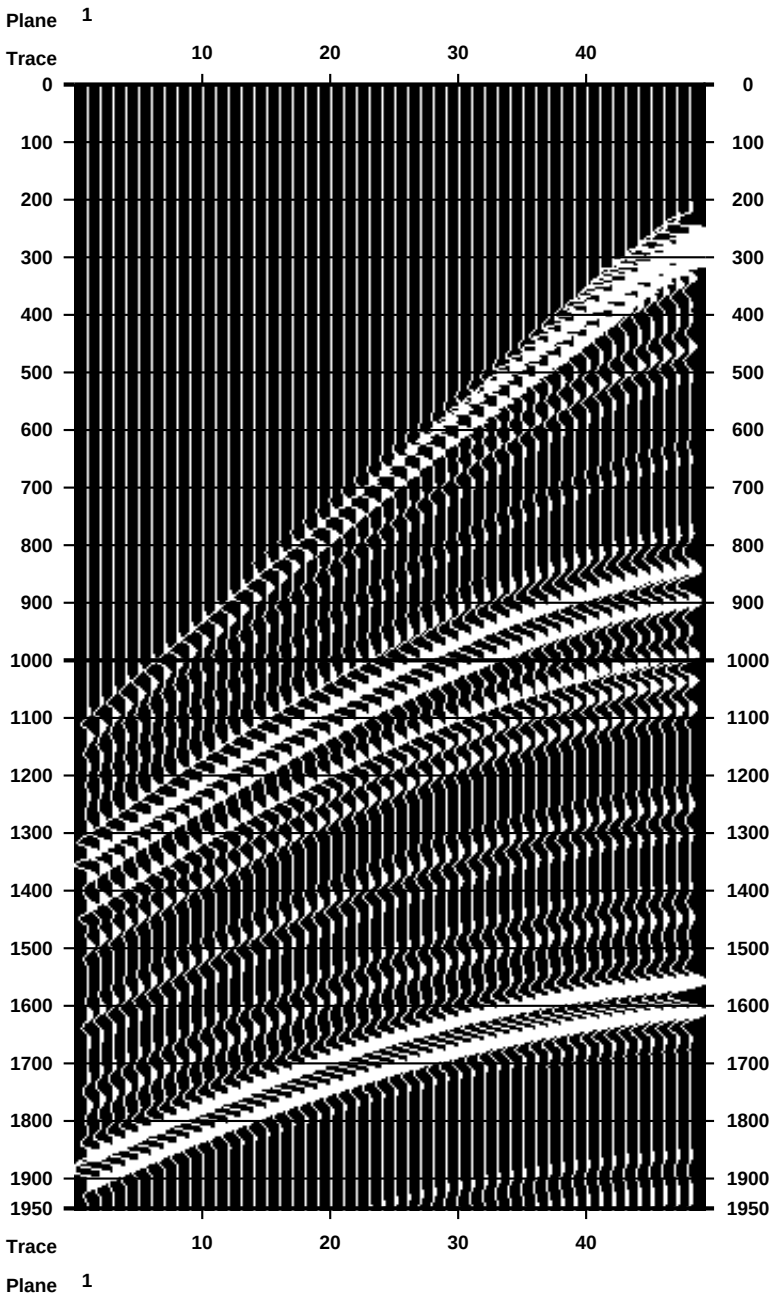

FIGURE 2(C): Linearized seismogram: reference velocity of Figure 3(a), perturbation velocity of Figure 3(b),

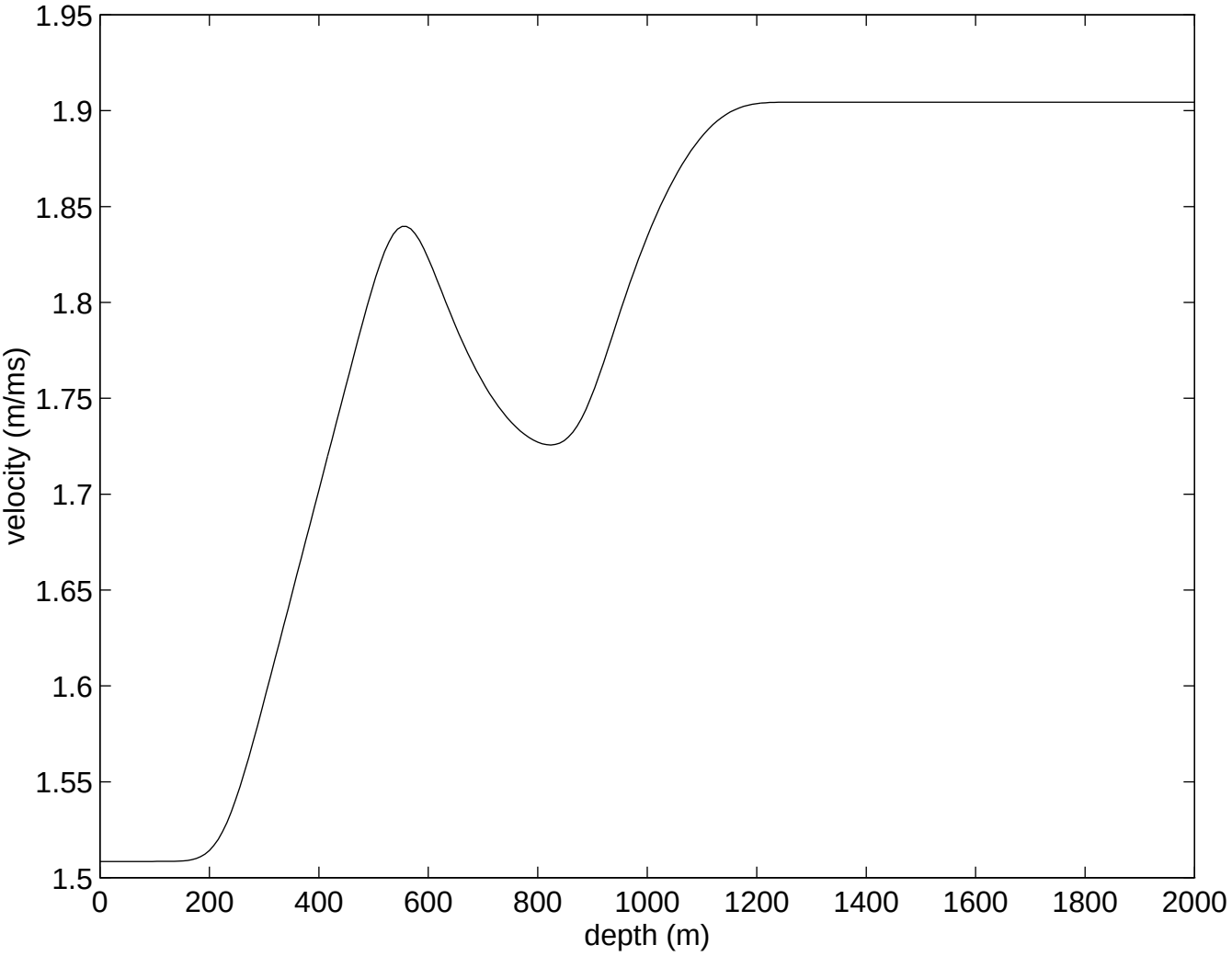

FIGURE 3(A): Velocity (function of depth only) used in synthetic experiments in this chapter.

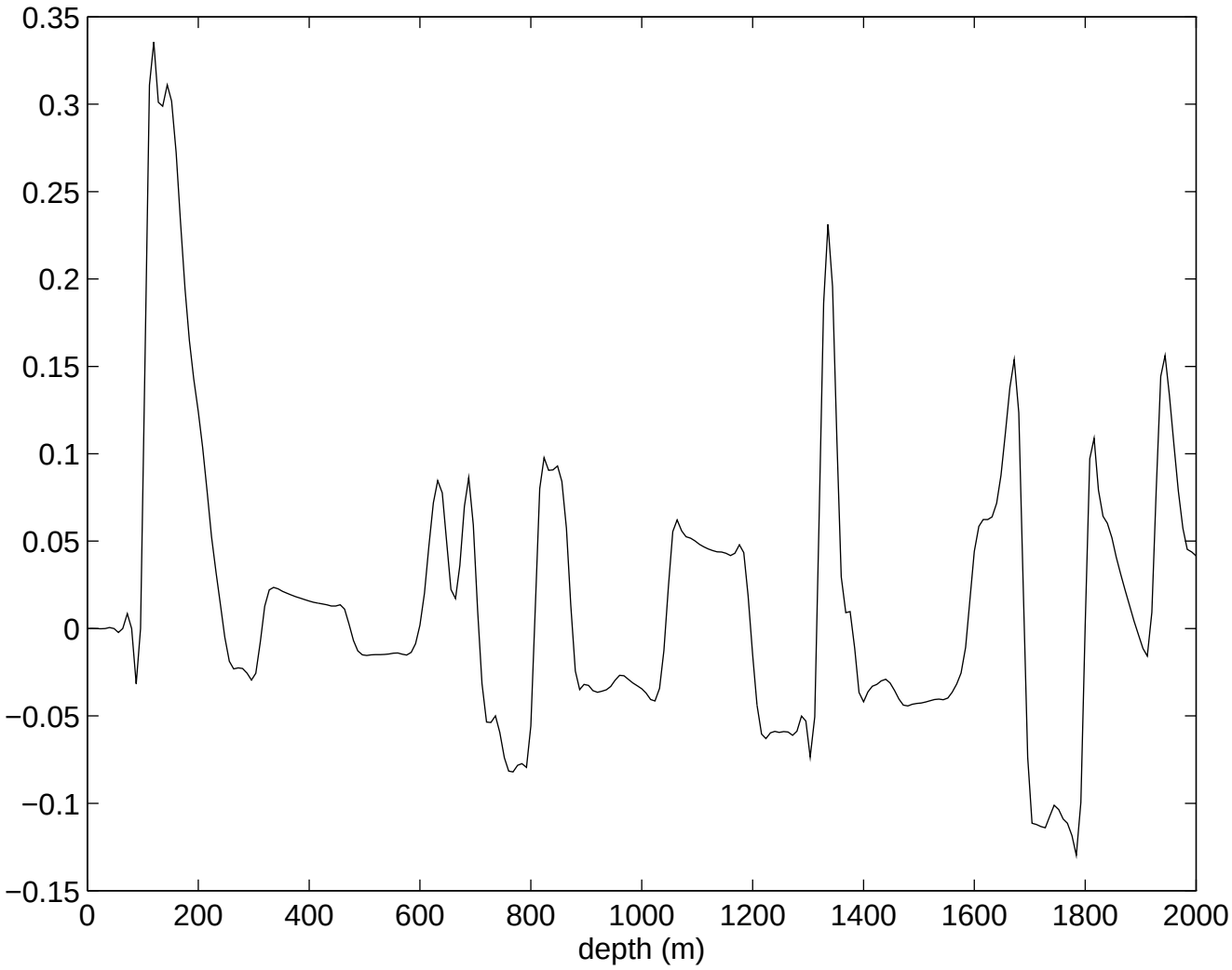

FIGURE 3(B): Relative velocity perturbation (i.e. $\delta c/c$) (function of depth only) used in synthetic experiments in this chapter.

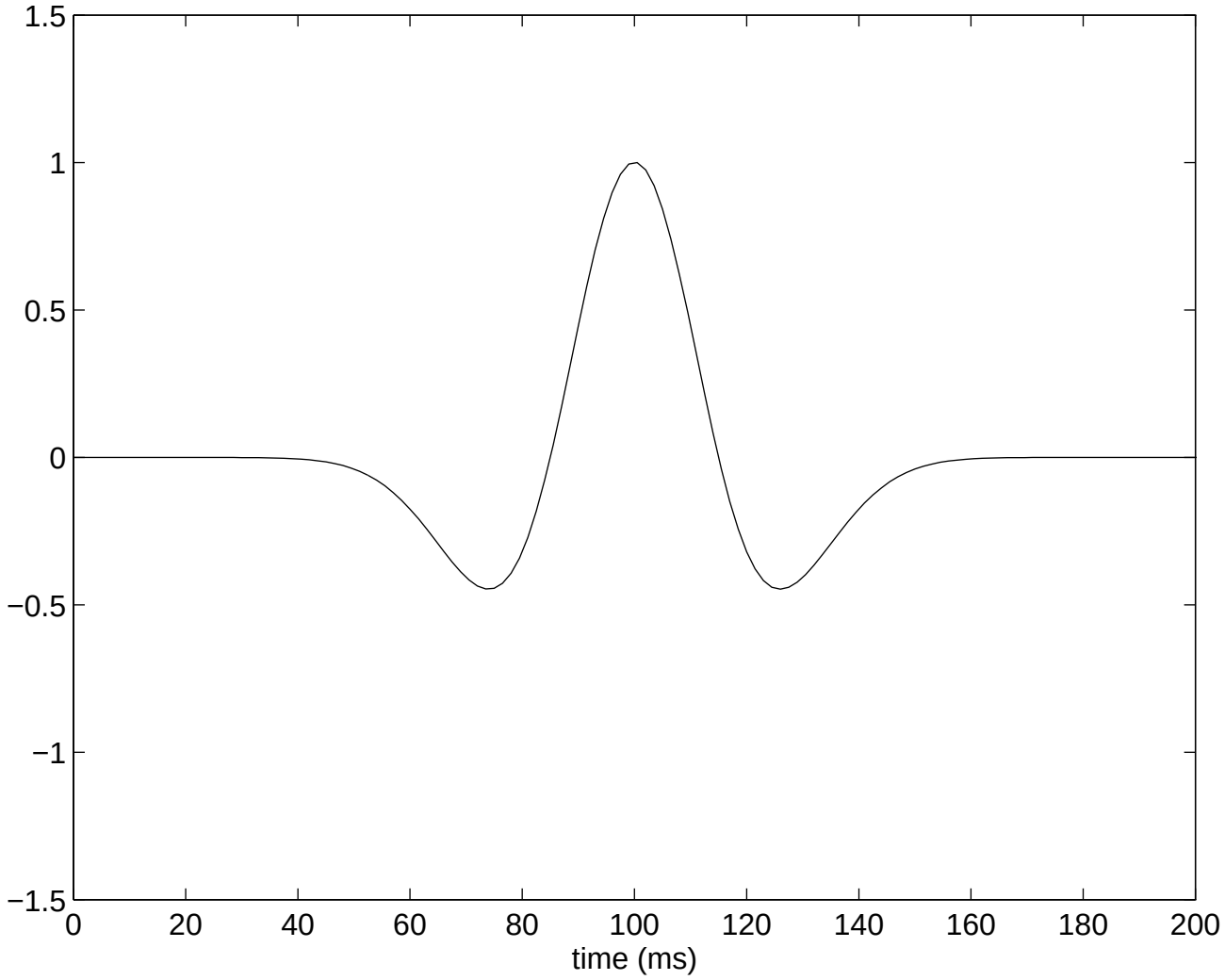

FIGURE 3(C): Source time function used in synthetic experiments in this chapter. Second derivative of Gaussian ("Ricker wavelet") scaled to have peak frequency at around 15 Hz.

Figure 2(a) shows the seismogram for the reference medium (Figure 3(a)). Note the non-appearance of reflected waves: the recorded signal consists almost entirely of a single pulse, apparently moving at constant velocity and decaying. The next section will explain this behaviour quite satisfactorily. Figure 2(b) shows the result of adding the oscillatory perturbation δc (Figure 3(b)) to the reference velocity. Reflected waves are now evident, having general character quite similar to that of the real data example (Figure 2) discussed above. In particular the reflected waves have very regular geometry. Figure 2(c) shows the linearized model. The similarity to the difference between Figure 2, (a) and (b), is obvious.

Since the bulk of the difference between the seismogram and its linearization lies in the early part of the signal (Figure 2(a)), a natural way to assess the result of linearization is to excise this component, by multiplying by a function $\equiv 1$ below a sloping line and $\equiv 0$ above it. In seismic jargon, such a cutoff function is a *mute*. Figure 4 shows the muted seismogram (a), the muted linearized seismogram (b), and the difference (c), plotted on the same scale. The difference appears quite small; actually it is roughly 23% RMS, or about20% in the sup norm. This is not a bad comparison, since δc is roughly 20% the size of c. Reducing the size of δc reduces the error quadratically, as one would expect of a differentiable function.

More importantly, the difference between the seismogram and its linearization is quite systematic and fraught with physical significance. Notice the coherent signal near the bottom of Figure 4(c). This part of the data arrives at about 1700 ms. It corresponds to the reflected waves in either Figure 4(a) or 4(b) arriving at about 850 ms - in fact it has traveled almost precisely twice as far, reflecting once from some subsurface model feature, then again from the surface, then yet again from the same model feature, in the process accumulating amost exactly twice the time of travel of the wave which reflects only once. The linearization does not model such *multiple reflections*, and for that reason is sometimes called *primaries only* or *primary reflection* modeling.

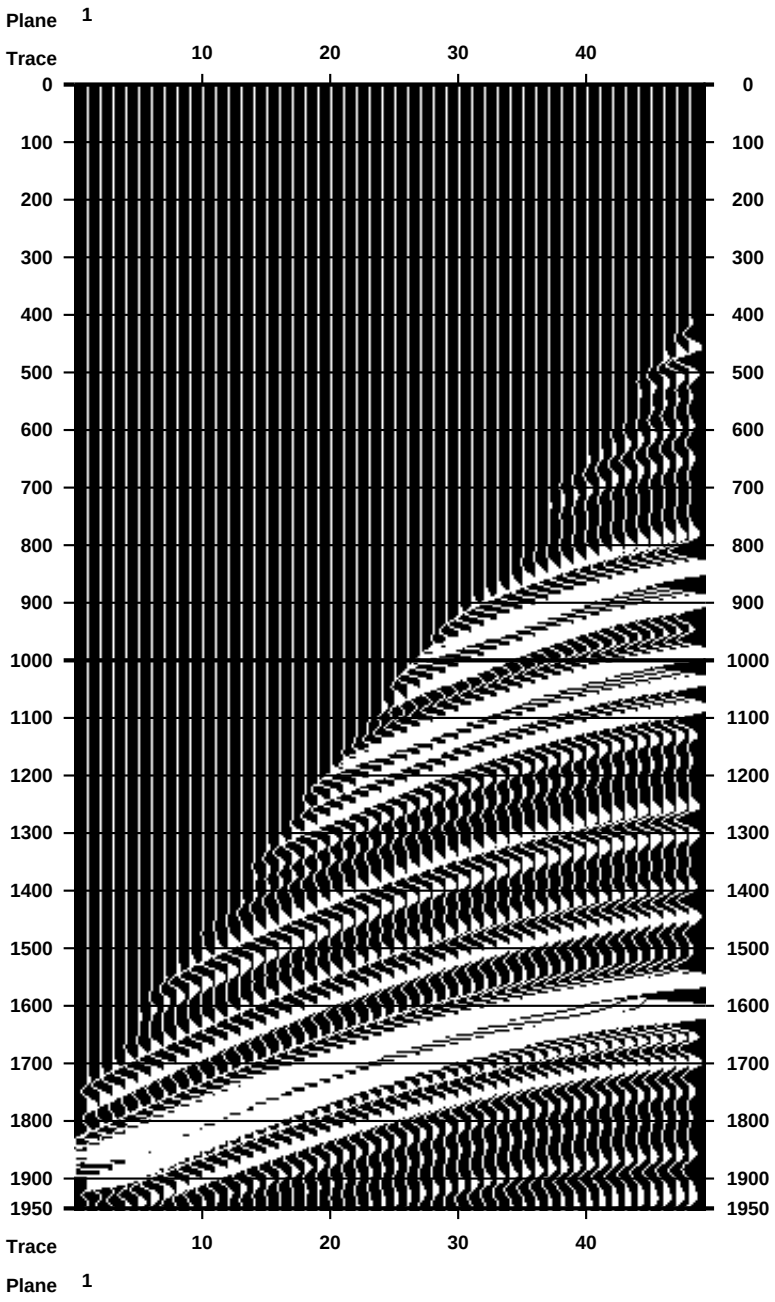

FIGURE 4(A): Muted version of Figure 2(a). Zero offset intercept (time at which mute would begin at zero offset = source-receiver distance) is 200 ms. First signal on rightmost trace occurs later because near offset is 150 m. Mute velocity = rate of first nonzero signal with offset = 1.2 m/ms.

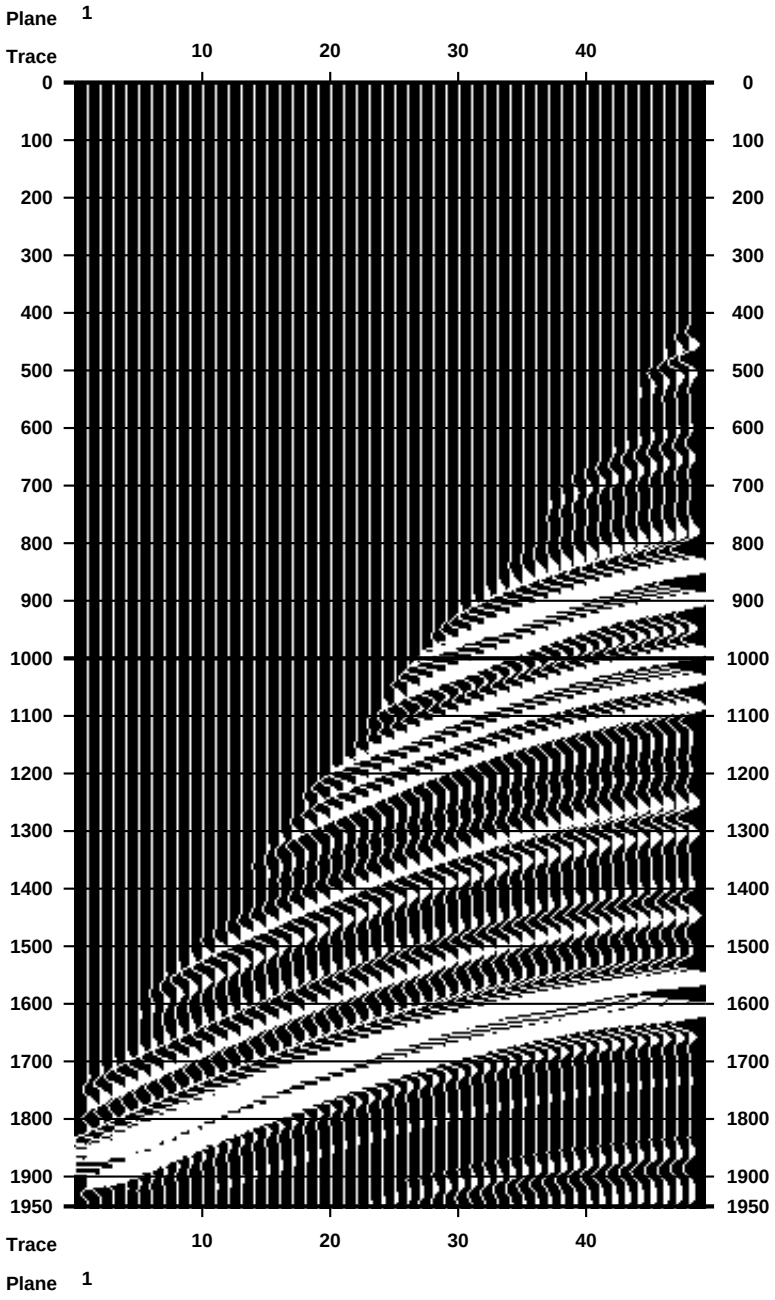

FIGURE 4(B): Muted version of Figure 2(b) (linearized seismogram).

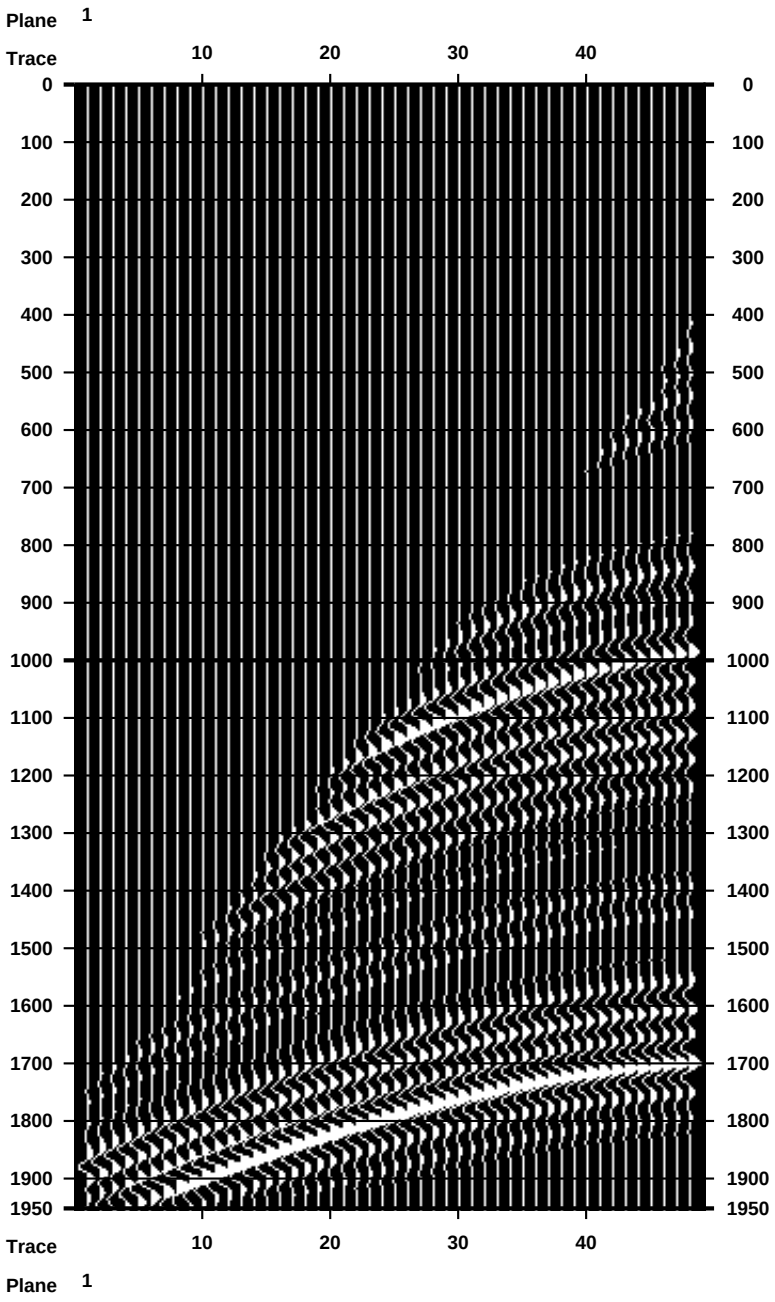

FIGURE 4(C): Difference between Figures 4(a) and 4(b). Note that strong signals correlate almost exactly with reflections in Figure 4(b) arriving at roughly half the time - these are multiple reflections.

This chapter is concerned almost entirely with primaries only modeling and its consequences. Chapter XXX by Weglein and Stolt will take up the issue of multiple reflections, which are present in many (but not all) real-world seismic reflection data sets. Seismologists have devoted much effort to devising processes to remove multiply reflected energy from data, so that it could be treated subsequently with processes based on primaries only modeling. The paper by Weglein and Stolt in this volume takes a fresh look at this problem, amongst other things.

One last example for this section emphasizes the importance of the heuristic rule, justified in the simplest (1D) instance by Lewis' result, that the reference velocity should be smooth, and the perturbation oscillatory, for the linearization to be an accurate approximation to the actual seismogram perturbation. Figure 5 shows another similar seismogram (a), the seismogram computed using the same reflectivity but a velocity only 2% lower (b), and the difference (c). The difference is now clearly on the same order as the data itself. This shows that the seismogram is a *very* nonlinear function of the smooth model components. We shall come back to this point in the sequel.

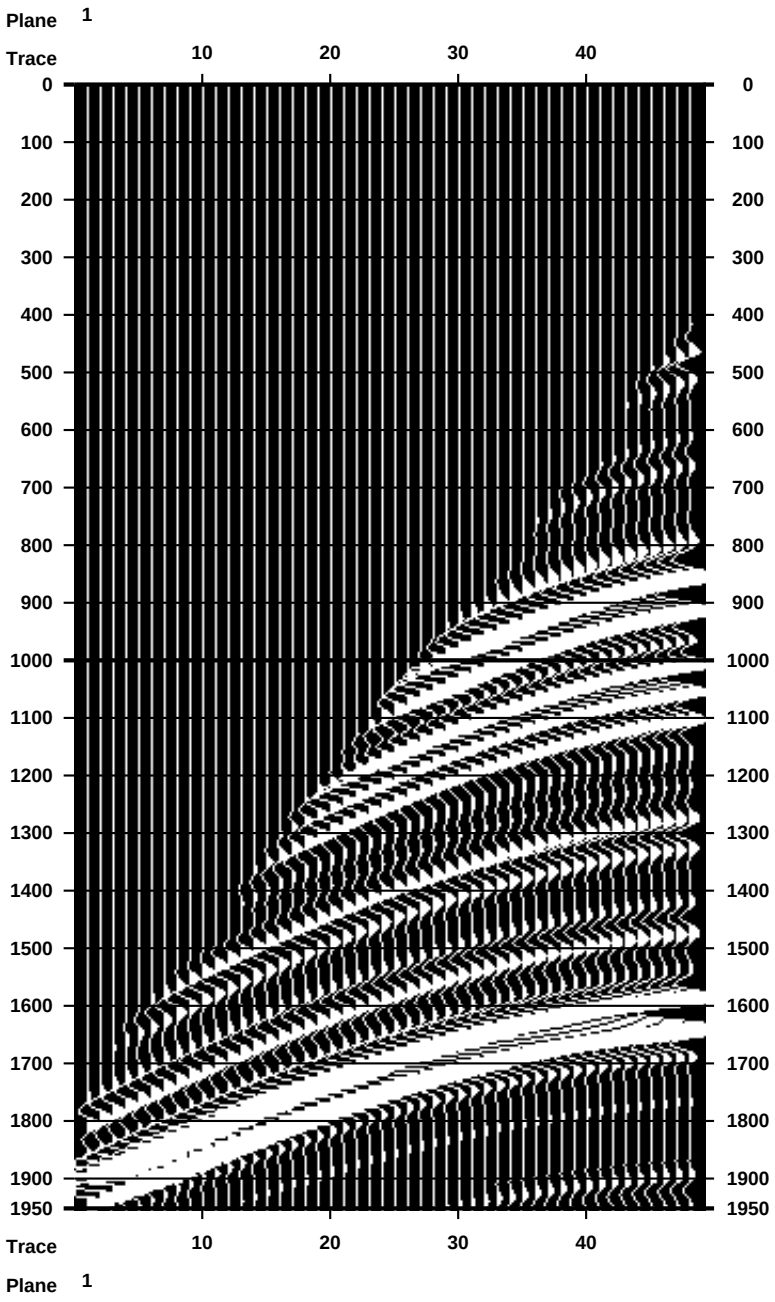

FIGURE 5(A): Muted primaries only (linearized seismogram) from model of Figure 3, except that velocity (Figure 3(a)) is reduced by 2%. Note that all reflections arrive slightly later than in the comparable Figure 4(b).

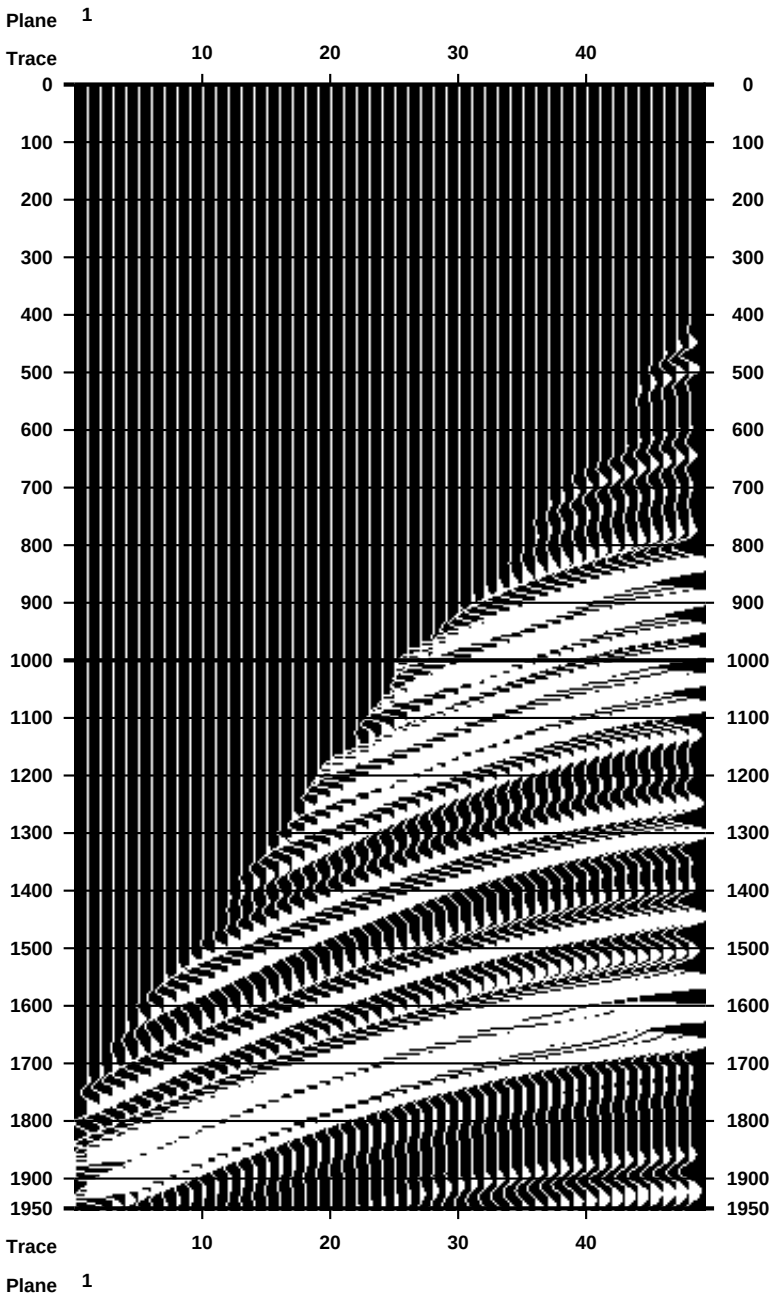

FIGURE 5(B): Difference of Figures 4(b), 5(a). The very large difference is a result of constructive interference, the *time shift effect*.

5 Progressing Wave Expansion

To understand the perturbational field δp, it is evident from 2 that we must first understand the background field p. As might be guessed from the point-source assumption, this field is singular — in fact, in view of the time-independence of the coefficients,

$$p(x_s, x, t) = \int dt' f(t - t') G(x_s, x, t)$$

where the fundamental solution (or Green's function) $G(x_s, x, t)$ solves

$$\frac{1}{\rho(x)c^2(x)} \frac{\partial^2 G(x_s, x, t)}{\partial t^2} - \nabla_x \frac{1}{\rho(x)} \nabla_x G(x_s, x, t) = \delta(t)\delta(x - x_s)$$
$$G(x_s, x, t) \equiv 0 \ , \quad t < 0 \ .$$

Since $\rho \equiv \rho_0, c \equiv c_0$ near the source (reflection configuration) and ρ_0 and c_0 are constant (for convenience), we can write explicit expressions for G, good for small t and $|x - x_s|$, in dimensions 1, 2, 3:

$$n = 1: \quad G(x_s, x, t) = \rho_0 H(c_0 t - |x - x_s|)$$
$$n = 2: \quad G(x_s, x, t) = \frac{\rho_0}{2\pi} \frac{H(c_0 t - |x - x_s|)}{\sqrt{c_0^2 t^2 - |x - x_s|^2}}$$
$$n = 3: \quad G(x_s, x, t) = \frac{\rho_0 \delta(c_0 t - |x - x_s|)}{4\pi |x - x_s|} \ .$$

While it is not possible to write such explicit expressions for the fundamental solution in the inhomogeneous region $\{z > z_d\}$, it is possible to describe the leading singularity of G quite precisely and this will be sufficient for our present purposes. This is accomplished *via* the *progressing wave expansion* (COURANT and HILBERT, 1962, Ch. VI). Each of the formulas for G above is of the form $a(x_s, x)S(t - \tau(x_s, x))$ where a and the travel time function τ are smooth except possibly at $x = x_s$, and $S(t)$ is singular at $t = 0$. The progressing wave expansion allows the extension of this expression away from $x = x_s$, up to a limit signaled by a fundamental change in the nature of the wavefield, and with an error which is *smoother* than S.

In general, suppose that

$$u(x_s, x, t) = a(x, x_s) S(t - \tau(x_s, x))$$

for $|x - x_s|$ small and t small, and write

$$u(x_s, x, t) = a(x, x_s) S(t - \tau(x_s, x)) + R(x_s, x, t)$$

where R is in some sense to be smoother than S, and a and τ are assumed to be smooth in some as-yet unspecified region. Applying the wave operator, we obtain

$$\left(\frac{1}{\rho c^2} \frac{\partial^2}{\partial t^2} - \nabla \frac{1}{\rho} \nabla \right) u$$
$$= \frac{a}{\rho} \left(\frac{1}{c^2} - |\nabla \tau|^2 \right) S''(t - \tau)$$

$$+\frac{1}{\rho}\left(2\nabla\tau\cdot\nabla a-\left(\nabla\tau\cdot\frac{\nabla\rho}{\rho}+\nabla^2\tau\right)a\right)S'(t-\tau)$$

$$+\left(\nabla\cdot\frac{1}{\rho}\nabla a\right)S(t-\tau)+\frac{1}{\rho c^2}\frac{\partial^2 R}{\partial t^2}-\nabla\cdot\frac{1}{\rho}\nabla R\,.$$

Formally, the terms written in the above order have decreasing orders of singularity, so that if u is to solve the wave equation for $x\neq x_s$, each of the coefficients above ought to vanish. Certainly, if

$$\frac{1}{c_2}-|\nabla\tau|^2\equiv 0 \tag{3}$$

$$2\nabla\tau\cdot\nabla a-(\nabla\tau\cdot\nabla\log\rho+\nabla^2\tau)a\equiv 0 \tag{4}$$

then the first two terms vanish. Using the special properties of the distributions S appearing in the fundamental solutions of the wave equation, it is possible to show that the last two terms can also be made to vanish for a particular choice of R. We will describe briefly how this is to be done below, after discussing the very important conditions 3 and 4.

Equation 3 is the *eikonal equation* of geometric optics (of which the progressing wave expansion is a variant). Inspecting the local fundamental solutions above, evidently it is required to satisfy 3 with a function $\tau(x,x_s)$ so that

$$\tau(x,x_s)=\frac{|x-x_s|}{c_0}\quad\text{for }|x-x_s|\text{ small.}$$

Fortunately, $c\equiv c_0$ for $|x-x_s|$ small so $\tau(x,x_s)$ given by the preceding formula satisfies the eikonal equation near the source. We will extend this solution by means of the *method of characteristics*.

Suppose first that τ solves the eikonal equation, and let $x(\sigma)$ be a solution of the system of ordinary differential equations

$$\dot{X}=c^2(X)\nabla\tau(X)\qquad\left(\dot{\ }=\frac{d}{d\sigma}\right)\,.$$

Then

$$\begin{aligned}\frac{d}{d\sigma}\tau(X(\sigma)) &= \nabla\tau(X(\sigma))\cdot\dot{X}(\sigma)\\ &= c^2(X(\sigma))|\nabla\tau(X(\sigma))|^2\ .\end{aligned}$$

Therefore we can identify τ with σ: if the segment $\{X(\sigma'):\sigma_0\leq\sigma'\leq\sigma\}$ lies entirely in a domain in which τ is defined, then

$$\tau(X(\sigma))=\tau(X(\sigma_0))+\sigma-\sigma_0 \tag{5}$$

Thus from knowledge of the characteristic curves (rays) $X(\sigma)$, we can construct τ. Somewhat more surprisingly, it is possible to construct the rays directly, which furnishes a construction of τ as well.

Indeed, if we write

$$\xi(\sigma) = \nabla\tau(X(\sigma))$$

then

$$\begin{aligned}
\dot{\xi}(\sigma) &= \nabla\nabla\tau(X(\sigma)) \cdot \dot{X}(\sigma) \\
&= c^2(X(\sigma))\nabla\nabla\tau(X(\sigma)) \cdot \nabla\tau(X(\sigma)) \\
&= \frac{1}{2}c^2(X(\sigma))\nabla|\nabla\tau(x)|^2 \mid_{x=X(\sigma)} \\
&= \frac{1}{2}c^2(x)\nabla(c^{-2}(x)) \mid_{x=X(\sigma)} \\
&= -\frac{1}{2}|\nabla\tau(x)|^2\nabla\nabla c^2(x) \mid_{x=X(\sigma)} \ .
\end{aligned}$$

If we write the *Hamiltonian*

$$H(x,\xi) = \frac{1}{2}c^2(x)|\xi|^2$$

then the equations for X and ξ read

$$\begin{aligned}
\dot{X} &= \nabla_\xi H(X,\xi) \\
\dot{\xi} &= -\nabla_x H(X,\xi)
\end{aligned}$$

which are *Hamilton's equations* of classical mechanics, a system of $2n$ autonomous ordinary differential equation.

Now note that for each unit vector $\theta \in S^{n-1}$, the trajectory

$$\sigma \to \left(c_0\sigma\theta + x_s,\ \frac{1}{c_0}\theta\right) = (X_\theta(\sigma), \xi_\theta(\sigma))$$

satisfies Hamilton's equations for small σ, and moreover

$$\dot{X}_\theta(\sigma) = c^2(X(\sigma))\nabla\tau(X_\theta(\sigma))$$

as is easily checked. Moreover, $(\sigma,\theta)) \mapsto X_\theta(\sigma)$ gives (essentially) polar coordinates centered at x_s. Now extend (X_θ, ξ_θ) as solutions of Hamilton's equations over their maximal intervals of definition for each $\theta \in S^{n-1}$, say $\{0 \le \sigma < \sigma_{\max}(\theta)\}$. Then every point in

$$\Omega(x_s) := \{x : x = X_\theta(\sigma) \quad \text{for some} \quad \theta \in S^{n-1},\ \sigma \in [0, \sigma_m ax(\theta_{\max})]\}$$

is touched by at least one ray. If every point in $\Omega(x_s)$ is touched by *exactly* one ray, then the formula (5) produces a unique value $\tau(x_s,x)$ at every point in $\Omega(x_s)$. *It is possible to show that, in that case, τ is a solution of the eikonal equation 3* (in fact, it's not even difficult, but we won't do it here. See the references cited at the end of the section.).

In general, some points in $\Omega(x_s)$ are touched by more than one ray. Let

$$\begin{aligned}
\Omega^0(x_s,t) = \{&x \in \Omega(x_s) : \text{ if } x = X_\theta(\sigma), \text{ then for} \\
&0 \le \sigma' \le \sigma\ , X_\theta(\sigma') \text{ lies } \textit{only} \text{ on the ray} \\
&X_\theta\ . \text{ Moreover } \tau(x_s,x) \le t\}\ .
\end{aligned}$$

Also for $\epsilon > 0$ define

$$\Omega^0_\epsilon(x_s, t) = \{x \in \Omega(x_s) : |y - x| < \epsilon \Rightarrow y \in \Omega^0(x_s, t)\} .$$

Then generally $\Omega^0(x_s, t) \not\subseteq \Omega(x_s)$. The boundary points of $\Omega^0(x_s, t)$ are located on envelopes of ray families, called *caustics*. Points in $\Omega^0_\epsilon(x_s, t)$ are at distance at least $\epsilon > 0$ from any caustic. The physics and mathematics of wave propagation and reflection both change substantially at caustics, in ways that are only poorly understood at present. We will discuss reflection from caustic locii briefly in Section 10. For the most part, *in these notes we will assume that the region to be examined lies inside* $\Omega^0(x_s, t)$ *for each source location* x_s.

To recapitulate: The method of characteristics ("ray tracing" in seismology) constructs a solution $\tau(x_s, x)$ of the eikonal equation which is for small $|x - x_s|$ identical to the travel-time $|x - x_s|/c_0$. Because of the parameterization of the rays for small σ, σ evidently has units of (time), so from (5) τ has units of time. For that reason, and because the zero-locus of $t - \tau$ is the locus of arrival of the singularity (in S) in the first term of the progressing wave expansion, we also call τ the *travel time* function.

Having computed τ, it is easy to compute a. Indeed, the *transport equation* 4 may be re-written

$$\frac{d}{d\sigma} a(X(\sigma)) - b(X(\sigma))a(X(\sigma)) = 0$$

where

$$b = \frac{1}{2}(\nabla\tau \cdot \nabla \log \rho + \nabla^2\tau) .$$

Thus a may be computed by quadrature along the ray family associated with τ. Initial values (for small (σ) for $a(X(\sigma))$ are read off from the small $(x - x_s)$ formulae for the fundamental solutions.

The solution of the transport equation has a nice geometric interpretation: it is proportional to the reciprocal square root of the change in volume of an infinitesimal transverse element, transported along a ray *via* the transport equation (e.g. FRIEDLANDER, 1958, Ch. 1). The solution becomes infinite at a caustic, or envelope of rays, where the transported transverse element collapses. Thus arrival at a caustics signals the breakdown of the progressing wave expansion.

The method of characteristics is used extensively in seismology, as a *numerical* method for the construction of travel-times. The first term in the progressing wave expansion is also computed by integration along rays, to produce *ray-theoretic seismograms*. Ironically, several people have presented evidence recently that both calculations may be performed far more efficiently by integrating the eikonal and transport equations directly as partial differential equations, using appropriate finite difference schemes, and avoiding entirely the construction of rays (VIDALE, 1988, VANTRIER and SYMES, 1991).

The entire construction is justified by the final step: the remainder R must satisfy

$$\frac{1}{\rho c^2}\frac{\partial^2 R}{\partial t^2} - \nabla \cdot \frac{1}{\rho}\nabla R = (\nabla \cdot \frac{1}{\rho}\nabla a)S(t - \tau)$$
$$R \equiv 0 , \quad t < 0$$

if u is to solve the wave equation. It is possible to show that the unique solution R of this initial value problem has singularities no worse than that of the indefinite integral of S. Thus the remainder R is indeed smoother than the first term, and the progressing wave expansion has captured the leading singularity of u.

The *meaning* of this construction may be understood by recalling that typical source time functions $f(t)$ are highly oscillatory. The pressure field is given by

$$p = f * G$$

(convolution in time). We have just seen how to write $G = aS(t-\tau) + R$, with R smoother than S — i.e. the Fourier coefficients of R decay more quickly than those of S. If f has most of its frequency content in a band in which the Fourier coefficients of R are much smaller than those of S, then $f * R << f * S(t-\tau)$, so

$$p = f * G \approx f * S$$

so that the first term of the progressing wave expansion *approximates* the pressure field. A careful quantification of this approximation relates the degree of smoothness of the reference coefficients ρ and c, the frequency band of the source f, and the ray geometry associated with c.

To give some idea of the accuracy of the progressing wave expansion, consider the velocity depicted in Figure 6(a). This (2D) velocity distribution has a slow zone, or lens, immediately below the location of the source point for this experiment. From the equations

$$\dot{x} = c^2\xi, \ \dot{\xi} = -\nabla(c^2)|\xi|^2$$

one sees that the acceleration vector $\ddot{x}$ will point towards decreasing c. Thus rays will tend to bend toward the slow zone, or center of the lens, creating an imperfect focus or *caustic* below it. Use of the (fractional) 3/2 derivative of a Gaussian pulse for the source wavelet f (Figure 6(b)) produces a 350 ms wavefront in 2D with the shape of the first derivative of the Gaussian (Figure 6(c)). The 325 ms contour of the earliest arrival time, also plotted in Figure 6(c), appears to lie almost exactly on the zero crossing over most of the wavefront (except in the caustic zone. This is natural, as the zero crossing of the source wavelet occurs at 25 ms. Figure 6(d) shows a plot of several vertical (z) sections through the wavefield at t=350 ms. On the sides, at points connected to the source by unique rays, the shape of the wave is an almost perfect shifted first derivative of a Gaussian, as predicted. Below the low velocity zone, the ray bending due to the lens causes several rays to pass over each point, producing several wavefront arrivals. The trailing pulse has had its phase shifted by $\pi/2$.

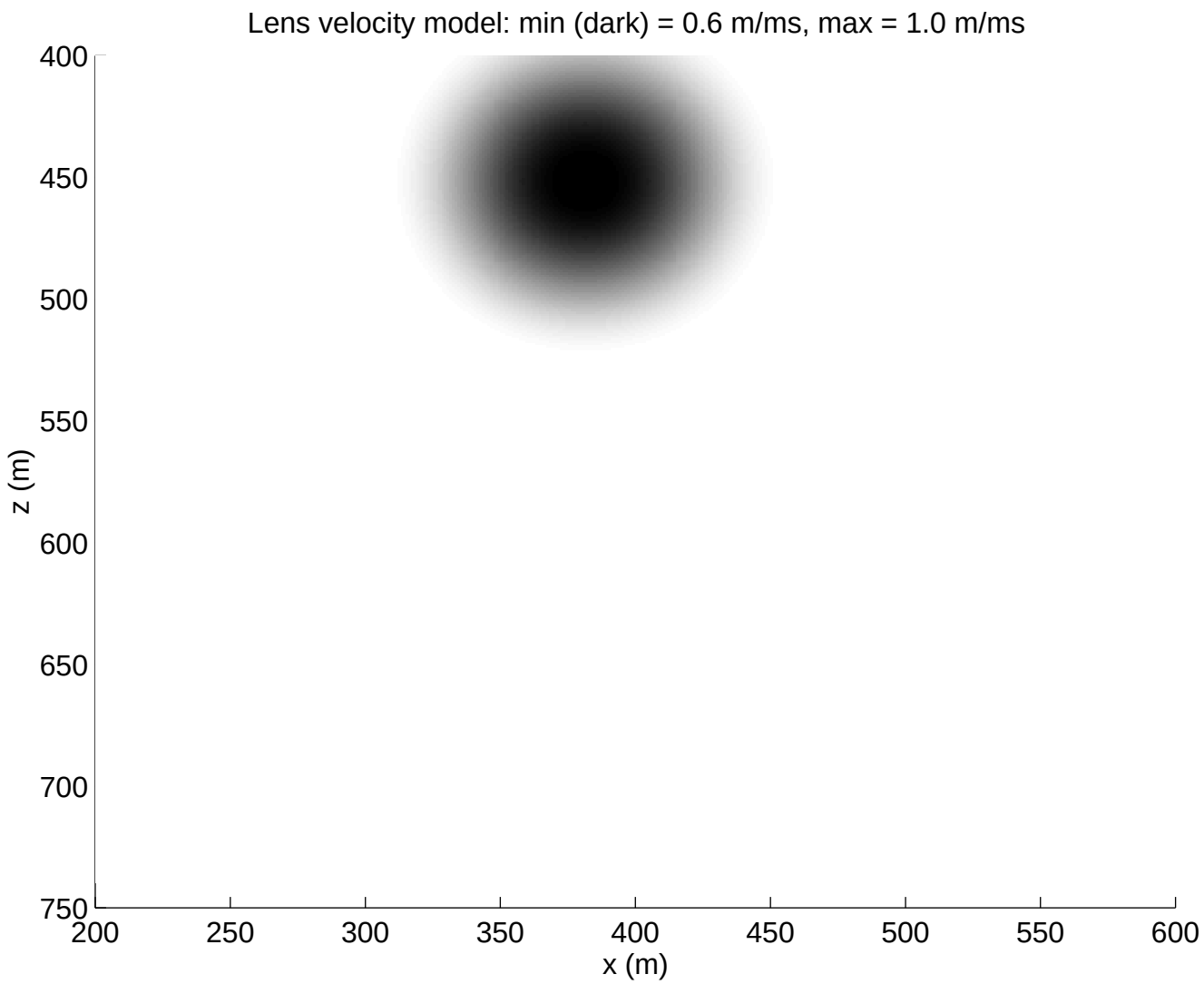

FIGURE 6(A): Velocity field with slow anomaly or lens just below source point. Velocity in center of lens is approximately half that in the surrounding region.

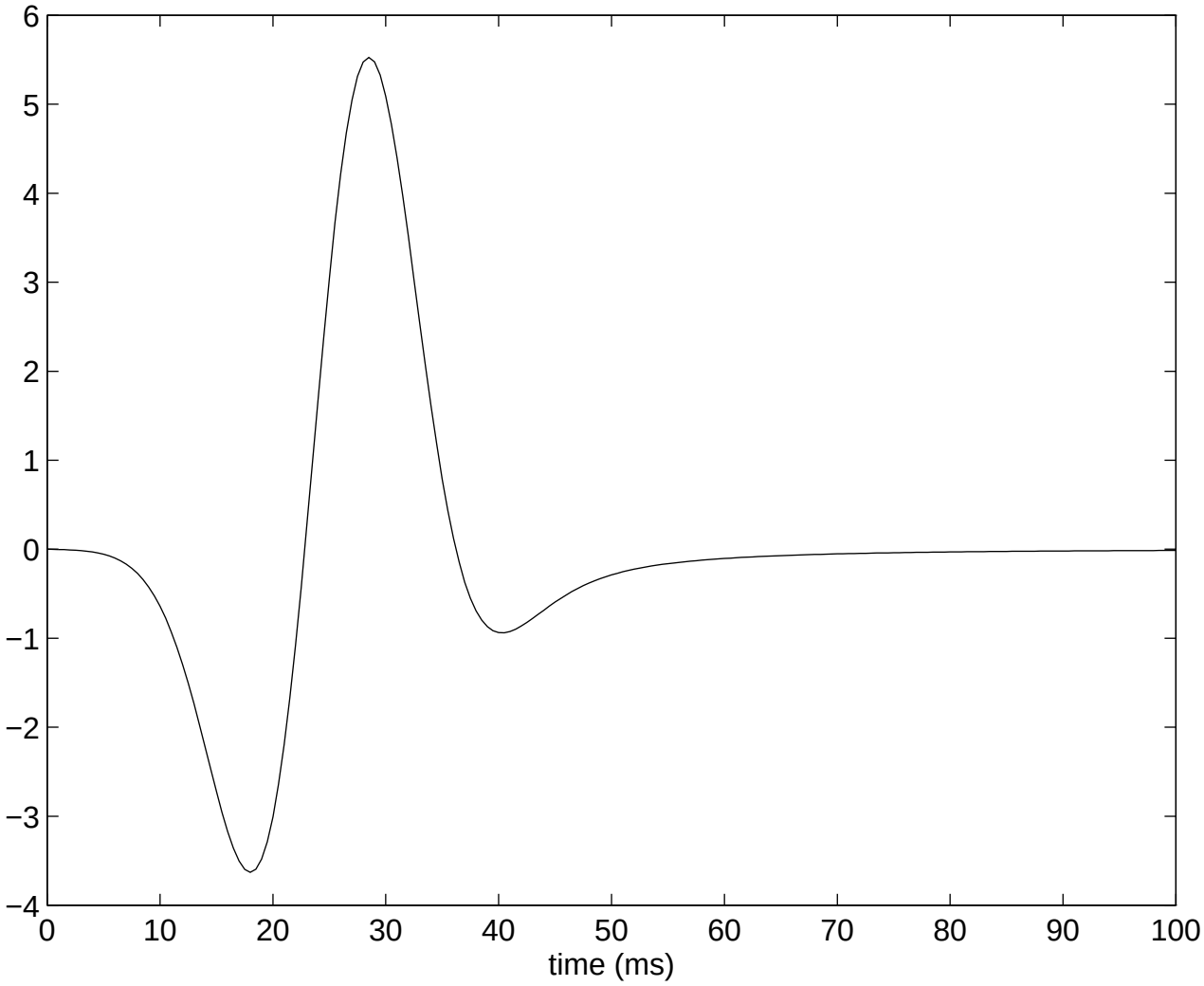

FIGURE 6(B): Source wavelet used in simulation. Derivative of Gaussian pulse of order 1.5. In 2D the field generated by this isotropic radiator has a leading pulse in the shape of the Gaussian first derivative, with one zero-crossing which can be used to calibrate traveltimes.

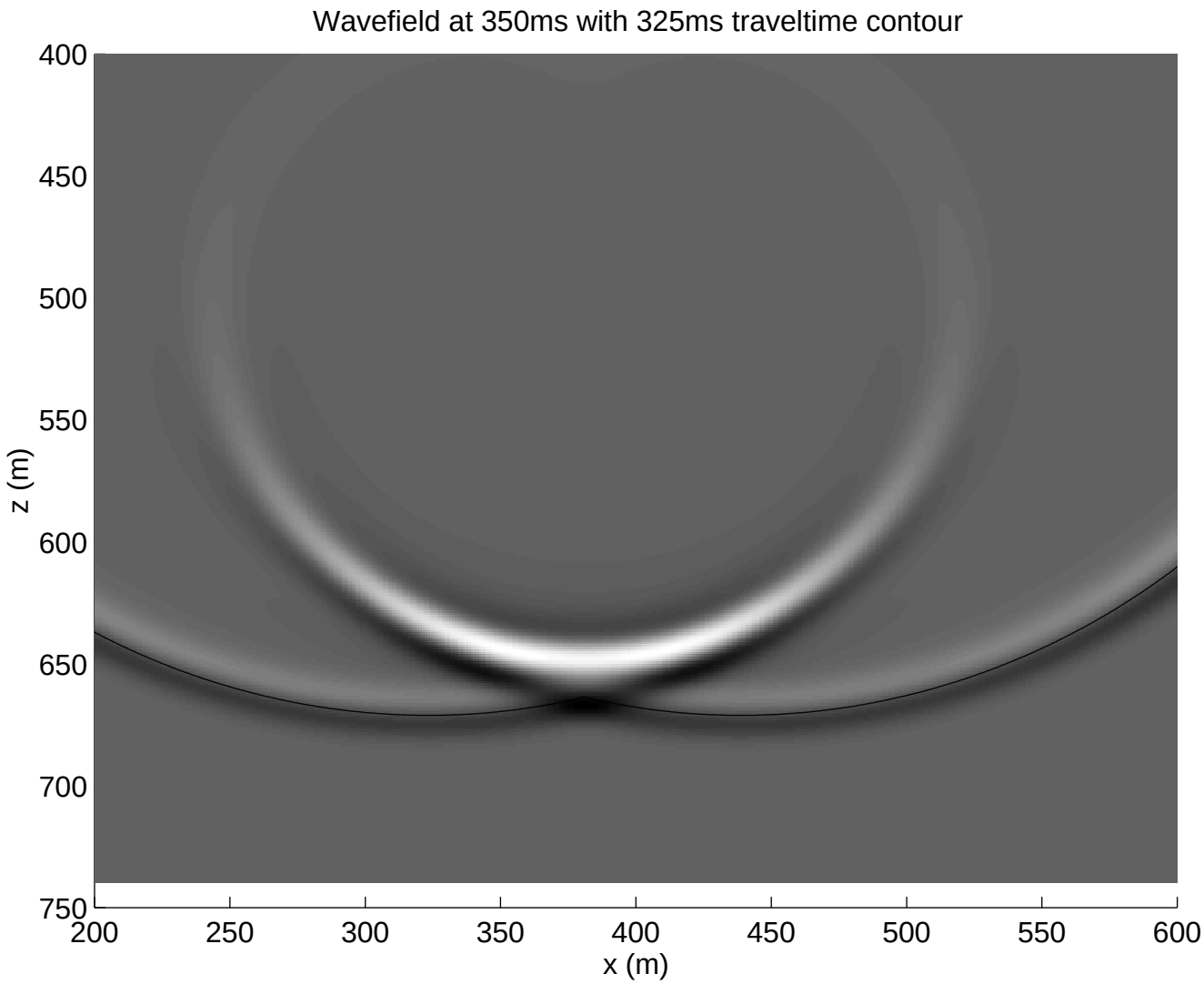

FIGURE 6(C): Grey scale plot of pressure field at 350 ms (function of the two space coordinates - NOT a seismogram!) with the 325 ms traveltime contour superimposed. Traveletime contour matches almost exactly the zero crossing of the leading pulse, as predicted by geometric acoustics. Only the first arrival time (computed by a finite difference eikonal equation solver) is plotted. Below the lens, a caustic has formed, with multiple wavefronts passing over each point.

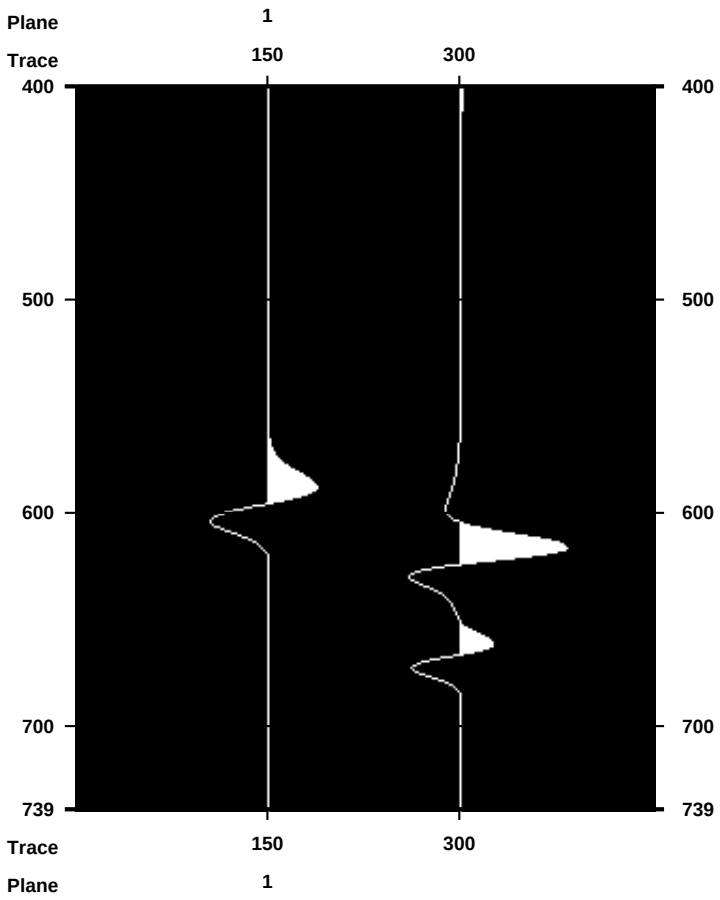

FIGURE 6(D): Two vertical slices through the pressure field. On the left is a slice taken outside of the caustic zone: each point is connected to the source point by a unique ray, and geometric acoustics predicts a single pulse having the Gaussian first derivative shape seen in the slide. On the right is a slice below and slightly to the left of the lens center, in the caustic zone. The lower pulse has traveled around the left side of the lens. The upper complicated signal is a superposition of a pulse traveling around the right side of the lense and a delayed and phase shifted pulse traveling through the center of the lens.

Excellent references for the progressing wave expansion are COURANT and HILBERT, 1962, Ch. 6, and FRIEDLANDER, 1958, Ch. 1. LUDWIG, 1966 and KRAVTSOV, 1968 gave the first satisfactory generalization of the progressing wave expansion accurate in the vicinity of caustics; see also STICKLER et al., 1981. For a modern differential geometric treatment of these topics, consult GUILLEMIN and STERNBERG, 1979

6 Linearized Reflection Operator as a Generalized Radon Transform

The progressing wave expansion allows us to give a very explicit construction of the "leading order" approximation to the pressure field perturbation δp resulting from the acoustic parameter perturbations $\delta c, \delta\rho$. The sense in which this approximation is "leading order" will become clearer in the sequel. Roughly, the error is of lower frequency content than the "leading" term, relative to the frequency content of $\delta\rho, \delta c$. Thus if $\delta\rho, \delta c$ are highly oscillatory, we would expect the "leading" term to constitute most of δp, and this proves to be the case.

We enforce throughout the requirement of *simple ray geometry*: for some $\epsilon > 0$, for all source and receiver positions $(x_s, x_r) \in X_{sr}$, signal duration T, and subsurface locations x,

$$\left.\begin{array}{r} \delta\rho(x) \neq 0 \\ \text{or} \quad \delta c(x) \neq 0 \end{array}\right\} \Rightarrow x \in \Omega^0_\epsilon(x_s, T) \cap \Omega^0_\epsilon(x_r, T) \; .$$

Let $\Omega = \{x : \delta\rho(x) \neq 0 \text{ or } \delta c(x) \neq 0\}$. Then we have assumed that

$$\Omega \subset \{x : z \geq z_d\} \cap \bigcap_{(x_s, x_r) \in X_{s,r}} \left[\Omega^0_\epsilon(x_s, T) \cap \Omega^0_\epsilon(x_r, T)\right] \; .$$

Note that if $c \equiv c_0$ in all of $\mathbb{R}^n$, the set on the right is simply $\{z \geq z_d\}$, but in general it is much smaller.

A robust approach to acoustic imaging must drop this assumption, which underlies almost all contemporary work.

I review briefly some recent progress towards removing the simple geometry assumption at the end of the chapter.

Since

$$\delta p = f * \delta G$$

where δG is the perturbation in the fundamental solution, it suffices to compute δG, which is the solution of

$$\frac{1}{\rho c^2} \frac{\partial^2 \delta G}{\partial t^2} - \nabla \cdot \frac{1}{\rho} \nabla \delta G = \frac{2\delta c}{\partial c^3} \frac{\partial^2 G}{\partial t^2} - \frac{1}{\rho} \left(\nabla \frac{\delta\rho}{\rho}\right) \cdot \nabla G$$
$$\delta G \equiv 0 \; , \quad t < 0 \; .$$

The key to an effective computation is the Green's formula

$$\int_{\mathbb{R}^n} dx \int dt \left(\frac{1}{\rho c^2} \frac{\partial^2 u}{\partial t^2} - \nabla \cdot \frac{1}{\rho} \nabla u \right) v = \int_{\mathbb{R}^n} dx \int dt \, u \left(\frac{1}{\rho c^2} \frac{\partial^2 v}{\partial t^2} - \nabla \cdot \frac{1}{\rho} \nabla v \right)$$

which holds so long as both sides make sense, e.g. if u, v are smooth and the support of the product uv is bounded. We will apply this Green's formula willy-nilly to singular factors as well, but in every case the result can be justified by limiting arguments, which we omit (trust me!).

Now

$$\begin{aligned}
\delta G(x_s, x_r, t_r) &= \int_{\mathbb{R}^n} dx \int dt \; \delta G(x_s, x_r, t) \delta(x_r - x) \delta(t_r - t) \\
&= \int_{\mathbb{R}^n} dx \int dt \; \delta G(x_s, x_r, t) \left[\frac{1}{\rho(x) c^2(x)} \frac{\partial^2 G}{\partial t^2}(x_r, x, t_r - t) \right. \\
&\qquad \left. - \nabla \cdot \frac{1}{\rho(x)} \nabla G(x_r, x, t_r - t) \right] \\
&= \int_{\mathbb{R}^n} dx \int dt \left[\frac{1}{\rho(x) c^2(x)} \frac{\partial^2 \delta G}{\partial t^2}(x_s, x, t) - \nabla \cdot \frac{1}{\rho(x)} \nabla \delta G(x_s, x, t) \right] \\
&\qquad \cdot G(x_r, x, t_r - t) \\
&= \int_{\mathbb{R}^n} dx \int dt \left[\frac{2\delta c(x)}{\rho(x) c^3(x)} \frac{\partial^2 G}{\partial t^2}(x_s, x, t) - \frac{1}{\rho(x)} \left(\nabla \frac{\delta \rho(x)}{\rho(x)} \right) \cdot \nabla G(x_s, x, t) \right] \\
&\qquad \cdot G(x_r, x, t_r - t) \, .
\end{aligned}$$

We have made use of Green's formula, and chosen for the other factor the advanced fundamental solution $G(x_r, x, t_r - t)$ to keep the product of supports bounded.

We claim that the "leading term" in the expression for δG results from substitution of the leading term in the progressing wave expansion for G in the above formula, and then systematically neglecting all expressions except those involving the highest derivatives of $\delta c, \delta \rho$. This claim will be justified later, to some extent. For now we proceed on this basis.

The dimension (i.e. n) now becomes important. Since the case $n = 3$ is slightly simpler than $n = 2$, we begin with it. Then

$$G(x, y, t) \approx a(x, y) \delta(t - \tau(x, y))$$

where a is the transport coefficient constructed in the last section, smooth except at $x = y$. Since x_s, x_r lie in the region $\{z < z_d\}$ and the support Ω of $\delta \rho, \delta c$ lies inside $\{z \geq z_d\}$, the integrand above vanishes near $x = x_s$ and $x = x_r$. Thus we may regard $a(x_s, x)$ and $a(x_r, x)$ as smooth.

Substituting the above expression for G, we get

$$\delta G(x_s, x_r, t_r) = \int_{\mathbb{R}^3} \frac{dx}{\rho(x)} \int dt \; a(x_r, x) \delta(t_r - t - \tau(x_r, x))$$

$$
\begin{aligned}
&\left\{ \frac{2\delta c(x)}{c^3(x)} \frac{\partial^2}{\partial t^2}(a(x_s,x)\delta(t-\tau(x_s,x)) \right. \\
&\left. - \left(\nabla \frac{\delta\rho(x)}{\rho(x)} \right) \cdot \nabla(a(x_s,x)\delta(t-\tau(x_s,x)) \right\} \\
= \;& \frac{\partial^2}{\partial t_r^2} \int \frac{dx}{\rho(x)} \int dt\; a(x_r,x)\delta(t_r-t-\tau(x_r,x))\; a(x_s,x)\delta(t-\tau(x_s,x)) \frac{2\delta c(x)}{c^3(x)} \\
&+ \int \frac{dx}{\rho(dx)} \int dt\; a(x_r,x)\delta(t_r-t-\tau(x_r,x)) \nabla \frac{\delta\rho(x)}{\rho(x)} \\
&\qquad \cdot \left(-\nabla_x a(x_s,x)\delta(t-\tau(x_s,x)) + a(x_s,x)\nabla_x\tau(x_s,x)\delta'(t-\tau(x_s,x)) \right) \\
= \;& \frac{\partial^2}{\partial t_r^2} \int \frac{dx}{\partial(x)} \int dt\; a(x_r,x)\delta(t_r-t-\tau(x_r,x)) a(x_s,x)\delta(t-\tau(x_s,x)) \frac{2\delta c(x)}{c^3(x)} \\
&+ \frac{\partial}{\partial t_r} \int \frac{dx}{\rho(x)} \int dt\; a(x_r,x)\delta(t_r-t-\tau(x_r,x)) a(x_s,x) \nabla \frac{\delta\rho(x)}{\rho(x)} \\
&\qquad \cdot \nabla_x\tau(x_s,x)\delta(t-\tau(x_s,x)) \\
&- \int \frac{dx}{\rho(x)} \int dt\; a(x_r,x)\delta(t_r-t-\tau(x_r,x)) a(x_s,x)\nabla_x a(x_s,x) \\
&\qquad \cdot \nabla \frac{\delta\rho(x)}{\rho(x)} \delta(t-\tau(x_s,x))
\end{aligned}
$$

We would like to carry out the t-integrations. This is possible provided that the hypersurfaces defined by

$$0 = t_r - t - \tau(x_r,x) \quad \text{and} \quad 0 = t - \tau(x_s,x)$$

intersect transversely: i.e., that the normals are not parallel at points of intersection. The correctness of the formula

$$\delta(t_r - \tau(x_s,x) - \tau(x_r,x)) = \int dt\; \delta(t_r - t - \tau(x_r,x))\delta(t-\tau(x_s x))$$

under this transversality condition is an exercise in the definition of compound distributions (see e.g. GEL'FAND and SHILOV, 1958). Transversality is guaranteed so long as

$$(-1, \nabla_x\tau(x_s,x)) \quad \text{is } \textit{not} \text{ parallel to } \; (1, \nabla_x\tau(x_r,x))\,.$$

Since $|\nabla_x\tau(x_s,x)| = |\nabla_x\tau(x_r,x)| = c^{-1}(x)$ (eikonal equation!), transversality is violated only when $\nabla_x\tau(x_s,x) = -\nabla_x\tau(x_r,x)$. We claim that this cannot occur when $x \in \Omega$, under the hypothesis enunciated at the beginning of this section. Indeed, if $\nabla\tau(x_s,x) = -\nabla\tau(x_r,x)$, then the ray from x_r to x, *traversed backwards*, is a continuation of the ray from x_s to x, because both are the x-projections of the solutions of Hamilton's equations with data $(x, \nabla\tau(x_s,x))$. In particular, points x' on this ray *near* x_r are touched by this "turned" ray, obviously, but also by the straight line to x_s, which lies entirely in $\{z \le z_d\}$ as soon as $|x' - x_r|$ is small enough. In this "surface layer," $c \equiv c_0$ is constant — so these lines

are rays, and x' is touched by two distinct rays — in contradiction to our assumption that $x \in \Omega^0(x_r, T)$.

The physical meaning of the violation of the "simple ray geometry" hypothesis just described is that a refracted ray connect the source and receiver points. Thus a segment of the initial wavefront propagates directly (according to geometrical acoustics!) from source to receiver. Such directly propagating waves are much more sensitive to short scale velocity fluctuations than are the primary reflections approximated by the linearized model, and must be treated by other means.

Thus t-integrations as indicated above. We obtain

$$\begin{aligned} Again \delta G(x_s, x_r, t_r) = \frac{\partial^2}{\partial t_r^2} \int \frac{dx}{\rho(x)} a(x_r, x) a(x_s, x) \frac{2\delta c(x)}{c^3(x)} \delta(t_r - \tau(x_r, x) - \tau(x_s, x)) \\ + \frac{\partial}{\partial t_r} \int \frac{dx}{\rho(x)} a(x_r, x) a(x_s, x) \nabla_x \tau(x_s, x) \cdot \nabla \frac{\delta \rho(x)}{\rho(x)} \delta(t_r - \tau(x_r, x) - \tau(x_s, x)) \\ - \int \frac{dx}{\rho(x)} a(x_r, x) \nabla a(x_s, x) \cdot \nabla \frac{\delta \rho(x)}{\rho(x)} \delta(t_r - \tau(x_s, x) - \tau(x_r, x)) \, . \end{aligned}$$

To interpret the t_r-derivatives as x-derivatives acting on δc, $\delta \rho$, we will introduce the vector field

$$N(x_s, x_r, x) = -(\nabla_x \tau(x_s, x) + \nabla \tau(x_r, x))$$

which does not vanish anywhere in Ω, according to previous reasoning. We compute

$$N \cdot \nabla \delta(t_r - \tau_s - \tau_r) = |N|^2 \frac{\partial}{\partial t_r} \, \delta(t_r - \tau_s - \tau_r)$$

where we have written $\tau_s(x) = \tau(x_s, x), \tau_r(x) = \tau(x_r, x)$ for convenience. Accordingly, we can replace each occurrence of $\frac{\partial}{\partial t_r}$ inside the integrals above by $|N|^{-2} N \cdot \nabla$ acting on δ, and then integrate by parts. We write explicitly only those resulting terms in which two spatial derivatives act on $\delta \rho$ or δc, dropping all others into "$\cdots$", including the third summand in the formula above:

$$\begin{aligned} \delta G(x_s, x_r, t_r) \;\; = \;\; & \int \frac{dx}{\rho} a_s a_r \left\{ |N|^{-4} (N \cdot \nabla)^2 \frac{2\delta c}{c^3} - |N|^{-2} (N \cdot \nabla) \nabla \tau_s \cdot \nabla \frac{\delta \rho}{\rho} \right\} \\ & \delta(t_r - \tau_s - \tau_r) \; + \; \cdots \end{aligned}$$

This expression gains significance when interpreted in terms of ray geometry. The ray from x_s to x ("incident") has velocity vector $\nabla \tau_s(x)$, similarly that from x_r to x ("reflected") has velocity vector $\nabla \tau_r(x)$. Thus, using the eikonal equation,

$$\begin{aligned} |N|^2 = |\nabla \tau_s + \nabla \tau_r|^2 \;\; &= \;\; |\nabla \tau_s|^2 + |\nabla \tau_r^2 + 2 \nabla \tau_r \cdot \nabla \tau_s \\ &= \;\; \frac{2}{c^2} (1 + \cos \theta) \end{aligned}$$

where $\theta(x_s, x_r, x)$ is the *opening angle*, i.e. the angle made by the velocity vectors of the incident and reflected rays. In view of the integrand above, it is convenient to introduce

$$b = \frac{1}{1 + \cos \theta} \, .$$

As we have seen, θ stays away from $\pm\pi$ for simple ray geometries, so b is smooth over $X_{sr} \times \Omega$.

Thus

$$\begin{aligned} |N|^{-4}(N\cdot\nabla)^2\,\frac{2\delta c}{c^3} &= \frac{2}{c^2}\cdot\left(\frac{c^2}{2}\right)^2 b^2(N\cdot\nabla)^2\frac{\delta c}{c}+\cdots \\ &= \frac{c^2}{2}\,b^2(N\cdot\nabla)^2\,\frac{\delta c}{c}+\cdots \end{aligned}$$

(Again, here and in the following, "$\cdots$" represent terms involving only lower derivatives of $\delta c, \delta\rho$.) while

$$\begin{aligned} &|N|^{-2}(N\cdot\nabla)\nabla\tau_s\cdot\nabla\frac{\delta\rho}{\rho} = -\frac{c^2}{4}\,b(N\cdot\nabla)(N\cdot\nabla+N_1\cdot\nabla)\frac{\delta\rho}{\rho} \\ &\text{(where } N_1=\nabla\tau_r-\nabla\tau_s) \\ &\quad= -\left(\frac{c^2}{2}b^2(N\cdot\nabla)^2+\frac{c^2}{2}\left(\frac{b}{2}-b^2\right)(N\cdot\nabla)^2+\frac{c^2}{4}\,b(N\cdot\nabla)(N_1\cdot\nabla)\right)\frac{\delta\rho}{\rho} \end{aligned}$$

so

$$\begin{aligned} \delta G(x_s,x_r,t_r) &= \int\frac{dx}{\rho}a_s a_r\frac{c^2}{2}\left[b^2(N\cdot\nabla)^2\left(\frac{\delta c}{c}+\frac{\delta\rho}{\rho}\right)+\left(\frac{b}{2}-b^2\right)(N\cdot\nabla)^2\frac{\delta\rho}{\rho}\right] \\ &\qquad\qquad \delta(t_r-\tau_s-\tau_r) \\ &\quad+\int\frac{dx}{\rho}a_r a_r\frac{c^2}{4}\,b(N\cdot\nabla)(N_1\cdot\nabla)\frac{\delta\rho}{\rho}\,\delta(t-\tau_s-\tau_r) \\ &\quad+\cdots \end{aligned}$$

Now because of the eikonal equation, $N\cdot N_1\equiv 0$. Hence

$$N_1\cdot\nabla\delta(t-\tau_s-\tau_r)\equiv 0$$

and we can integrate by parts in the second term above to see that it is actually a sum of terms of the form we are throwing away — (smooth functions) $\times$ (derivatives of $\delta\rho, \delta c$ of order ≤ 1) $\times(\delta(t_r-\tau_s-\tau_r))$.

The upshot of all this is the expansion

$$\begin{aligned} \delta G(x_s,x_r,t_r) &= \int dx\frac{c^2 a_s a_r}{2\rho}\left[b^2(N\cdot\nabla)^2\left(\frac{\delta c}{c}+\frac{\delta\rho}{\rho}\right)+\left(\frac{b}{2}-b^2\right)(N\cdot\nabla)^2\frac{\delta\rho}{\rho}\right] \\ &\qquad\qquad \delta(t_r-\tau_s-\tau_r) \\ &\quad+\int dx(Q_1\delta c+Q_2\delta\rho)\delta(t-\tau_s-\tau_r) \\ &\quad+\int dx(K_1\delta c+K_2\delta\rho) \end{aligned}$$

where Q_1 and Q_2 are differential operators of order ≤ 1 and K_1 and K_2 are piecewise smooth functions, all depending on (x_s, x_r, x).

A closer examination of the first term is warranted. The expression

$$\frac{\delta c}{c} + \frac{\delta \rho}{\rho} =: \frac{\delta \sigma}{\sigma}\,, \quad \sigma = \rho c$$

is important enough to have a name: σ is the *acoustic impedance*. In the special "zero-offset" case of coincident source and receiver ($x_s = x_r$), about which we will have more to say later, $\tau_s = \tau_r$, so $\theta = 0$, $b = \frac{1}{2}$, and we obtain

$$\delta G(x_s, x_s, t) \cong \int dx\, \frac{c^2 a_s^2}{2\rho} (\nabla \tau_s \cdot \nabla)^2 \frac{\delta \sigma}{\sigma}$$

i.e. the "leading" order" reflected signal depends only on the perturbation in the acoustic impedance. Moreover, in general

$$\frac{b}{2} - b^2 = \frac{b^2}{2}(\cos\theta - 1) = -b^2 \sin^2 \frac{\theta}{2}$$

so we can rewrite the leading term as

$$\delta G(x_s, x_r, t_r) \approx \int dx \frac{c^2 b^2 a_s a_r}{2\rho} (N \cdot \nabla)^2 \left(\frac{\delta \sigma}{\sigma} - \sin^2(\frac{1}{2}\theta) \frac{\delta \rho}{\rho} \right) \delta(t_r - \tau_s - \tau_r)\,.$$

or alternatively

$$\delta G(x_s, x_r, t_r) \approx \frac{\partial^2}{\partial t_r^2} \int dx \frac{2 a_x a_r}{c^2 \rho} \left(\frac{\delta \sigma}{\sigma} - \sin^2 \frac{1}{2}\theta \frac{\delta \rho}{\rho} \right) \delta(t_r - \tau_s - \tau_r)$$

The different angular dependence of the perturbation in G on $\frac{\delta \sigma}{\sigma}$ and $\frac{\delta \rho}{\rho}$ respectively has led to a number of suggested schemes to determine them separately.

The integral above is simply a formal way of writing the family of integrals over the hypersurfaces

$$\{x : t_r = \tau(x_r, x) + \tau(x_s, x)\}$$

which are indexed by t_r, x_r, and x_s. Under our standing "simple geometry" hypothesis, these surfaces are all smooth, and the associated integral transform is a generalization of the Radon transform, hence the name. This observation is due to G. BEYLKIN, 1985; see also BEYLKIN and BURRIDGE, 1990 and BLEISTEIN, 1987.

The 2-dimensional case follows immediately from the observation that

$$G = t_+^{-1/2} * \tilde{G}$$

where $t_+^{-1/2} = t^{-1/2} H(t)$ interpreted as a generalized function, and $\tilde{G} = a\delta(t - \tau)$ just as in 3d. The Green's formula becomes

$$\begin{aligned} &\delta G(x_s, x_r, t) \\ &\quad = \int_{\mathbb{R}^2} dx \int dt\, \delta G(x_s, x_r, t)\, \delta(x_r - x)\, \delta(t_r - t) \end{aligned}$$

$$
\begin{aligned}
&= \int_{\mathbb{R}^2} dx \int dt\, \delta G(x_s, x_r, t) \left[\frac{1}{\rho(x) c^2(x)} \frac{\partial^2 G}{\partial t^2}(x_r, x, t_r - t) - \nabla \cdot \frac{1}{\rho(x)} \nabla G(x_r, x, t_r - t) \right] \\
&= \int_{\mathbb{R}^2} dx \int dt \left(\frac{2\delta c}{\rho c^3} \frac{\partial^2}{\partial t^2} - \frac{1}{\rho} \frac{\nabla \delta \rho}{\rho} \cdot \nabla \right) G(x_s, x, t) \cdot G(x_r, x, t_r - t) \\
&= t_+^{-\frac{1}{2}} * t_+^{-\frac{1}{2}} * \int_{\mathbb{R}^2} dx \int dt \left(\frac{2\delta c}{\rho c^3} \frac{\partial^2}{\partial t^2} - \frac{1}{\rho} \frac{\nabla \delta \rho}{\rho} \cdot \nabla \right) \tilde{G}(x_s, x, t) \tilde{G}(x_r, x, t_r - t) \\
&\approx t_+^{-\frac{1}{2}} * t_+^{-\frac{1}{2}} * \int dx \frac{c^2 b^2 a_s a_r}{2\rho} (N \cdot \nabla)^2 \left(\frac{\delta \sigma}{\sigma} - \sin^2 \left(\frac{1}{2} \theta \right) \frac{\delta \rho}{\rho} \right) \delta(t_r - \tau_s - \tau_r) + \cdots
\end{aligned}
$$

Now $t_+^{-\frac{1}{2}} * t_+^{-\frac{1}{2}}$ is a multiple of the Heaviside function $H(t)$, (GEL'FAND and SHILOV, 1958, p. 116, formula (3′)) so we obtain

$$
\begin{aligned}
&\delta G(x_s, x_r, t) \\
&\quad \approx \Gamma \left(\frac{1}{2} \right)^2 \int dx \frac{c^2 b^2 a_s a_r}{2\rho} (N \cdot \nabla)^2 \left(\frac{\delta \sigma}{\sigma} - \sin^2 \left(\frac{1}{2} \theta \right) \frac{\delta \rho}{\rho} \right) H(t_r - \tau_s - \tau_r) \\
&\quad \approx -\frac{\pi}{2} \int dx \frac{c^2 b^2 a_s a_r}{2\rho} |N|^2 (N \cdot \nabla) \left(\frac{\delta \sigma}{\sigma} - \sin^2 \left(\frac{1}{2} \theta \right) \frac{\delta \rho}{\rho} \right) \delta(t_r - \tau_s - \tau_r) \\
&\quad = -\frac{\pi}{2} \int dx \frac{b a_s a_r}{\rho} (N \cdot \nabla) \left(\frac{\delta \sigma}{\sigma} - \sin^2 \left(\frac{1}{2} \theta \right) \frac{\delta \rho}{\rho} \right) \delta(t_r - \tau_s - \tau_r) \\
&\quad = \frac{\partial}{\partial t_r} \int dx \frac{\pi a_s a_r}{c\rho} \left(\frac{\delta \sigma}{\sigma} - \sin^2 \frac{1}{2} \theta \frac{\delta \rho}{\rho} \right) \delta(t_r - \tau_s - \tau_r)
\end{aligned}
$$

Each step involves integration by parts and throwing away the same sort of terms as before.

The formula just given is as noted before an integration over a family of curves with curve-dependent weight, or a generalized Radon transform. Such formulae have come to be known as *Kirchhoff formulae* in the exploration seismic literature, and I shall refer to the formula just given as the 2D acoustic Kirchhoff simulation approximation.

It is possible to write energy estimate for the error in the approximations just developed, but a numerical example is more instructive. Figure 7(a) displays a muted linearized seismogram for the model of Figure 3, with slightly different boundary conditions than were used in Figures 2 and 4. Numerical evaluation of the Kirchhoff simulation formula (similarly muted) gives the data displayed in Figure 7(b). The difference between the data of Figures 7(a) and (b) is plotted in Figure 7(c). The traveltimes necessary to evaluate the Kirchhoff simulation came from a refine ment of the technique presented in VANTRIER and SYMES, 1991 in which the eikonal equation is solved by an upwind finite difference scheme. A related difference scheme for the transport equation yielded the amplitudes a. Trapezoidal rule integration and piecewise linear interpolation gave a feasible and compatibly accurate evaluation of the integral.

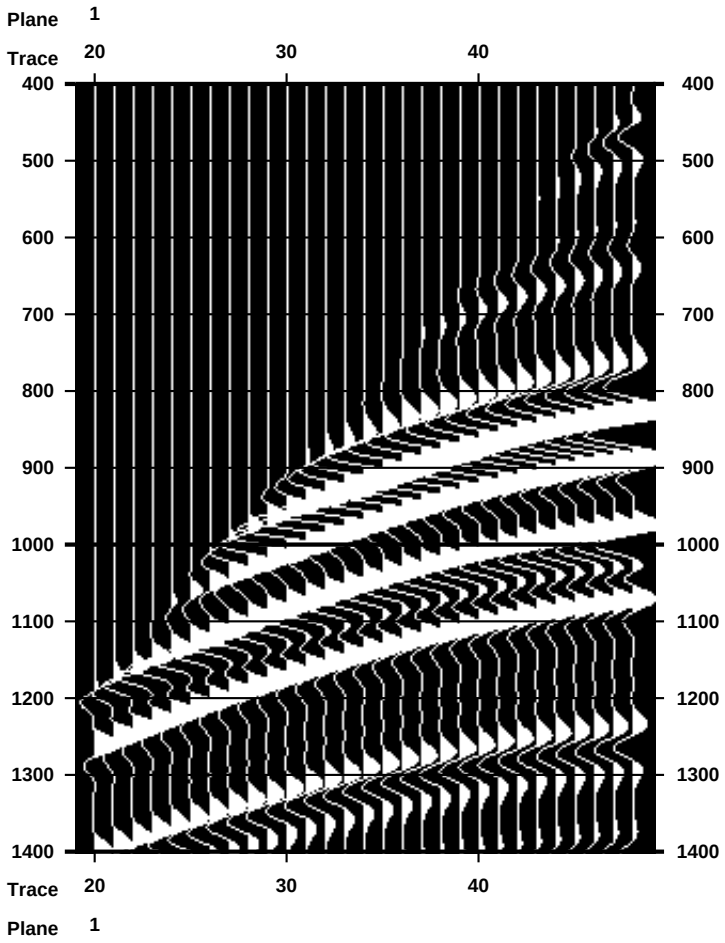

FIGURE 7(A): Finite difference seismogram for the model of Figure 3, using absorbing boundary conditions on all sides of computational domain.

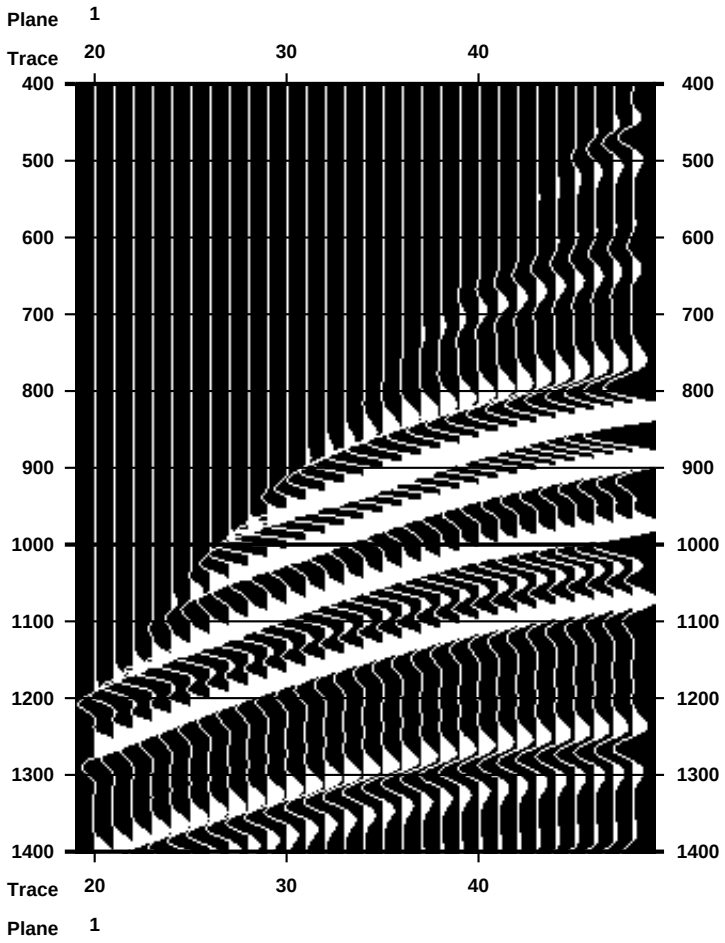

FIGURE 7(B): Kirchhoff seismogram for the model of Figure 3, from numerical evaluation of the generalized Radon transform representation developed in this section.

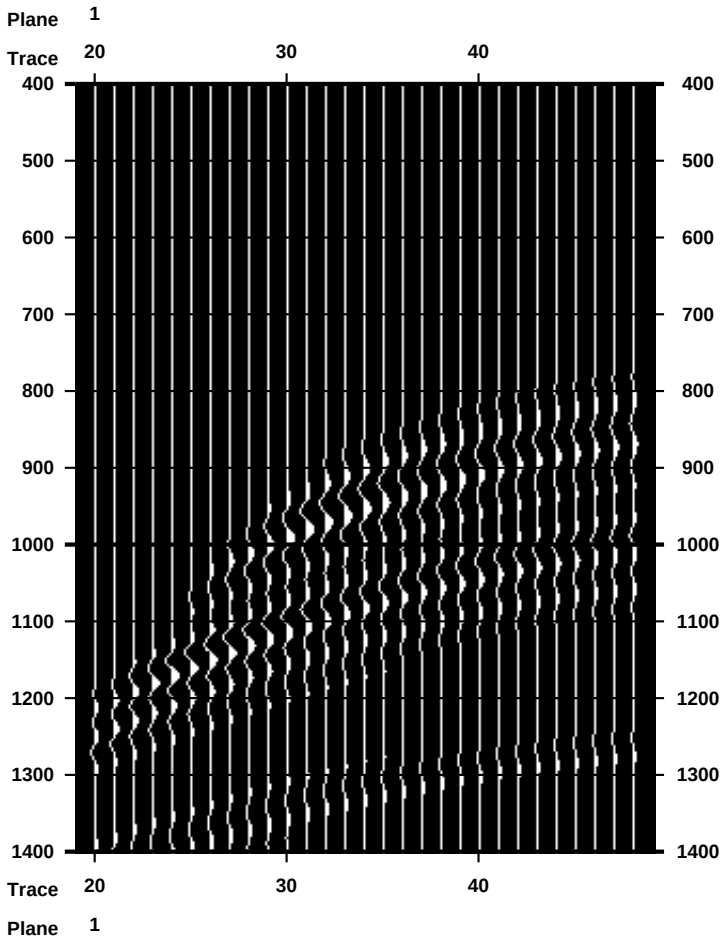

FIGURE 7(C): Difference, Figure 7(b) - Figure 7(a).

Evidently the approximation embodied in the Kirchhoff simulation formula is quite accurate in this case. Such accuracy is typical of problems in which the assumed separation of scales actually occurs. Moreover, these formulae can be evaluated very economically, because the multiplicity of sources and receivers in seismic survey design permits re-use of the components of the integral. The computational cost of a properly designed Kirchhoff simulation or migration is far lower than that of direct approximate solution of the wave equations for the linearized simulation problem by finite difference schemes, for instance. For 3D migration (see section 9), the most computation intesive process commonly employed in exploration seismic data processing, Kirchhoff formulae analogous to the above formula form the basis of most contemporary codes.

7 Kinematics of Reflection

In reflection seismic work, it was established long ago that reflected signals are caused by localized, rapid changes in rock properties. Inspection of direct measurements (well logs) often shows that these reflection zones exhibit oscillatory or abrupt changes in mechanical properties. Similarly, ultrasonic reflections occur at sharp edges (cracks, voids). In all cases, the material parameters in reflecting zones have rather large high-spatial-frequency components.

The approximation to the reflected field derived in the preceding section is quite successful in explaining the relation between oscillatory mechanical parameter perturbations and their corresponding reflected signals, at least up to a point. This relation emerges most clearly from consideration of perturbations of the form

$$\frac{\delta\sigma}{\sigma}(x) = \chi(x)e^{i\xi\cdot x}$$

where χ is a smooth function of bounded support (for simplicity, we assume temporarily that $\delta\rho \equiv 0$). A couple of remarks are in order. Of course we do not really mean to consider complex parameter perturbations — but since the rest of the expression for δG is real, we can take the real part either before or after computing δG! Second, any perturbation $\delta\sigma/\sigma$ in impedance (with support contained in that of χ) can be represented as a sum of such simple oscillatory perturbations. Since δG is linear in $\delta\sigma/\sigma$, it suffices to study their effect on the acoustic field.

Because of the observations mentioned at the beginning of this section, we expect highly oscillatory $\delta\sigma/\sigma$ (i.e. large $|\xi|$) to give rise to highly oscillatory reflected waves. We would like to know *where* these waves arrive at $z = z_r$, say (so we will temporarily imagine that the receivers fill the entire plane $\{z = z_r\}$. Our idea is that a very efficient detector of high-frequency waves arriving near $x_r = (x_r', z_r)$ (x_r' are the tangential coordinates of the receiver point — either one or two) at a time t_r is obtained by integrating δG against an oscillatory function

$$\chi(x_r', t_r) = e^{i(\omega t_r + \xi_r' x_r')} .$$

If δG has a significant component with almost the same phase surfaces and frequency the integral should be substantial; otherwise destructive interference should render the integral

small. More precisely, consider first the approximation

$$\begin{aligned}
&\int\int dx'_r \int dt_r \chi_r(x'_r,t_r)\, e^{i(\omega t_r+\xi'_r x'_r)}\delta G(x_s,x'_r,z_t,t) \\
&\cong \int dx'_r \int dt_r \int dx\ R(x_s,x_r,x)(N(x_s,x_r,x)\cdot\nabla_x)^2\frac{\delta\sigma(x)}{\sigma(x)} \\
&\qquad \times \chi(x'_r,t_r)e^{i(\omega t_r+\xi'_r x'_r)}\delta(t_r-\tau(x_s,x)-\tau(x_r,x))
\end{aligned}$$

from the "leading term" calculation of the previous section: we have written

$$R(x_s,x_r,x) := \frac{c^2(x)\, b^2(x_s,x_r,x)\, a(x_s,x)\, a(x_r,x)}{2\rho(x)}\ .$$

Inserting the oscillatory form for $\frac{\delta\sigma}{\sigma}$ and carrying out the t-integral,

$$\begin{aligned}
\cong \int dx'_r \int dx\ &\chi_r(x'_r,\tau(x_s,x)+\tau(x_r,x))\,\chi(x)\, R(x_s,x_r,x)(N(x_s,x_r,x)\cdot\xi)^2\cdot \\
&e^{i(\omega(\tau(x_s,x)+\tau(x_r,x))+\xi'_r\cdot x'_r+\xi\cdot x)}+\dots
\end{aligned}$$

where we have written out explicitly only the terms of highest order (possibly) in $|\xi|$. Note the identities

$$\begin{aligned}
&\nabla_x\cdot e^{i[\omega(\tau(x_s,x)+\tau(x_r,x))+\xi'_r\cdot x'_r+\xi\cdot x]} \\
&\quad = i(-\omega N(x_s,x_r,x)+\xi)e^{i[\cdots]} \\
&\nabla_{x'_r} e^{i[\omega(\tau(x_s,x)+\tau(x_r,x))+\xi'_r\cdot x'_r+\xi\cdot x]} \\
&\quad = i(\omega\nabla_{x'_r}\tau(x_r,x)+\xi'_r)e^{i[\cdots]}
\end{aligned}$$

so

$$\begin{aligned}
&\left(\tfrac{-i(\xi-\omega N)}{|\xi-\omega N|^2}\cdot\nabla_x+\tfrac{-i(\xi'_r+\omega\nabla_{x'_r}\tau_r)}{|\xi'_r+\omega\nabla_{x'_r}\tau_r|^2}\nabla_{x'_r}\right)\cdot e^{i(\omega(\tau_s+\tau_r)+\xi'_r\cdot x'_r+\xi\cdot x)} \\
&\qquad = 2e^{i(\omega(\tau_s+\tau_r)+\xi'_r\cdot x'_r+\xi\cdot x)}\ .
\end{aligned}$$

We can substitute the above expression for the exponential and integrate by parts any number of times, say K, so long as one of the quantities

$$|\xi-\omega N| \quad\text{and}\quad |\xi'_r+\omega\nabla_{x'_r}\tau_r|$$

is non-vanishing at each point m of integration, i.e. the support of the product $\chi\cdot\tilde\chi_r$ where $\tilde\chi_r(x_s,x_r,x)=\chi_r(x'_r,\tau(x_s,x)+\tau(x_r,x))$. Granted this assumption, the integral is bounded by a multiple of

$$|\xi|^2 \sup_{x'_r\in\operatorname{supp}\chi_r} \max\left(|\xi-\omega N|,\ |\xi'_r+\omega\nabla_{x'_r}\tau_r|\right)^{-K}\ .$$

This expression is homogeneous in (ξ,ξ'_r,ω) of order $2-K$. So, if ξ,ξ'_r and ω are made large in fixed ratio, and if

$$\frac{\xi}{\omega}-N\ ,\quad \frac{\xi'_r}{\omega}+\nabla_{x'_r}\tau_r$$

don't both vanish over the domain of integration, then the leading term decays like an ω^{2-K}. What is more, one can show that all the terms neglected above also decay with increasing ω.

So we have established: for fixed envelope functions χ, χ_r, and tolerance $\epsilon > 0$, a *necessary* condition that a perturbation $\delta\sigma/\sigma = \chi e^{i\xi\cdot x}$ give rise to a fundamental solution perturbation δG which when localized by multiplication with χ_r has significant high Fourier components with frequency ω proportional to $|\xi|$, is that

$$\frac{\xi}{\omega} - N\,, \quad \frac{\xi_r'}{\omega} + \nabla_{x_r'}\tau_r$$

both vanish at some point in the support of $\tilde{\chi}_r\chi$.

The geometric significance of these conditions is profound. The first one states that ξ is parallel to the sum $N = \nabla_x\tau_s + \nabla_x\tau_r$ of the velocity vectors of incident and reflected rays. In view of the equal length of these vectors (eikonal equation!) the sum is also their bisector. Since ξ is the normal to the equal-phase surfaces of $\delta\sigma/\sigma$, these surfaces act like reflecting surfaces, at which incident and reflected rays are related by Snell's law. That this condition hold for $(x_s, x_r, x) \in$ supp $\tilde{\chi}_r\chi$ means that a pair of incident and reflected rays must exist touching $x \in$ supp χ with $t_r = \tau(x_s, x) + \tau(x_r, x)$ for $(x_r, t_r) \in$ supp χ_r.

The second condition states that we will find a high-frequency component in the reflected field at (x', t_r) with wavenumber (ξ_r', ω) if $0 = \xi_r' + \omega\nabla_x \cdot \tau_r$. Given x and x_s, the *moveout (or arrival time) surface* is the graph of

$$x_r' \mapsto \tau(x_s, x) + \tau(x_r, x) \quad (x_r = (x_r', z_r))\,.$$

A typical tangent vector to the moveout surface has the form $(\eta', \eta' \cdot \nabla_{x_r'}, \tau_r)$. The second condition means precisely that (ξ_r', ω) is orthogonal to all such vectors. That is, a *high-frequency component appears in δG only with wavevector normal to the moveout surface.*

Looked at slightly differently, we have constructed a kinematic relation between high-frequency components of the medium perturbation $\delta\sigma/\sigma$ and of the reflected field δG. Given a location/direction pair (x, ξ),

(1) Connect the source x_s with x by a (unique!) ray!

(2) Construct a reflected ray vector at x, i.e, a η_r with $|\eta_r| = c(x)^{-1}$ and $\eta_r + \nabla_x\tau(x_s, x) \| \xi$.

(3) Solve the Hamiltonian equations with initial conditions $(x, -\eta_r)$. If the reflected ray (i.e. x-projection of the solution) so produced crosses $z = z_r$, let x_r be the intersection point. Then $\eta_r = \nabla_x\tau(x_r, x)$, and set $t_r = \tau(x_s, x) + \tau(x_r, x)$.

(4) Set $\omega = \frac{|\xi|}{|\nabla_x\tau(x_s,x)+\nabla\tau(x_r,x)|}$, $\xi_r' = -\omega\nabla_{x_r'}\tau(x_r, x)$.

Set $C(x, \xi) := (x_r', t_r, \xi_r', \omega)$. Then

(i) For $\frac{\delta\sigma(x)}{\sigma(x)} = \chi(x)e^{i\xi\cdot x}$ with ξ sufficiently large, and envelope function χ_r, $\chi_r \delta G\,|_{z=z_r}$ has a large Fourier component with wave vector (ξ_r', ω) only if

$$(x_r' t_r, \xi_r', \omega) = C(x, \xi)$$

for $x \in$ supp χ and $(x_r', t_r) \in$ supp χ_r.

(ii) The map C is not well-defined at all (x, ξ) — the reflected rays may go "off to China," and never pass over the receiver surface $\{z = z_r\}$. This accounts for the intrinsic aperture-limitation of reflection imaging, as we shall see.

(iii) C is a canonical transformation in the sense of classical mechanics. We shall call it the canonical reflection transformation (or "CRT", for short). Moreover, C is homogeneous of degree 1 in ξ, ξ_r', ω.

An even stronger statement than (i) is true:

(i′) For sufficiently large $|\omega|$, $\chi_r \delta G$ has a large Fourier component with wave vector (ξ_r', ω), and $\chi_r(x_r' t_r) \neq 0$ if and only if $\chi \frac{\delta c}{c}$ has a large Fourier component with wave vector ξ so that

$$(x_r', t_r, \xi_r', \omega) = C(x, \xi)\ .$$

Here χ is any envelope function non-zero at x.

This statement follows from the inversion theory of Section 6; essentially, we use the principle of stationary phase to show that our analysis of component decay is sharp.

This stronger statement suggests a positive resolution to the *migration problem*:

> *Given locii of highly oscillatory components in the data, find the locii of highly oscillatory components of the acoustic coefficients.*

Highly oscillatory components in the acoustic coefficients are the result of rapid changes in material type, which typically occur at structural boundaries. So the information to be got *via* solution of the migration problem is the *identification of structural units.*

8 Normal Operator

In order to make the preceding section more precise, and to develop the inversion theory of the subsequent sections, it is necessary to study the so-called *normal operator*. This study requires a more precise definition of the linearized seismogram. Many of our subsequent developments will assume *densely sampled* surface data, so we will idealize the receiver set for each source position as a continuum. We choose a window function $m(x_s, x_r', t_r)$ which for each x_s is $\equiv 1$ over most of the receiver (space-time) domain, going to zero smoothly

at the boundaries (i.e. a "tapered receiver window"). We define the impulsive linearized forward map L_δ as

$$L_\delta[\rho, c]\left[\frac{\delta\sigma}{\sigma}, \frac{\delta\rho}{\rho}\right](x_s, x_r', t_r) = m(x_s, x_r', t_r)\delta G(x_s, x_r, t_r) \ .$$

Then the linearized map for an isotropic point source with time function $f(t)$ is simply

$$f * L_\delta[\rho, c]\left[\frac{\delta\sigma}{\sigma}, \frac{\delta\rho}{\rho}\right]$$

whereas L_δ has the approximation (in 3-d):

$$\begin{aligned} & L_\delta[\rho, c]\left[\frac{\delta\sigma}{\sigma}, \frac{\delta\rho}{\rho}\right](x_s, x_r, t_r) \approx L_\delta^a[\rho, c]\left[\frac{\delta\sigma}{\sigma}, \frac{\delta\rho}{\rho}\right](x_s, x_r, t_r) \\ = & \int dx\, m(x_s, x_r', t_r) R(x_s, x_r, x)[N(x_s, x_r, x)\cdot\nabla_x]^2 \\ & \left(\frac{\delta\sigma}{\sigma}(x) - \sin^2\left(\frac{1}{2}\theta(x_s, x_r, x)\right)\frac{\delta\rho}{\rho}(x)\right)\delta(t_r - \tau(x_s, x) - \tau(x_r, x)) \ . \end{aligned}$$

Remark. One of the byproducts of our analysis of the normal operator will be precise statements about the sense of the above approximation.

We introduce the formal adjoint L_δ^* of L_δ, defined by

$$\begin{aligned} & \int dx_r' \int dt_r \left(L_\delta[\rho, c]\left[\frac{\delta\sigma}{\sigma}, \frac{\delta\rho}{\rho}\right](x_s, x_r, t_r)\right) u(x_r', t_r) \\ = & \int dx \left(\frac{\delta\sigma}{\sigma}(x), \frac{\delta\rho}{\rho}(x)\right)(L_\delta^*[\rho, c]u(x_s, x))^T \ . \end{aligned}$$

The object of this section is to describe precisely the normal operator $L_\delta^* L_\delta$. Presumably $L_\delta^{a*} \approx L_\delta^*$ in the same sense that $L_\delta^a \approx L_\delta$. L_δ^a can be written as a sum of operators of the form

$$w = \frac{\delta\rho}{\rho} \quad \text{or} \quad \frac{\delta\sigma}{\sigma} \mapsto AP(D)w$$

where $P(D)$ is a constant-coefficient differential operator and

$$Aw(x_r', t_r) = \int dx\, \alpha(x, x_r', t_r)\delta(t_r - \tau(x_s, x_r) - \tau(x_r, x))w(x)$$

so L_δ^{a*} can be written as a sum of operators of the form

$$P(D)A^*$$

whence $L_\delta^{a*} L_\delta^a$ is a sum of operators of the form $P_1(D)A_1^* AP(D)$. The key is therefore to understand the structure of operators of the form $A_1^* A$. Note that if

$$A_1 w(x_r', t_r) = \int dx\, \alpha_1(y, x_r', t_r)\delta(t_r - \phi(x_r, y))w(y)$$

then

$$\begin{aligned} A_1^* w(x) &= \int dt_r \int dx'_r \int dt\ \alpha_1(x_1 x'_r, t_r)\, \delta(t_r - \phi(x_r, x)) u(x'_r, t_r) \\ &= \int dx'_r\ \alpha_1(x, x'_r, \phi(x_r, x)) u(x'_r, \phi(x_r, x))\ . \end{aligned}$$

Here we have written $\phi(x_r, x) = \tau(x_s, x) + \tau(x_r, x)$ and temporarily suppressed x_s from the notation. Thus

$$A_1^* A w(x) = \int dx'_r \int dy\ \alpha_1(x, x'_r, \phi(x_r, y))\ \alpha(y, x'_r, \phi(x_r, y))\ \delta(\phi(x_r, y) - \phi(x_r, x)) w(y)\ .$$

We can divide the domain of y-integration into subdomains on which the equation $\phi(x_r, y) = t$ has a solution for one or another of the y-coordinates. We will only treat the case in which this equation can be solved for the last coordinate y_n; the other cases go in exactly the same way, and the end result is independent of the choice.

Thus we will assume that over the domain of y-integration, there exists a unique solution $Y_n(x, x'_r, y')$ to the equation

$$\phi(x_r, y', Y_n) = \phi(x_r, x)$$

and also that for $y_n = Y_n$,

$$\frac{\partial \phi}{\partial y_n}(x_r, y) \neq 0$$

(here $y' = (y'_1, \ldots y_{n-1})$, as usual). Then

$$A_1^* A w(x) = \int dx'_r \int dy' \beta(x, x'_r, y')\ w(y', Y_n(x, x'_r, y'))$$

with

$$\begin{aligned} \beta(x, x'_r, y') = & \\ & \alpha_1(x, x'_r \phi(x'_r, y', Y_n(x, x'_r, y')))\ \alpha(y', Y_n(x, x'_r, y'), \\ & x'_r, \phi(x'_r, y', Y_n(x, x'_r, y'))) \left(\frac{\partial \phi}{\partial y_n}(x'_r, y', Y_n(x, x'_r, y')) \right)^{-1}\ . \end{aligned}$$

The support of the coefficients α etc. appearing in the operators A is necessarily bounded, because of the introduction of the window function m and because of our standing assumption that the perturbations $\delta\sigma/\sigma$, etc. are of fixed, bounded support. Therefore we can introduce the definition of the Fourier transform of w and interchange orders of integration to get

$$= \frac{1}{(2\pi)^n} \int d\xi\ \hat{w}(\xi) \int dx'_r \int dy' \beta(x, x'_r, y') e^{i(\xi' \cdot y' + \xi_n Y_n(x, x'_r, y')}\ .$$

We re-write the inner integral using polar coordinates $\xi = \omega \hat{\xi}$, and evaluate it using the stationary phase principle viewing ω as large parameter. This procedure will justify itself shortly. The phase of the integrand is

$$\hat{\xi}' \cdot y' + \hat{\xi}_n \cdot Y_n(x, x'_r, y')$$

so the stationary phase conditions are

$$\begin{aligned} \hat{\xi}' + \hat{\xi}_n \frac{\partial Y_n}{\partial y'} &= 0 \\ \hat{\xi}_n \frac{\partial Y_n}{\partial x'_r} &= 0 \ . \end{aligned}$$

Throughout the following, these are to be regarded as determining y' and x'_r. From the first condition $\hat{\xi}_n \neq 0$, else $\hat{\xi}$ could not be a unit vector. So the factor of $\hat{\xi}_n$ can be dropped from the second condition.

Understanding the first condition requires computation of $\partial Y_n / \partial y'$. From its definition

$$\begin{aligned} 0 &= \frac{\partial}{\partial y'} \left[\phi(x_r, x) - \phi(x_r, y', Y_n(x, x'_r, y')) \right] \\ &= \left(\frac{\partial \phi}{\partial y'} + \frac{\partial \phi}{\partial y_n} \frac{\partial Y_n}{\partial y'} \right) (x, x_r, y', Y_n(x, x'_r, y')) \ . \end{aligned}$$

So $\partial Y / \partial y' = -(\partial \phi / \partial y')(\partial \phi / \partial y_n)^{-1}$. Thus the first condition is equivalent to

$$\frac{\partial \phi}{\partial y_n}(x_r, y', Y_n(x, x'_r, y'))\hat{\xi}' = \hat{\xi}_n \frac{\partial \phi}{\partial y'}(x_r, y', Y_n(x, x'_r, y')) \ .$$

That is

$$\boxed{\hat{\xi} \| \nabla_y \phi(x_r, y) \mid_{y_n = Y_n(x, x'_r, y')}}$$

(This condition should be familiar from the last section.)

To understand the second condition, compute the x'_r derivative of Y_n in the obvious way, to get

$$\left(\frac{\partial \phi}{\partial y_n} \frac{\partial Y_n}{\partial x'_r} + \frac{\partial \phi}{\partial x'_r} \right) (x_r, y', Y_n) = \frac{\partial \phi}{\partial x_r}(x_r, x)$$

so the second condition implies that

$$\frac{\partial \phi}{\partial x'_r}(x'_r, y', Y_n(x, x'_r, y')) = \frac{\partial \phi}{\partial x_r}(x_r, x) \ .$$

Recalling the definition of ϕ, this means

$$\frac{\partial \tau}{\partial x'_r}(x_r, y', Y_n(x, x'_r, y')) = \frac{\partial \tau}{\partial x'_r}(x'_r, x) \ .$$

To see the meaning of this condition: recall that $\nabla \tau(x, y)$ is the velocity vector of a ray at x, which also passes over y in the past (or vice-versa). Thus the above condition means: The rays passing over x_r, emanating from (y', Y_n) and x respectively, have tangent vectors

at x_r identical in their first $n-1$ components. Because of the eikonal equation, the n^{th} components are the same up to sign. Because the velocity field is constant for $x_n < 0$, so that the rays there are straight lines, the n^{th} components must be negative, since otherwise the ray segment preceding x_r would have to lie entirely in $x_n < 0$, and could not pass over (y', Y_n) or x. Therefore the tangent vectors at x_r are identical, so — from Hamilton's equations and the basic theorem on systems of ordinary differential equations — the rays are identical. That is (y', Y_n) and x lie on the same ray through x_r. On the other hand, from the definition of Y_n,

$$\phi(x_r, y', Y_n(x, x_r', y')) = \phi(x_r, x)$$

i.e.

$$\tau(x_s, y', Y_n(x, x_r', y')) + \tau(x_r, y', Y_n(x, x_r', y')) = \tau(x_s, x) + \tau(x_r, x) \ .$$

We claim that this imples $(y', Y_n) = x$. Otherwise, let $\sigma \mapsto x(\sigma)$ C^1 parameterize the segment between (y', Y_n) and x of the ray emanating from x and passing over x_r, so that $X(0) = x$ and $X(1) = (y', Y_n)$. Then

$$\phi(x_r, X(0)) = \phi(x_r, X(1))$$

so from elementary calculus there exists $\sigma_o \in [0,1]$ at which

$$0 = \frac{d}{d\sigma}\phi(x_r, X(\sigma))\bigg|_{\sigma=\sigma_0} = [\nabla\tau(x_s, X(\sigma_0)) + \nabla\tau(x_r, X(\sigma_0))] \cdot \dot{X}(\sigma_0) \ .$$

There must exist $f(\sigma)$ so that

$$\dot{X}(\sigma) = f(\sigma)\nabla\tau(x_r, X(\sigma))$$

and since τ is monotone along rays, $f \not\equiv 0$. Thus at $\sigma = \sigma_0$

$$0 = \nabla\tau(x_s, X(\sigma_0)) \cdot \nabla\tau(x_r, X(\sigma_0)) + \frac{1}{c^2(X(\sigma_0)} \ .$$

From the eikonal equation,

$$\nabla\tau(x_s, X(\sigma_0)) = -\nabla\tau(x_r, X(\sigma_0))$$

which contradicts the "simple geometry" hypothesis of Section 2.

So we conclude that the meaning of the second stationary phase condition is:

$$\boxed{(y', Y_n(x, x_r', y')) = x}$$

In particular there is only one stationary point. In order to employ the stationary phase formula, we must also compute the determinant of the phase Hessian. Write

$$\Phi(x, x_r', y', \theta) = \hat{\xi}' y' + \hat{\xi}_n Y_n(x, x_r', y') \ .$$

Then the Hessian (with respect to x'_r, y') has a natural block structure:

$$\begin{aligned} \text{Hess} &= \begin{pmatrix} \frac{\partial^2\Phi}{\partial x_r'^2} & \frac{\partial^2\Phi}{\partial x'_r \partial y'} \\ \frac{\partial^2\Phi}{\partial x'_r \partial y'} & \frac{\partial^2\Phi}{\partial y'^2} \end{pmatrix} \\ &= \begin{pmatrix} \hat{\xi}_n \frac{\partial^2 Y_n}{\partial x_r'^2} & \hat{\xi}_n \frac{\partial^2 Y_n}{\partial x'_r \partial y'} \\ \hat{\xi}_n \frac{\partial Y_n}{\partial x'_r \partial y'} & \hat{\xi}_n \frac{\partial^2 Y_n}{\partial y'^2} \end{pmatrix} \end{aligned}$$

so we continue differentiating:

$$\begin{aligned} &\left[\frac{\partial\phi}{\partial y_n} \frac{\partial^2 Y_n}{\partial x_r'^2} + \frac{\partial^2\phi}{\partial y_n^2} \left(\frac{\partial Y_n}{\partial x'_r} \right)^2 + 2 \frac{\partial^2\phi}{\partial y_n \partial x'_r} \frac{\partial Y_n^T}{\partial x'_r} + \frac{\partial^2\phi}{\partial x_r'^2} \right] (x_r, y', Y_n) \\ &= \frac{\partial^2\phi}{\partial x_r'^2}(x_r, x) \\ &\quad \left[\frac{\partial\phi}{\partial y_n} \frac{\partial^2 Y_n}{\partial x'_r \partial y'} + \frac{\partial^2\phi}{\partial y_n^2} \frac{\partial Y_n}{\partial x'_r} \frac{\partial Y_n^T}{\partial y'} + \frac{\partial^2\phi}{\partial y_n \partial x'_r} \frac{\partial Y_n^T}{\partial y'} + \frac{\partial^2\phi}{\partial x'_r \partial y'} \right] (x_r, y', Y_n) \\ &= 0 \, . \end{aligned}$$

Now we employ the stationary phase conditions since (for the form of the stationary phase formula to be used below) the Hessian need only be evaluated at the stationary points. Since $\partial Y_n / \partial x'_r \equiv 0$ and $(y', Y_n) = x$ (both versions of the second condition), the first equation in the above group implies that $\partial^2 Y_n / \partial (x'_r)^2 \equiv 0$. Thus

$$\det \text{Hess } \Phi = \det \left[\hat{\xi}_n \frac{\partial^2 Y_n}{\partial x'_r \partial y'} \right]^2 \, .$$

From the first condition, $\hat{\xi}_n = (\partial\phi/\partial y_n)(|\nabla\phi|)^{-1}$ so our determinant is

$$\begin{aligned} &|\nabla\phi|^{-2(n-1)} \det \left| \frac{\partial\phi}{\partial y_n} \frac{\partial^2 Y_n}{\partial x'_r \partial y'} \right|^2 \\ &= |\nabla\phi|^{-2(n-1)} \det \left| \frac{\partial\phi}{\partial y_n \partial x'_r} \frac{\partial\phi Y_n^T}{\partial y'} + \frac{\partial^2\phi}{\partial y' \partial x'_r} \right|^2 \\ &= |\nabla\phi|^{-2(n-1)} \det \left| -\frac{\partial\phi}{\partial y_n \partial x'_r} \frac{\partial\phi^T}{\partial y'} \left(\frac{\partial\phi}{\partial y_n} \right)^{-1} + \frac{\partial^2\phi}{\partial y' \partial x'_r} \right|^2 \, . \end{aligned}$$

Now use the determinant identity

$$\det(A - vw^T) = \det \left(\begin{array}{c|c} A & v \\ \hline w^T & 1 \end{array} \right)$$

with

$$v \sim \left(\frac{\partial\phi}{\partial x_n} \right)^{-1} \frac{\partial\phi}{\partial x'_r \partial y_n} \, , \quad w \sim \frac{\partial\phi}{\partial y'} \, , \quad A \sim \frac{\partial^2\phi}{\partial x'_r \partial y'}$$

to write the above as

$$\begin{aligned} &= |\nabla\phi|^{-2(n-1)} \det \left(\begin{array}{c|c} \frac{\partial\phi}{\partial x'_r \partial y'} & \frac{\partial\phi}{\partial x'_r \partial y_n}\left(\frac{\partial\phi}{\partial y_n}\right)^{-1} \\ \hline \frac{\partial\phi^T}{\partial y'} & 1 \end{array} \right)^2 \\ &= |\nabla\phi|^{-2(n-1)} \left(\frac{\partial\phi}{\partial x_n}\right)^{-2} \det \left(\begin{array}{c} \frac{\partial}{\partial x'_r}\nabla_y\phi \\ \nabla_y\phi \end{array} \right)^2 \end{aligned}$$

which is the form we want for the Hessian determinant.

Next, employment of stationary phase demands that we verify the nonvanishing of Hessian determinant. The condition that this determinant vanish is that $\gamma' \in \mathbb{R}^{n-1}$, $\gamma_n \in \mathbb{R}$ (not all zero) exist so that

$$\begin{aligned} &\sum_{j=1}^{n-1} \gamma'_j \frac{\partial}{\partial x'_{r,j}} \nabla_x \phi(x_s, x_r, x) + \gamma_n \nabla\phi(x_s, x_r, x) = 0 \\ &= \sum_{j=1}^{n-1} \gamma'_j \frac{\partial}{\partial x'_{r,j}} \nabla_x \tau(x_r, x) + \gamma_n (\nabla_x \tau(x_s, x) + \nabla_x \tau(x_r, x)) = 0 \ . \end{aligned}$$

Take the dot product of both sides with $\nabla_x \tau(x_r, x)$ to get

$$\begin{aligned} &\nabla_x \tau(x_r, x)^T \left(\sum_{j=1}^{n-1} \gamma'_j \frac{\partial}{\partial x'_{r,j}} \nabla_x \tau(x_r, x) + \gamma_n (\nabla_x \tau(x_s, x) + \nabla_x \tau(x_r, x)) \right) \\ &= \frac{1}{2} \left(\sum_{j=1}^{n-1} \gamma'_j \frac{\partial}{\partial x'_{r,j}} \right) \cdot |\nabla_x \tau(x_r, x)|^2 + \gamma_n (\nabla_x \tau(x_s, x) \cdot \nabla_x \tau(x_r, x) \\ &\qquad + |\nabla_x \tau(x_r, x)|^2) \\ &= \gamma_n (1 + \cos\theta(x_s, x_r, x)) \end{aligned}$$

since $|\nabla_x \tau(x_r, x)|^2 = c^{-2}(x)$ is independent of x_r. As we have seen, the "simple geometry" hypothesis implies $\cos\theta > -1$, so $\gamma_n = 0$ necessarily.

The remaining condition is the infinitesimal violation of the "simple geometry" assumption, as explained in Section 2. Thus we conclude that $\gamma' = 0$, i.e. that the determinant is indeed nonsingular.

It is finally required to determine the *signature* sgn Hess Φ, that is, the number of positive eigenvalues, less the number of negative. In fact, it follows from the block structure

$$\text{Hess } \Phi \sim \left(\begin{array}{c|c} 0 & B \\ \hline B^T & C \end{array} \right)$$

of the Hessian at the stationary point that there are exactly the same number of positive as negative eigenvalues.

This fact follows easily from the nonsingularity of B. Let $B^T B = UDU^T$ with D positive diagonal, U orthogonal. Since B is nonsingular, $D \neq 0$. Choose a C^0 family of $2(n-1) \times 2(n-1)$ nonsingular matrices $\Gamma(t)$ for which $\Gamma(0) = I$,

$$\Gamma(1) = \left(\begin{array}{cc} U & 0 \\ 0 & UD^{-\frac{1}{2}} \end{array} \right) \ .$$

Now $\det \Gamma(1) = (\det U)^2 \det D^{-1} > 0$, and the nonsingular matrices of positive determinant form an arcwise connected family, so this is possible. Now the determinant of $\Gamma(\sigma)^T \text{Hess } \Phi \Gamma(\sigma)$ is clearly positive for $0 \leq \sigma \leq 1$. Therefore none of the eigenvalues of $\Gamma(\sigma)^T \text{Hess } \Phi \Gamma(\sigma)$ change sign, and so Hess Φ has the same signature as

$$\begin{aligned} \Gamma(1)^T \text{Hess } \Phi \Gamma(1) &= \left(\begin{array}{c|c} 0 & U^T B U D^{-\frac{1}{2}} \\ \hline D^{-\frac{1}{2}} U^T B^T U & D^{-\frac{1}{2}} U^T C U D^{-\frac{1}{2}} \end{array} \right) \\ &=: \left(\begin{array}{c|c} 0 & B_1 \\ \hline B_1^T & C_1 \end{array} \right) = \Phi_1 \ . \end{aligned}$$

Now C_1 is symmetric, so has real spectrum $\mu_1, \ldots, u_{n-1}$, with orthonormal family of eigenvectors $v_1, \ldots, v_{n-1}$. On the other hand $w = (w_1, w_2)^T$ is an eigenvector of Φ with eigenvalue λ if and only if

$$\begin{aligned} B_1 w_2 &= \lambda w_1 \\ B_1^T C w_1 &= \lambda w_2 \ . \end{aligned}$$

Assuming momentarily that $\lambda \neq 0$, we get for w_2

$$\left(\frac{1}{2} B_1^T B_1 + C \right) w_2 = \lambda w_2 \ .$$

But $B_1^T B_1 = D^{-\frac{1}{2}} U^T B^T U U^T B U D^{-\frac{1}{2}} = I$, so the above reads

$$C w_2 = (\lambda - \frac{1}{\lambda}) w_2 \ .$$

Now the solutions $\lambda_i^{\pm}$ of

$$\lambda_i^{\pm} - \frac{1}{\lambda_i^{\pm}} = \mu_i \ , \quad i = 1, \ldots, n-1$$

are

$$\lambda_i^{\pm} = \frac{1}{2} \left(\mu_1 \pm \sqrt{\mu_i^2 + 1} \right)$$

which are (a) never zero, and (b) of opposite signs: $\lambda_i^+ > 0$, $\lambda_i^- < 0$, regardless of the sign of μ_i. Build corresponding eigenvectors according to

$$w_i^{\pm} = \left(\begin{array}{c} \lambda_i^{\frac{1}{\pm}} B_1 v_i \\ v_i \end{array} \right) \ .$$

Then $\{w_i^{\pm}\}$ are an orthogonal family of eigenvectors with eigenvalues $\{\lambda_i^{\pm}\}$. Since there are $2(n-1)$ of them, they represent the spectral decomposition of Φ_1. Thus Φ_1, hence Hess Φ, has signature zero.

We now have all of the information required to employ the stationary phase principle, which we state here in sufficiently general form:

Suppose that ψ and g are smooth on $\mathbb{R}^n$, with g having bounded support. Suppose moreover that

$$\begin{aligned} z \in \text{supp } g\,, \quad \nabla\psi(z) &= 0 \\ \Rightarrow \qquad \det \text{Hess } \psi(z) &\neq 0 \end{aligned}$$

and suppose moreover that

$$\Lambda = \{z \in \text{supp } g: \quad \nabla\psi(z) = 0\} \quad \textit{is finite.}$$

Then

$$\begin{aligned} &\int_{\mathbb{R}^m} dx\; g(x) e^{i\omega\psi(x)} \\ &\sum_{x^* \in \Lambda} \left(\frac{2\pi}{\omega}\right)^{\frac{m}{2}} e^{\frac{\pi i}{4}\text{sgn Hess } \psi(x^*)} |\det \text{Hess } \psi(x^*)|^{-\frac{1}{2}} g(x^*) e^{i\omega\psi(x^*)} \\ &\qquad + R(\omega) \end{aligned}$$

where for some K depending on g and ψ,

$$|R(\omega)| \leq K|\omega|^{-\frac{m}{2}-1}\,.$$

More is true: one can actually develop an asymptotic series

$$\int_{\mathbb{R}^m} dx\; g(x) e^{i\omega\psi(x)} \sim |\omega|^{-\frac{m}{2}} \left(\sum_{j=0}^{\infty} g_j \omega^{-j}\right)$$

where the g_j are explicitly determined in terms of derivatives of g, ψ and associated quantities. We shall make explicit use only of the first term g_0, given above.

Collecting the facts proved above, we evaluate

$$\begin{aligned} &\int dx_r' \int dy' \beta(x, x_r', y') e^{i\omega(\hat{\xi}'\cdot y' + \hat{\xi}_n Y_n(x, x_r', y'))} \\ &= \left(\frac{2\pi}{|\omega|}\right)^{n-1} |\nabla\phi(x_s, x_r, x)|^{n-1} \left|\frac{\partial\phi}{\partial x_n}(x_s, x_r, x)\right| \left|\det \begin{pmatrix} \frac{\partial}{\partial x_r'}\nabla\phi(x_s, x_r, x) \\ \nabla\phi(x_s, x_r, x) \end{pmatrix}\right| |\cdots|^{n-1} \\ &\qquad \times \beta(x, x_r', x') e^{i\omega\hat{\xi}\cdot x} + O(|\omega|^{n-2})\,. \end{aligned}$$

In this and succeeding formulas, $x_r = x_r(x_s, x, \hat{\xi})$ as determined by the stationarity conditions. The formula for β simplfies considerably because, at the stationary point $(y', Y_n) = x'$, we obtain

$$\beta(x, x_r', x') = \alpha_1(x, x_r', \phi(x_r, x))\alpha(x, x_r', \phi(x_r, x)) \left(\frac{\partial\phi}{\partial y_n}(x_r', x)\right)^{-1}\,.$$

By more reasoning of the sort of which the reader has become tired, it is possible to show that $\frac{\partial\phi}{\partial x_n}$ remains positive. Thus the integral is

$$p_0(x_s, x, \xi) e^{i\xi\cdot x} + O(|\xi|^{-n-2})$$

where

$$p_0(x_s,x,\xi) = \left(\frac{2\pi}{|\xi|}\right)^{n-1} |\nabla\phi(x_s,x_r,x)|^{n-1} \left|\det\begin{pmatrix} \frac{\partial}{\partial x_r'}\nabla\phi(x_s,x_r,x) \\ \nabla\phi(x_s,x_r,x)\end{pmatrix}\right|^{-1} \times\alpha_1(x,x_r',\phi(x,x_r')\alpha(x,x_r',\phi(x,x_r'))$$

(where as before x_r is regarded as a function of x_s, x, and $\frac{\xi}{|\xi|}$).

The full-blown stationary phase series yields

$$\cong \left(\sum_{j=0}^{\infty} p_j(x,\xi)\right) e^{i\xi,x}$$

where p_0 is given above, and p_j is homogeneous in ξ of degree $n-1-j$.

Note that p_0 indeed shows no traces of our special use of y_n, as promised; it turns out that all of the other terms are similarly "coordinate-free."

Inserting this result in the expression for A_1^*A, we obtain formally

$$A_1^*Aw(x) = \frac{1}{(2\pi)^n}\int d\xi \left(\sum_{j=0}^{\infty} p_j(x,\xi)\right) e^{i\xi\cdot x}\hat{w}(\xi)\ .$$

It is possible to make good sense out of this expression: it defines a so-called *pseudodifferential operator*. A development of the theory of pseudodifferential operators can be found in TAYLOR, 1981, for example. The essential points are these:

(1) Given a series like the above, $\sum p_j(x,\xi)$ with p_j smoothness in $\{x,\xi : |\xi| > 0\}$ and homogeneous in ξ of degree $s-j$, one can find a (nonunique) smooth function $p(x,\xi)$ for which

$$p(x,\xi) - \sum_{j=0}^{N-1} p_j(x,\xi) = O(|\xi|^{s-N}) \qquad N = 1,2,\dots\ .$$

p_0 is called the principal part of p. p should satisfy some inequalities involving derivatives — essentially, differentiating in ξ should lower the order in ξ, and differentiating in x should not raise it. (These properties follow easily for the A_1^*A construction above.) Such a function is called a *symbol*. The summand $p_0(x,\xi)$ of highest order (s) is called the principal symbol, or principal part of p.

(2) Given such p, the oscillatory integral

$$u \mapsto \frac{1}{(2\pi)^n}\int d\xi\ p(x,\xi)e^{ix\xi}\hat{u}(\xi) =: p(x,D)u(x)$$

defines a map from smooth functions of bounded support to smooth functions (and between many other function classes as well). Such an operator is called *pseudodifferential*. (It is conventional to denote the operator associated with the symbol by replacing the Fourier vector ξ with the derivative vector $D = -\sqrt{-1}\nabla$. The reason will become obvious in (5) below.)

(3) Two symbols with the same asymptotic development define operators differing by a smoothing operator — i.e. an integral operator with an infinitely smooth kernel. Smoothing operators yield small results when applied to oscillatory functions, so the *entire importance of pseudodifferential operators for the theory of wave imaging lies in their ability to describe approximately the behaviour of high-frequency signals.* To a limited extent it is possible to make estimates concerning this approximation; some examples appear below.

(4) With minor further restriction on support, the class of pseudodifferential operators is closed under composition. Moreover, if p and q are symbols with principal parts p_0 and q_0, then

$$p(x,D)q(x,D) = r(x,D)$$

and the principal part of $r(x,\xi)$ is $p_0(x,\xi)q_0(x,\xi)$ — so far as principal parts go, one composes pseudodifferential operators simply by multiplying their symbols! This and some related facts give a *calculus* of pseudodifferential operators.

(5) Differential operators with smoothly varying coefficients are naturally pseudodifferential operators. Indeed

$$\sum_{|\alpha|\le m} a_\alpha(x) D^\alpha u(x) = \frac{1}{(2\pi)^n} \int d\xi \left(\sum_{|\alpha|\le m} a_\alpha(x)(i\xi)^\alpha \right) e^{i\xi x} \hat{u}(\xi) \ .$$

Thus differential operators have finite asymptotic expansions, all terms of which have positive integral degree.

We can combine the remarks to finish the job of this chapter, namely the representation of the normal operator. Examining the representation of L^a_δ given at the beginning, we recognise that

$$\begin{aligned} & L^a_\delta[\rho,c] \left[\frac{\delta\sigma}{\sigma}, \frac{\delta\rho}{\rho} \right] (x_s, x_r, t_r) \\ = & \int dx \ m(x_s, x'_r, t_r) \ R(x_s, x_r, x) \sum_{i,j=1}^{n} N_i(x_s, x_r, x) \ N_j(x_s, x_r, x) \\ & \left\{ \frac{\partial^2}{\partial x_i \partial x_j} \left(\frac{\delta\sigma}{\sigma}(x) \right) - \sin^2\left(\frac{1}{2}\theta(x_s, x_r, x)\right) \frac{\partial^2}{\partial x_i \partial x_j} \frac{\delta\rho}{\rho}(x) \right\} \\ & \delta(t_r - \tau(x_s, x) - \tau(x_r, x)) + \cdots \end{aligned}$$

where the "$\cdots$" represents terms involving lower derivatives of $\frac{\delta\sigma}{\sigma}$ and $\frac{\delta\rho}{\rho}$. These will not figure in the computation of the principal symbol, and in any case have the same importance as contributions already neglected in the approximation $L_\delta \sim L^a_\delta$. Then:

Remarks (4) and (5) above combine to yield our principal result:

$$\Lambda := L^*_\delta[\rho,c] L_\delta[\rho,c] = \begin{bmatrix} \Lambda_{\sigma\sigma} & \Lambda_{\sigma\rho} \\ \Lambda_{\rho\sigma} & \Lambda_{\rho\rho} \end{bmatrix}$$

is a two-by-two matrix of pseudodifferential operators of order 2.

The principal symbols of $\Lambda_{\sigma\sigma}$, etc. are products of the *geometrical factor*

$$g(x_s, x, \hat{\xi}) = |\nabla\phi(x_s, x_r, x)|^2 \det \begin{pmatrix} \frac{\partial}{\partial x'_r}\nabla\phi(x_s, x_r, x) \\ \nabla\phi(x_s, x_r, x) \end{pmatrix}$$

and terms from the integral kernel defining L^a_δ, above. In all cases these are evaluated at $t_r = \phi(x_s, x_r, x)$ and $x'_r = x'_r(x_s, x, \hat{\xi})$ chosen to satisfy the stationary phase conditions.

Recall (Section 3) that

$$R(x_s, x_r, x) = \frac{c^2(x)\, b^2(x_s, x_r, x)\, a(x_s, x)\, a(x_r, x)}{2\rho(x)}$$

and

$$\begin{aligned} b(x_s, x_r, x) &= \frac{1}{1 + \cos\theta(x_s, x_r, x)} = \frac{2}{c^2(x)|N(x_s, x_r, x)|^2} \\ N(x_s, x_r, x) &= \nabla_x\tau(x_s, x) + \nabla_x\tau(x_r, x)\ . \end{aligned}$$

The first stationary condition implies that

$$|N(x_s, x_r(x_s, x, \hat{\xi}), x) \cdot \hat{\xi}| = |N(x_s, x_r(x_s, x, \hat{\xi}), x)|\ .$$

So the principal symbol of $\Lambda_{\sigma\sigma}$ is the product of the geometrical factor $g(x_s, x, \hat{\xi})$ and

$$\begin{aligned} & m(x_s, x'_r, t_r)\ R(x_s, x_r, x)(N(x_s, x_r, x) \cdot \xi))^2 \\ &= |\xi|^2 m(x_s, x'_r, t_r)\frac{c^2(x)}{2\rho(x)}\ \frac{a(x_s, x)\,(a(x_r, x)}{(1 + \cos\theta(x_s, x_r, x))^2}|N(x_s, x_s, x)|^2 \\ &= |\xi|^2 \frac{m(x_s, x'_r, t_r)\ a(x_s, x)\ a(x_r, x)}{\rho(x)(1 + \cos\theta(x_s, x_r, x))} \\ &= |\xi|^2 \frac{2m(x_s, x'_r, t_r)\ a(x_s, x)\ a(x_r, x)}{\rho(x)\ c^2(x)|\nabla\phi(x_s, x_r, x)|^2}\ . \end{aligned}$$

Accordingly ($n = 3$!).

$$\begin{aligned} &\Lambda_{\sigma\sigma}(x_s, x, \xi) = \\ &\quad |\xi|^2 \left(\frac{2m(x_s, x'_r, t_r)\ a(x_s, x)\ a(x_r, x)}{\rho(x)c^2(x)}\right)^2 |\nabla\phi(x_s, x_r, x)|^{-2} \\ &\qquad \det \begin{pmatrix} \frac{\partial}{\partial x'_r}\nabla\phi(x_s, x_r, x) \\ \nabla\phi(x_s, x_r, x) \end{pmatrix}^{-1} \\ &\Lambda(x_s, x, \xi) = \\ &\quad \Lambda_{\sigma\sigma}(x_s, x, \xi) \begin{pmatrix} 1 & \sin^2\frac{1}{2}\theta(x_s, x_r, x) \\ \sin^2\frac{1}{2}\theta(x_s, x_r, x) & \sin^4\frac{1}{2}\theta(x_s, x_r, x) \end{pmatrix}\ . \end{aligned}$$

This expression simplifies still further through use of the (stationary point) identity

$$\nabla\phi(x_s, x_r, x) = \frac{\sqrt{2}}{c}(1 + \cos\theta)\hat{\xi}$$

and

$$\frac{\partial}{\partial x_r'}\nabla\phi = \frac{\partial}{\partial x_r}\nabla_x\tau(x_r,x)\ .$$

These identities allow one to write the symbol as a sum of products of function of (x_s,ξ) and (x_r,ξ), which is useful in actual calculations.

Similar calculations hold for the 2-d case. Then (see end of Section 3; we have absorbed factors of π, etc., into the definition of a):

$$R(x_s,x_r,x) = \frac{b(x_s,x_r,x)\ a(x_s,x)\ a(x_r,x)}{\rho(x)}$$

and only one factor of the vector field $N\cdot\nabla$ occurs. Then we get for the principal part of $\Lambda_{\sigma\sigma}$ the expression

$$\begin{aligned}
&|\xi| g(x_s,x,\xi)(m(x_s,x_r,x)b(x_s,x_r,x)a(x_s,x)a(x_r,x)\rho(x)^{-1})^2 \\
&\qquad\cdot (N(x_s,x_r,x)\cdot\xi)^2 \\
&= \quad |\xi|\left(\frac{2m(x_s,x_r',t_r)a(x_s,x)a(x_r,x)}{\rho(x)c^2(x)}\right)^2 \\
&\qquad\times |\nabla\phi(x_s,x_r,x)|^{-1}\det\begin{pmatrix} \frac{\partial}{\partial x_r'}\nabla\phi(x_s,x_r,x) \\ \nabla\phi(x_s,x_r,x)\end{pmatrix}^{-1}\ .
\end{aligned}$$

Some further, instructive geometric interpretation is easy in the 2-d case. Writing

$$\nabla\phi = |\nabla\phi|(\sin\psi\ ,\cos\psi)$$

we have

$$\det\begin{pmatrix} \frac{\partial}{\partial x_r'}\nabla\phi \\ \nabla\phi\end{pmatrix} = |\nabla\phi|^2\cos\psi^2\frac{\partial}{\partial x_r'}\tan\psi = |\nabla\phi|^2\frac{\partial\psi}{\partial x_r}\ .$$

Thus the determinant measures the rate at which the direction of $\nabla\phi$ changes with receiver position. Consequenlty, the principal symbol can be written entirely in terms of angles and local quantities:

$$\begin{aligned}
&\Lambda_{\sigma\sigma}(x_s,x,\xi) = |\xi|\cdot \\
&\qquad\frac{\sigma(x)^{-1}(m(x_s,x_r,t_r)\ a(x_s,x)\ a(x_r,x))^2\sqrt{\frac{2}{c(x)}}}{(1+\cos\theta(x_s,x_r,x))^{\frac{3}{2}}\frac{\partial\psi}{\partial x_r'}(x_s,x_r,x)}\ .
\end{aligned}$$

9 Migration

The solution of the migration problem, hinted at the end of Section 4, can now be placed on firm footing. We shall give both a straightforward discussion of the "ideal" migration (the so-called before-stack variety), and a derivation of a number of standard "real-world" approximations.

Recall that the *migration problem* is: given a data set $\{\delta p(x_s, x_r, t_r) : 0 \le t_r \le t_{max}, (x_s, x_r) \in X_{rs}\}$, find the locii of high-frequency components in the coefficient perturbations $\delta\sigma/\sigma$, $\delta\rho/\rho$. Of course it is presumed that

$$\delta p \approx L_f[\rho, c]\,[\delta\sigma/\sigma, \delta\rho/\rho]$$

for suitable reference parameters ρ, c. If ρ, c are smooth, then the analysis of the previous section shows that

$$L_\delta[\rho, c]^* f^{-1} * \delta p \approx L_\delta[\rho, c]^*\, L_\delta[\rho, c]\,[\delta\sigma/\sigma, \delta\rho/\rho]$$

is pseudodifferential. That is, if the inverse convolution operator $f^{-1}*$ is first applied to the data δp, followed by the adjoint of the perturbational forward map, then the result is related by a matrix of pseudodifferential operators to the causative coefficient perturbations.

This yields a solution of the migration problem because pseudodifferential operators are *pseudolocal*: they preserve the locii of high frequency components. In fact:

> *Suppose $P = p(x, D)$ is pseudodifferential, and u is a distribution, smooth near $x_0 \in \mathbb{R}^n$. Then Pu is smooth near x_0.*

This statement replaces the vague "locii of high frequency components": pseudodifferential operators do not create singularities in new locations. Thus any singularities of the processed data set above are amongst the singularities of $[\delta\sigma/\sigma, \delta\rho/\rho]$. In fact, the converse is also true, as follows from the inversion theory of the next section. Thus the locations of the singularities of $[\delta\sigma/\sigma, \delta\rho/\rho]$ are found by the above "before-stack migration" procedure. This view of migration and the interpretations advanced below for the various migration algorithms are due, for the most part, to Albert Tarantola, Patrick Lailly, Gregory Beylkin, and Rakesh. Their original papers are cited in the introduction, and should be consulted for additional insight and different emphases.

The proof of the pseudolocal property is simple and revealing, and we shall give it below. We will also describe algorithms for before-stack migration. First, though, we record some deficiencies in the approach.

The interpretation of "high-frequency locii" as "singularities" increases precision at the cost of scope. Available direct evidence shows that real earth parameter distributions are singular — i.e., not smooth — virtually everywhere. Therefore, strictly speaking no information is to be gained by identifying the singularities of model parameters, as these parameters ought to be singular everywhere in any event! In practice, the mechanical properties of sedimentary rocks have abnormally large fluctuations in a limited number of locations — boundaries of geological units and gas or oil reservoirs, for example. Therefore the goal of migration ought to be identification of a measure of local singularity strength, rather than identification of of singularities *per se*. It is difficult to define precisely such a measure of strength. Geophysicists have tended to rely on output signal strength from migration algorithms as giving qualitative estimates of strong parameter fluctuations (or at least their locii). (Often geophysicists claim to access only phase information in this way — but of course phases can only be recognised by virtue of associated signal amplitudes!) The quantitative

differences in output between different migration algorithms can sometimes masquerade as qualitative differences, however. The inversion theory of the next section suggests one way to make more precise and standardized estimates of parameter fluctuations, but a definitive resolution of the singularity strength issue remains to be achieved.

A second difficulty is that the convolution inverse "$f^{-1}*$" in the migration formula above does not exist, because the source function $f(t)$ is essentially bandlimited, as discussed in §2. (It is also known only with some difficult-to-assess error, though we shall treat it as known.) Thus the best practically achievable "normal operator" is something like

$$L^*_\delta[\rho, c]\, L_{\tilde{f}}[\rho, c]$$

where $\tilde{f}$ is a "bandlimited delta." Such operators are "not quite" pseudodifferential, and the extent to which their properties approximate those of pseudodifferential operators is not known with any precision to this author's knowledge.

To see the extent to which singularities are reproduced under mildly realistic circumstances, consider the data displayed in Figure 8(a), resulting from Kirchhoff simulation applied to the model of Figure 3, but with a difference source time dependence (Figure 8(b), a bandpass trapezoidal filter with $5 - 7.5 - 30 - 35$ Hz profile. Shot record migration *via* the Kirchhoff migration formula (i.e. application of the adjoint $L^*_{\sigma\sigma}$) produces Figure 8(c). For comparison Figure 8(d) shows the relative velocity perturbation $\delta c/c$ used to produce the data, plotted in the same way. The very close correspondence between the high frequency signal locations in the two fields is clear, as are the differences. While a large part of the high frequency signal in the migration output coincides in location with part of that in the velocity perturbation, quite a lot of the latter is not present in the former. In fact only the singularities preserved by application of the normal operator are present in the migration result (or rather their finite frequency "ghosts" are!). The construction of the normal operator shows that only *Snell points*, i.e. connected to source and receiver by rays whos bisector is the reflector normal, appear with significant high frequency energy in the migration output. The resulting *imaging aperture* is evident in Figure 8(c).

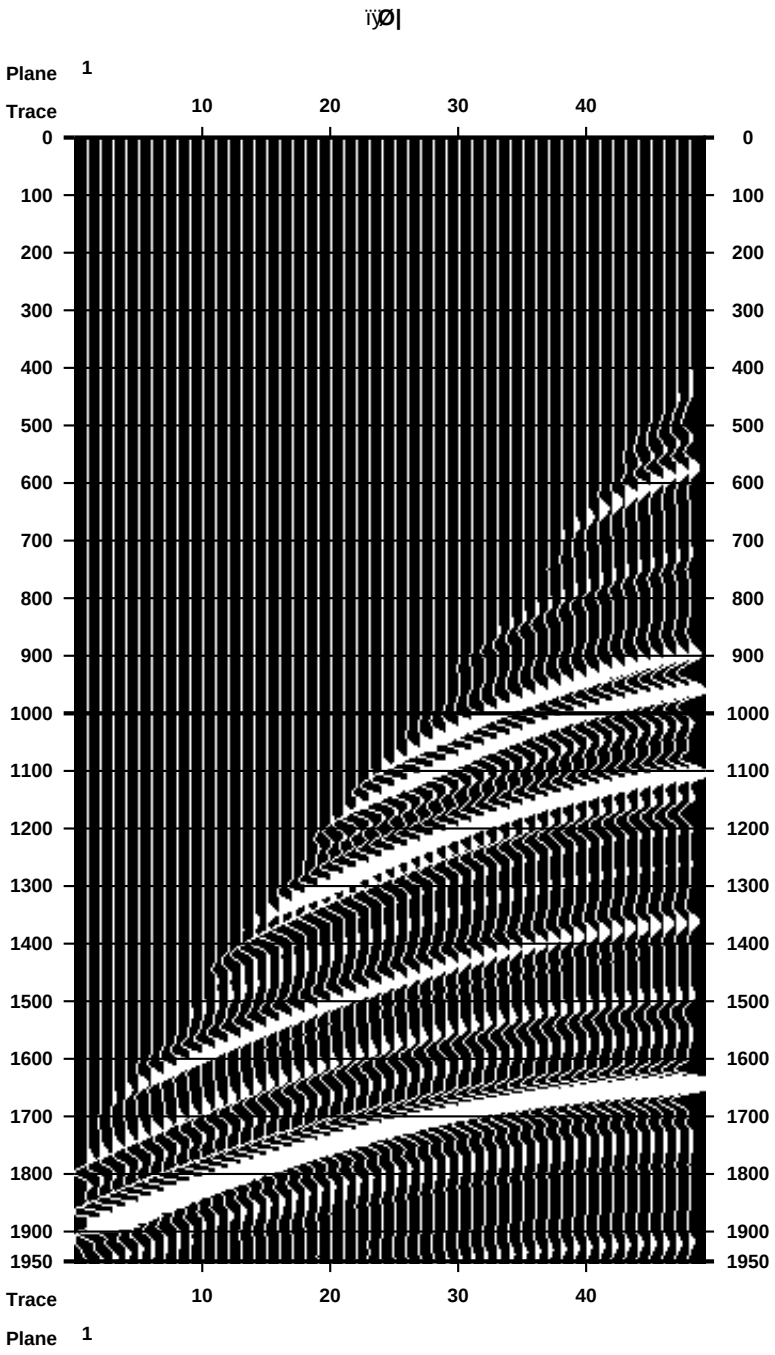

FIGURE 8(A) Data simulated from velocity and velocity perturbation of Figure 3 and same acquisition geometry, but using the bandpass filter of Figure 8(b) as source.

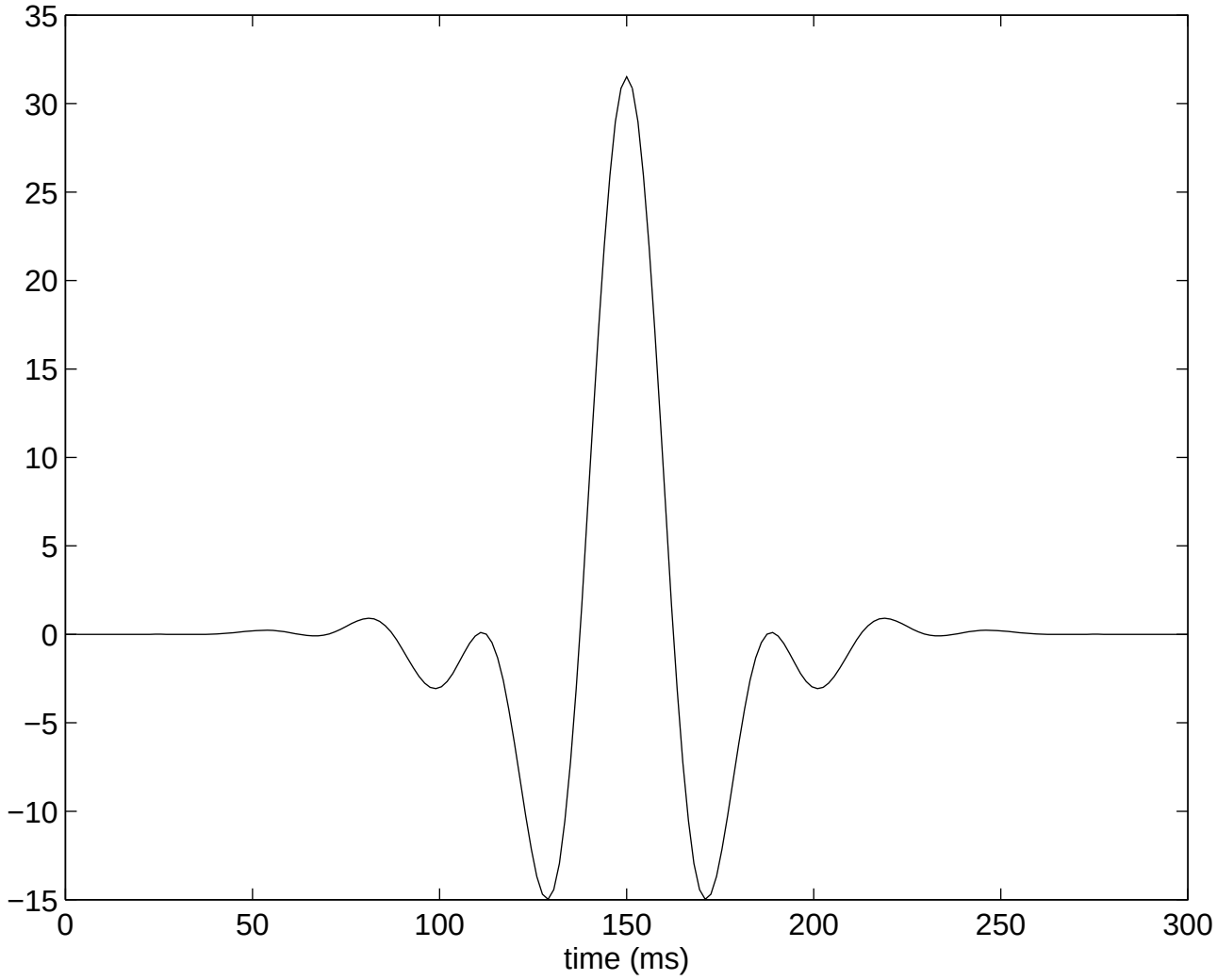

FIGURE 8(B) Bandpass filter with 5 - 7.5 - 30 - 35 Hz trapezoidal kernel, used as source.

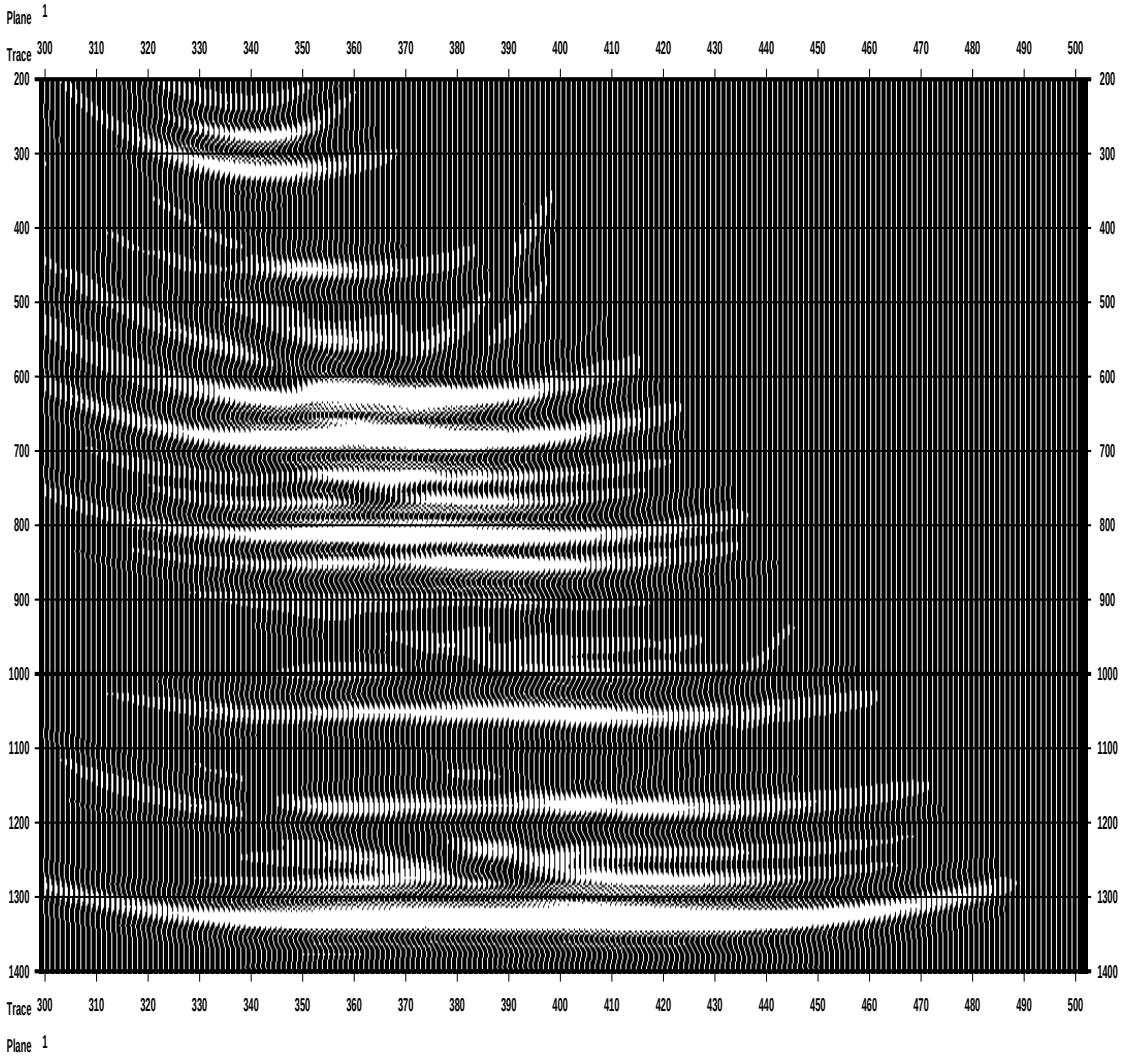

FIGURE 8(C): Prestack Kirchhoff migration of the shot gather in Figure 7(b). Note the limited aperture and migration artifacts.

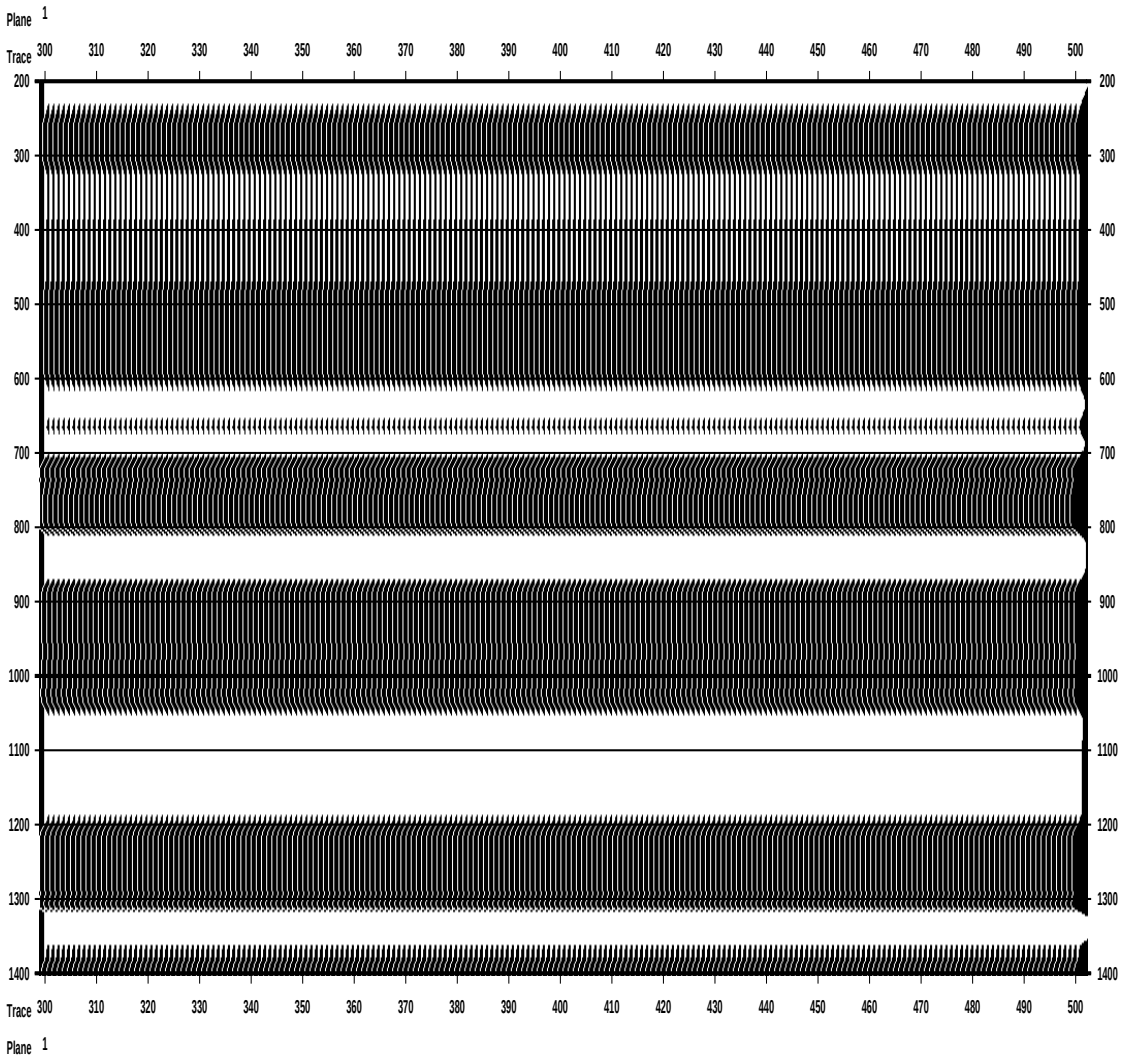

FIGURE 8(D): Relative velocity perturbation - Figure 3(b) as a function of 2 variables, constant in x, depending only on z. Note that the locii of rapid change line up well with those in Figure 8(c).

Also evident are signal components unrelated to the parameter fluctuations, so called "migration artifacts". Much of this unwanted signal is due to truncation of the integration range in the discrete implementation of the generalized Radon transform formula. These are largely removed by use of more data: the adjoint of the map from $\delta c, \delta\rho$ to all shot records simultaneously involves an integration over the shot coordinate x_s as well. This summation over shots tends to cancel destructively the artifacts, enlarge the inversion aperture, and enhance the signal. For example, the shot record shown above is the first of 60, spaced 32 m apart, which were migrated collectively to produce Figure 8(e). This collective migration (i.e. application of the appropriate adjoint) amounts to migration of the individual shot records followed by summation ("stack") of the outputs ("migrated partial images"). Hence the application of the adjoint to a multi-shot data set is termed "post migration stack" (at least by some - the reader should be forewarned that most of the concepts introduced in this chapter go by many names, and this one is no exception!).

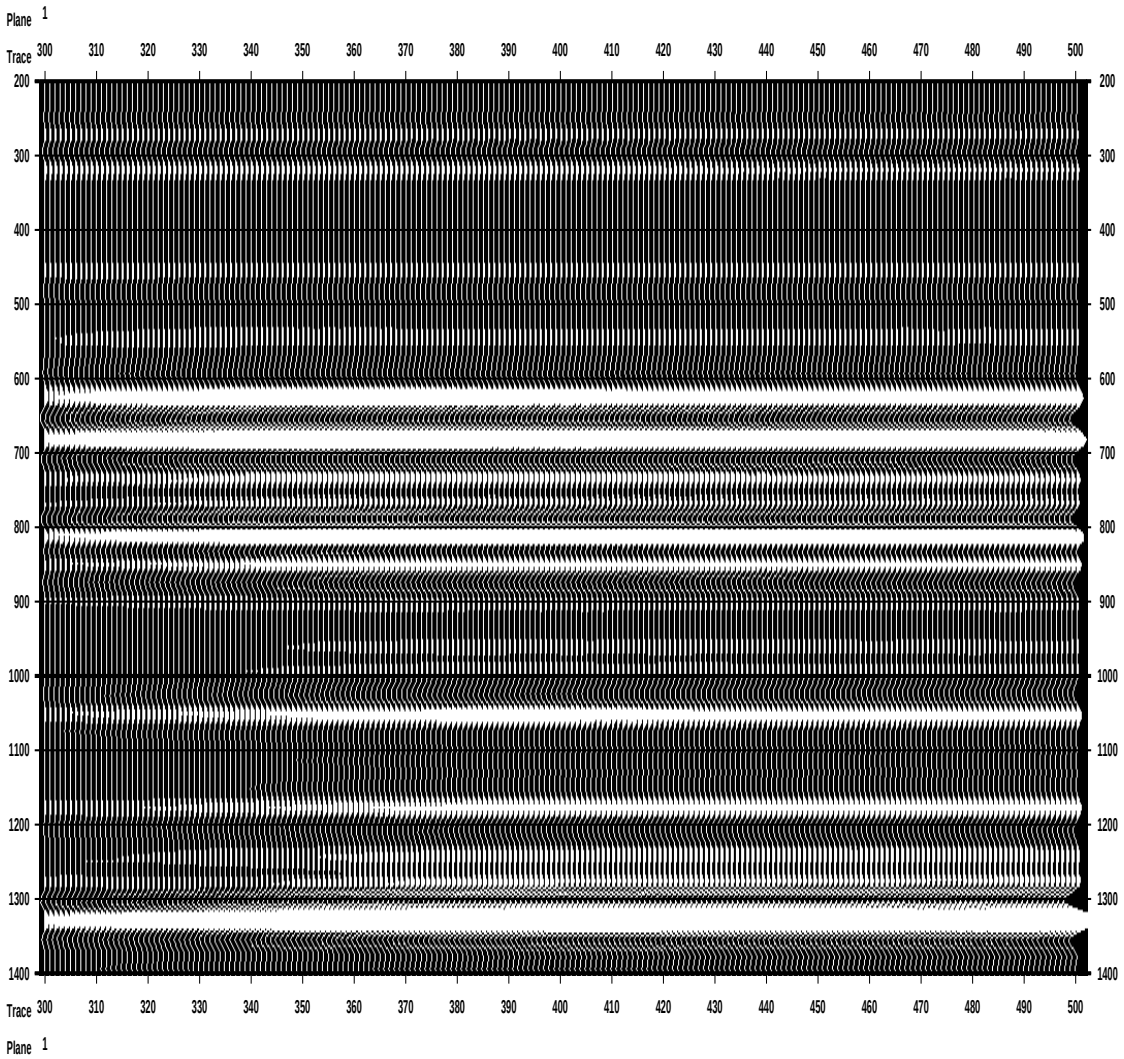

FIGURE 8(E): Post migration stack = output of adjoint operator of map from velocity perturbation to 61 shot records over the model depicted in Figure 3 with shot locations separated by 32 m. Note that migration artifacts have been eliminated for the most part by the summation over shots implicity in the adjoint construction.

A very important feature of the post-migration stack is its sensitivity to errors in the background parameters ρ and c (especially c!). If the data are well-approximated by the perturbational map at ρ, c and if L^* is computed with ρ_m, c_m, then we obtain

$$L^*_\delta[\rho_m, c_m]\ L_\delta[\rho, c]$$

which is in general no longer pseudodifferential. In fact the output of this operator will generally have singularities in different positions than does its input. Even worse, if we write

$$L_\delta[\rho, c; x_s]\ [\delta\sigma/\sigma, \delta\rho/\rho] = \delta G(x_s, \cdot, \cdot)$$

then

$$L_\delta[\rho_m, c_m]^*\ L_\delta[\rho, c] = \sum_{x_s} L_\delta[\rho_m, c_m, x_s]^*\ L[\rho, c, x_s]\ .$$

If $c_m = c$, then each individual operator

$$L_\delta[\rho_m, c, x_s]^*\ L_\delta[\rho, c, x_s]$$

is pseudodifferential, and therefore so is their sum. If $c_m \neq c$, then generally the above operator moves an input singularity to an x_s-dependent output position. Then summation over x_s "smears" the singularity out; destructive interference may actually convert a singularity to a smooth signal. This smearing phenomenon is analysed in a simple special case, in Appendix A of SANTOSA and SYMES, 1989. In any case, if $c \neq c_m$, singularities in $[\delta\sigma/\sigma, \delta\rho/\rho]$ are moved, and possibly lost altogether in the final summation over x_s ("stack").

To illustrate this phenomenon, I display in Figure 8(f) the postmigration stack of the data used to generate Figure 8(e), but this time the adjoint is computed with a constant velocity of $c_m = 1.5$ m/ms. Reference to Figure 3(a) shows that this velocity is correct only near the surface. The output of this adjoint scattering operator with incorrect velocity is plotted on the same scale as was used in Figure 8(e). Evidently considerable destructive interference has occurred. Also those locii of high frequency energy ("events") which remain recognizable are located incorrectly: use of an incorrect velocity has translated time into distance ("migrated") the events incorrectly.

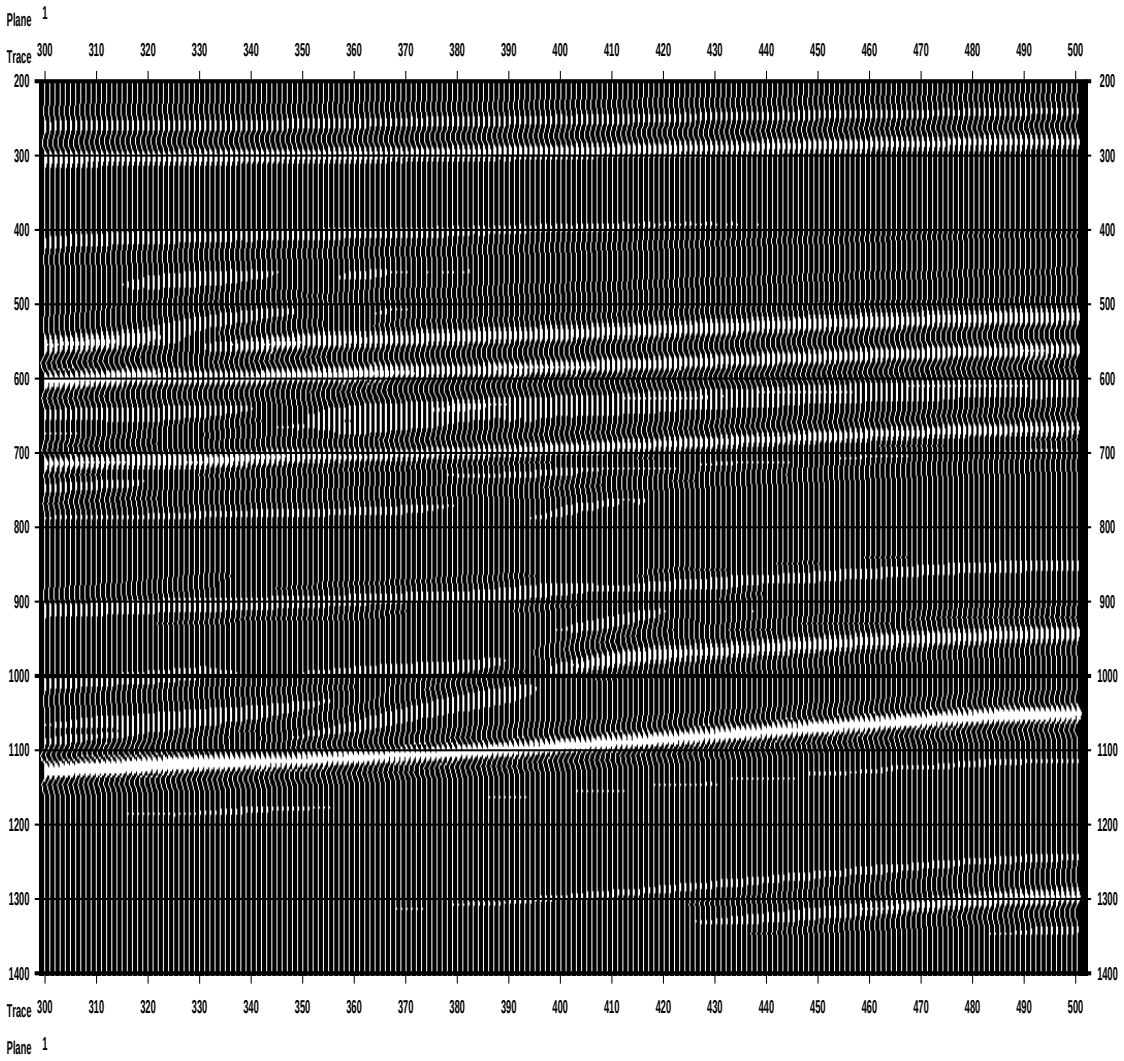

FIGURE 8(F): Post migration stack = output of adjoint scattering operator, but with incorrect velocity ($c \equiv 1.5$ m/ms). Much destructive interference occurs and remaining events are positioned incorrectly.

This sensitivity of before-stack migration performance to reference velocity has led seismologists to rely on a number of imaging techniques less directly motivated by the physics of wave propagation, but much more robust against reference velocity error. These "after-stack" migration processes are also dramatically cheaper, requiring far smaller computational resources than before-stack migration. For these reasons after-stack migration was the most common migration process applied to seismic reflection data, until rather recently. A large research effort has provided the seismic industry with tools to estimate velocity with sufficient accuracy to give usable before-stack migration results, in many cases. Together with the increasing power of computers, these improved velocity analysis tools have made before-stack migration practical: it is now routine for 2D data, and carried out with increasing frequency for 3D data. Note that the "difficult" cases for velocity estimation still abound, and as a research topic velocity estimation is far from exhausted.

We shall also describe a simple version of after-stack migration at the end of the section. Before doing so, we shall

(i) discuss the pseudolocal property of pseudodifferential operators;

(ii) describe the major families of before-stack migration agorithms.

The crucial fact which underlies the effectiveness of migration is the pseudolocal property of pseudodifferential operators. To state this property precisely, we give a simple criterion for detecting local smoothness: a function u (locally integrable, say) is smooth at $x_0 \in \mathbb{R}^n$ if we can find a smooth envelope function χ with $\chi(x_0) \neq 0$ so that χu is smooth.

Now suppose that $p(x,\xi)$ is the symbol of a pseudodifferential operator, and that u is smooth at x_0. We claim that $p(x,D)u$ is also smooth at x_0 (this is the pseudolocal property). In fact, let χ_1 be another smooth envelope function, so built that $\chi_1(x_0) \neq 0$ and for some $\delta > 0$

$$\chi_1(x) \neq 0\,, \quad \chi_1(y) = 0 \Rightarrow |x-y| \geq \delta\,.$$

In fact, we can arrange that χu is smooth and that $\chi(x) \equiv 1$ if $\chi_1(x) \neq 0$. Write

$$\begin{aligned}\chi_1(x)p(x,D)u(x) &= \int d\xi \int dy\; p(x,\xi)e^{i(x-y)\cdot\xi}\chi_1(x)\chi(y)u(y) \\ &\quad + \int d\xi \int dy\; p(x,\xi)e^{i(x-y)\cdot\xi}\chi_1(x)(1-\chi(y))u(y)\,.\end{aligned}$$

Since χu is smooth, we can integrate by parts repeatedly in the first integral using the identity

$$(1-\Delta_y)e^{i(x-y)\cdot\xi} = (1+\xi)^2 e^{i(x-y)\cdot\xi}$$

and loading the derivatives onto $\chi u(y)$. This gives sufficiently many negative powers of $1+|\xi|^2$ eventually that the first integral is convergent even after any fixed number of differentiations in x. Thus the first term is smooth. For the second, note that $|x-y| \geq \delta$ when $\chi_1(x)(1-\chi(y)) \neq 0$, so we can integrate by parts in ξ:

$$\begin{aligned}&\int d\xi \int dy\; p(x,\xi)e^{i(x-y)\cdot\xi}\chi_1(x)(1-\chi(y))u(y) \\ &= \cdots = \int d\xi \int dy (1-\Delta_\xi)^N p(x,\xi)(1+(x-y)^2)^{-N}\chi_1(x)(1-\chi(y))u(y)\end{aligned}$$

As mentioned in the last section, it is characteristic of symbols that, when differentiated in ξ, their order drops: the defining estimates for the symbol classes in fact take the form (for symbols of order m):

$$|D_x^\alpha D_\xi^\beta p(x,\xi)| \leq C_{\alpha,\beta,K}(1+|\xi|)^{m-|\beta|}$$

for any compact $K \subset \mathbb{R}^n$. (We have used multi-index notation here: $\alpha = (\alpha_1, \ldots \alpha_n)$, $|\alpha| = \sum_i \alpha_i$

$$D_x^\alpha u = (-i)^{|\alpha|} \frac{\partial^{|\alpha|}}{\partial x_1^{\alpha_1} \cdots \partial_{x_n}^{\alpha_n}}$$

etc.). Thus integration by parts in ξ causes the integrand to decrease in $|\xi|$, and so eventually to support differentiation in x under the integral sign.

Note that the size of the x-derivatives of $\chi_1 p(x,D)u$ will be influenced by the size of the support of χ (hence by $\delta > 0$): The smaller this support is, the larger typically are the two integrands after the integration-by-parts manipulations above. Thus the resolution, with which smooth and non-smooth points may be distinguished, is limited.

Next we address the computation of the before-stack migration result: clearly, the key issue is the calculation of the adjoint operator L^*. There are two general approaches to this computation.

The first approach begins with the "integral" representation

$$L[\delta\sigma/\sigma, \delta\rho/\rho] = \int dx\ R\,(N\cdot\nabla_x)^2 \left(\frac{\delta\sigma}{\sigma} - \sin^2(\frac{1}{2}\theta)\frac{\delta\rho}{\rho}\right)\ \delta(t-\tau_s-\tau_r)\ .$$

Evidently

$$\begin{aligned} L^*\,u(x_s,x) &= \int dx_r'\ R\,(x_s,x_r,x)(N\cdot\nabla_x)^2 u(x_r',\tau_s(x)+\tau_r(x)) \\ &\quad \times \begin{pmatrix} 1 \\ -\sin^2\frac{1}{2}\theta(x_s,x_r,x) \end{pmatrix}\ . \end{aligned}$$

Apart from the derivative, each component of the output is a weighted integral over the moveout curves $t = \tau_s + \tau_r$.

Since one wants only an "image," i.e. a function of location rich in high-frequency energy, the presence of two components represents redundancy. An obvious way to prune the output is to compute only the first component, i.e. the "impedance" image:

$$\begin{aligned} Mu(x_s,x) &= \int dx_r' R(x_s,x_r,x)(N\cdot\nabla_x)^2 u(x_r',\tau_s(x)+\tau_r(x)) \\ &\cong \int dx_r' \tilde{R}(x_s,x_r,x)\frac{\partial^2 u}{\partial t^2}(x_r',\tau_s(x)+\tau_r(x)) \end{aligned}$$

where $\tilde{R}$ is a modified amplitude function. In fact, it follows from the calculations in the previous section that $\tilde{R}$ could be greatly modified, and the image of u under the resulting *shot record migration operator* M would still have the same locii of high-frequency components. The essential point is that these are mapped by the inverse of the canonical reflection

transformation constructed in Section 4 — which property depends on the choice of phase (i.e. $\tau_s(x) + \tau_r(x)$) and hardly at all on the amplitude ($\tilde{R}$).

The family of integral migration formulas so obtained goes under the name "Kirchhoff migration" in the literature. A great variety of such formulae have been suggested, but all fit in the general scheme just explained.

Another family of migration algorithms comes from the recognition that the adjoint operator L^* is itself defined by the solution of a boundary value problem. As noted above, it suffices to compute the impedance component, i.e. to assume that $\delta\rho = 0$. Thus M is adjoint to the map

$$\delta c/c \mapsto \delta G \,|_{x=x_r}$$

defined by solving

$$\left(\frac{1}{\rho c^2}\,\frac{\partial^2}{\partial t^2} - \nabla\frac{1}{\rho}\nabla\right)\delta G = \frac{2\delta c}{c^3}\,\frac{\partial^2 G}{\partial t^2} \qquad\qquad \delta G \equiv 0\ , \quad t << 0\ .$$

Suppose v solves

$$\left(\frac{1}{\rho c^2}\,\frac{\partial^2}{\partial t^2} - \nabla\cdot\frac{1}{\rho}\nabla\right)v = F \qquad\qquad v \equiv 0\ , \quad t >> 0\ .$$

Then Green's formula (Section 3) gives

$$\begin{aligned}&\int dx \frac{\delta c}{c(x)}\left\{\frac{2}{c^2(x)}\int dt\ v(x,t)\frac{\partial^2 G}{\partial t^2}(x_s,x,t)\right\}\\ &\quad = \int dx \int dt\ \delta G\,(x_s,x,t)\,F\,(x,t)\ .\end{aligned}$$

Therefore, if $F(x,t) = \sum_{x_r} u(x_r',t)\delta(x - x_r)$, we see that

$$Mu(x_s,x) = \frac{2}{c^2(x)}\int dt\ v(x,t)\frac{\partial^2 G}{\partial t^2}(x_s,x,t)\ .$$

That is, the adjoint (shot record migration) operator is obtained by "propagating the data backwards in time, using the receivers as sources" (i.e. solving the final-value problem given above) and "cross-correlating the back-propagated field with the second t-derivative of the direct field." In practice G is often replaced by the leading term in its progressing wave expansion, and often the leading singularity is changed so that $\partial^2 G/\partial t^2$ has a δ-singularity; then M becomes something like

$$Mu(x_s,x) \approx v(x,\tau(x_s,x))\ .$$

None of these manipulations changes the basic singularity-mapping property of M.

Algorithms following this pattern usually employ a finite-difference scheme to solve the final-value problem numerically, and so are known as "finite-difference reverse-time before-stack shot record migration."

Remark. The literature exhibits a great deal of confusion about the identity of the adjoint field v. Many authors clearly regard v as a time-reversed version of δp or δG, i.e. "the scattered field, run backwards in time." Obviously v is *not* identical to δp or δG: it is a mathematical device used to compute the adjoint operator *and nothing more.*

As mentioned before, the final image is produced from data $\{u(x_s, x_r, t)\}$ by *stacking*, i.e. forming the sum of shot migrations over source ("shot") locations

$$\sum_{x_s} Mu(x_s, x) \; .$$

This sum is exceedingly sensitive to errors in background velocity. Accordingly, other algorithms have been devised which are markedly less sensitive to this velocity. These "after-stack" processes depend on two main observations. First, suppose that one is given the *zero-offset dataset* $\delta G(x_s, x_s, t) =: u(x_s, t)$. Then (Section 3)

$$u(x_s, t) \approx \int dx \; R \, (\nabla \tau_s \cdot \nabla)^2 \frac{\delta \sigma}{\sigma} \delta(t - 2\tau_s) \; .$$

Now $2\tau_s$ is the travel-time function (from x_s) for the medium with velocity field $c(x)/2$ (as follows directly from the eikonal equation). Thus *except for amplitudes*, u is high-frequency asymptotic to the solution $U \, |_{x=x_s}$ of the problem

$$\left(\frac{4}{c^2(x)} \, \frac{\partial^2}{\partial t^2} - \nabla^2 \right) U(x,t) = \frac{\delta \sigma(x)}{\sigma(x)} \delta(t) \, ; \qquad U \equiv 0 \, , \quad t < 0$$

as is easily verified by use of Green's formula, the progressing wave expansion, and high-frequency asymptotics. This approximation is called the "exploding reflector model," as the impedance perturbation functions as a $t = 0$ impulse. A reverse-time migration algorithm is easily generated, by identifying the adjoint of the map

$$\frac{\delta \sigma}{\sigma} \mapsto U \, |_{x=x_s}$$

via Green's formula; one obtains the prescription:

Solve:

$$\left(\frac{4}{c(x)} \, \frac{\partial^2}{\partial t^2} - \nabla^2 \right) v(x,t) = \sum_{x_s} u(x_s, t) \, \delta(x - x_s) \qquad v \equiv 0 \, , \quad t >> 0$$

Image:

$$\{ v(x, 0) \} \; .$$

There is also a Kirchhoff-style version of this algorithm, obtained by expressing the solution v as an integral against the fundamental solution, and truncating its progressing wave expansion. Also, paraxial approximations to the wave equation have been used in an attempt to speed up the numerical calculations. We refer the reader to the SEG reprint collection on migration (GARDNER, 1985) for many original references, with the warning that these papers are often mathematically self-contradictory. See also the excellent recent comprehensive reference YILMAZ, 1987.

So far, the reason for the appellation "after-stack" is not evident. The reason is the second main observation: to some extent, zero-offset data can be approximated by summing multi-offset data (i.e. $\{p(x_s, x_r, t)\}$) over certain trajectories in (x_s, x_r, t). In rough outline, the crudest version of this construction depends on the assumption that "*reflectors are all flat*" i.e. that $\delta\sigma/\sigma$ has high-frequency components only with vertical wave-vectors (ideally, $\delta\sigma/\sigma = \delta\sigma/\sigma(z)$).Indeed, sedimentary rocks originate in flat-lying sediment layers. In many places, subsequent geological processes have not distorted too much this flat structure, so the "flat reflector hypothesis" is not too inaccurate. *If it were not for this fact, reflection seismology would probably not have attained its current importance in geophysical exploration technology.*

Given that the reflectors are flat, a *unique* family of moveout curves is picked out for each source, by the kinematic construction of Section 4: in general, for each source/receiver location pair (x_s, x_r), and time t_r, at only one place on the reflector locus $\{x : t_r = \tau(x_s, x) + \tau(x_r, x)\}$ is the virtual reflector normal $N = \nabla\tau_s + \nabla\tau_r$ vertical — and by symmetry this point lies under the midpoint of the source-receiver segment $x' = \frac{1}{2}(x'_s + x'_r)$. Thus the data is sorted into common midpoint bins (or gathers) $\{p(x_s, x_r, t_r) : \frac{1}{2}(x'_s + x'_r) = x_m\}$. An approximate phase correction is applied, depending on t_r and the half-offset $x_h = \frac{1}{2}(x_r - x_s)$:

$$\tilde{p}(x_m, x_h, t) = p(x_m - x_h, x_{m+}x_h, t + \phi(x_m, x_h, t))$$

where ϕ is constructed to approximately remove the offset-dependence of the signal. This is the so-called *normal-moveout (NMO) correction.* Then the data is stacked:

$$P_{st.}(x_m, t) = \sum_{x_h} \tilde{p}(x_m, x_h, t) \ .$$

This *stacked section* is regarded as an approximate zero-offset section and submitted to the zero-offset migration algorithms outlined above (hence "after-stack migration"). Ignoring amplitudes, one can justify this point of view using the same geometric-optics tools employed in the rest of these notes.

The effectiveness of this strategy obviously depends on the choice of phase correction $\phi(x_m, x_h, t)$. The secret of success of after-stack processing is that ϕ is chosen so that the "energy" of the stacked section

$$\sum_{x_m, t} |p_{st}(x_m, t)|^2$$

is maximized relative to the energy of the input common midpoint gathers. In principle, ϕ ought to be determined by the velocity model; in practice, it is determined to obtain the best possible image, i.e., the least destructive cancellation. In this way the result of after-stack migration becomes much less sensitive to the velocity model, *because the velocity model is adjusted to produce the most robust result.* In the subsequent zero-offset migration, the velocity $c(x)$ is either set equal to some convenient constant ("time migration") or adjusted to approximate the true distribution of earth velocities ("depth migration"). In either case, this second-stage use of velocity has a subsidiary effect to that of the NMO correction.

Note that the physical meaning of velocity in the NMO correction step is essentially lost: the kinematics are merely adjusted to give the best stack. Under some circumstances

(notably, when the data really come from flat-lying reflectors) there is arguably some connection between the physical velocity and the stack-optimizing kinetics — in general, there is no such connection.

In the last fifteen years, so-called *dip moveout correction* has been advanced as a partial cure for this defect in the kinematic treatment of reflections, the idea being to treat non-flat-lying ("dipping") reflectors consistently, at least regarding kinematics. Dip moveout is beyond the scope of these notes.

Finally, note that none of the after-stack processes take physically consistent account of signal amplitudes: only phases are preserved — and, as previously remarked, phases are only recognizable through amplitudes, so even phases must be regarded with suspicion in after-stack output.

10 Inversion, Caustics, and Nonlinearity

The formulas derived at the end of Section 5 lead to a number of so-called *inversion methods*, i.e. techniques for direct estimation of parameters $(\delta\sigma, \delta\rho)$. For example, if we restrict ourselves to the 2-D, $\delta\rho \equiv 0$ case, then for each shot formally

$$S(x_s, x_r, t_r) = f * L_\delta[\rho, c]\,[\delta\sigma/\sigma, 0]$$

implies that

$$\delta\sigma/\sigma = \Lambda_{\sigma\sigma}^{-1} M\,[\rho, c, x_s](f*)^{-1} S(x_s, \cdot, \cdot)$$

where $M[\rho, c, x_s]$ is the before-stack migration operator introduced in Section 6, i.e. M is adjoint to $\delta\sigma/\sigma \mapsto L_\delta[\rho, c]\,[\delta\sigma/\sigma, 0](x_s, \cdot, \cdot)$. This is a prototypical inversion formula, which we pause to examine critically.

As observed in Section 6, $(f*)^{-1}$ doesn't exist; at best one can produce a bandlimited partial inverse to $(f*)$, i.e. a convolution operator f_1* for which

$$f_1 * f * u \approx u$$

for a linear space of bandlimited signals u.

The production of such deconvolution operators f_1 is well understood, but the influence of the defect $f_1 * f - \delta$ on the remainder of the inversion process is not.

Next we observe that $\Lambda_{\sigma\sigma}^{-1}$ also does not exist, strictly speaking. We can write (Section 5) for the principal symbol

$$\Lambda_{\sigma\sigma,0}(x_s, x, \xi) = m(x_s, x_r(x_s, x, \xi), t_r(x_s, x, \xi))p(x_s, x, \xi)$$

where $p(x_s, x, \xi)$ is a symbol of order 1 and m is the window or mute, introduced in Section 5, the presence of which reflects the finite size of the measurement domain (finite cable length). The reflected receiver location $x_r(x_s, x, \xi)$ is determined by the reflection kinematics, and is homogeneous of degree zero in ξ. Thus $m(x_s, x_r, t_r)$ is an *aperture filter*, homogeneous of degree zero and nonzero only over the range of reflector normals at x mapped into the

"cable," i.e. support of $m(x_s, \cdot, \cdot)$, by the CRT. This *inversion aperture* is typically far less than the full circle S^1, so m vanishes over a large part of S^1.

The composition of pseudodifferential operators corresponds to the product of principal symbols, as noted in Section 5. Thus $(\Lambda_{\sigma\sigma})^{-1}$ ought to be a pseudodifferential operator with principal symbol $1/\Lambda_{\sigma\sigma,0}$; unfortunately $\Lambda_{\sigma\sigma,0}$ vanishes outside the aperture just constructed. Therefore the best we can do is to construct an *aperture-limited high-frequency approximate inverse.*

Remark. In the modern p.d.e. literature, the term *microlocal* has roughly the same meaning as "aperture limited" here. A high-frequency approximate inverse is called a *parametrix.*

First we build a *cutoff operator* to project out the undetermined components of the solution. In fact, we already have such an operator:

$$Q(x_s, x, \xi) := m(x_s, x_r(x_s, x, \hat{\xi}), t_r(x_s, x, \hat{\xi}))$$

is its symbol. The "simple geometry" hypothesis implied that $\Lambda_{\sigma\sigma,0}(x_s, x, \xi)$ is well-defined and non-vanishing when $Q(x_s, x, \xi) \neq 0$.

Now first consider the (hypothetical) case $f = \delta$, so that $(f*)^{-1}$ really does exist, and is in fact the identity map. Let $\Gamma(x_s, x, \xi)$ be any symbol satisfying

$$\Gamma(x_s, x, \xi)\Lambda_{\sigma\sigma}(x_s, x, \xi) = 1$$
$$\text{when} \quad Q(x_s, x, \xi) \neq 0$$

Then

$$Q\Gamma\Lambda_{\sigma\sigma} = Q + \cdots$$

where "$\cdots$" represents a smoothing operator. That is,

$$Q\frac{\delta\sigma}{\sigma} = Q\Gamma MS + \cdots .$$

Thus the sequence of operations $S \to (\text{migration})MS \to (\text{amplitudecorrection})\Gamma MS$ "inverts" the model-seismogram relation to a limited extent, in that it recovers the Fourier components of the model within the inversion aperture with an error decreasing with spatial frequency.

If we drop the unrealistic hypothesis $f = \delta$, then another limitation emerges: $(f*)^{-1}$ doesn't exist and we can at best replace it with a bandlimited deconvolution operator f_1*. Then $f_1 * f$ is a "bandlimited delta," and the operator

$$\delta\sigma/\sigma \to Mf_1 * S$$

is no longer a pseudodifferential operator with symbol $\Lambda_{\sigma\sigma}$. There is presumably a class of "spatially bandlimited" impedance perturbations for which the above operator is well approximated by $\Lambda_{\sigma\sigma}$. If this class includes perturbations of sufficiently high frequency content, presumably these are recovered accurately by the above formula. The characterization of such "recoverable classes" has not been carried out, to the author's knowledge.

BEYLKIN, 1985 proposed a slightly different approach: it is possible to write the product $Q\Gamma M$ as a generalized Radon transform. In fact, this follows from the calculations very similar to those in Section 5. This sort of inversion formula also suffers from the limitations just outlined.

Despite the theoretical imperfections, the sort of accuracy achievable with this approach is impressive. My research group at Rice University has implemented a version of Beylkin's construction, using the same techniques as in the implementation of Kirchhoff migration described previously (finite difference solution of eikonal and transport equations, simple second order quadrature and interpolation). The cost of getting the amplitudes right is a roughly 50% premium over Kirchhoff migration (i.e. the adjoint operator).

Figure 9(a) shows a synthetic shot gather created from a least-squares inversion (described below) of the North Sea data of Figure 1. This synthetic data has lower frequency content, but some of the same complexity as the field data. The model acquisition geometry is the same as that used in the field, as described in the caption of Figure 1. The source used in the simulation was a 5-7.5-30-35 Hz trapezoidal bandpass filter. This simulates ideal preprocessing in which the bandlimited data is rendered as close to a perturbational Green's function as possible, by *deconvolution*, i.e. application of a convolution pseudoinverse to the source signature. [Robinson discusses the deconvolution of seismic data extensively in Chapter XXX]. The application of the high frequency asymptotic inversion to this data produced the rather complex pattern of velocity perturbation displayed in Figure 9(b). For comparison the actual input velocity perturbation used to produce the data is displayed in Figure 9(c). One can see similarities, as well as differences to be expected in a result derived from a single shot record, notably aperture limitation and truncation artifacts. Figure 9(d) presents the *resimulation* of the data, using this time the high frequency asymptotic inversion estimate of the velocity perturbation (Figure 9(b)) instead of the input (Figure 9(c)). Figure 9(e) shows the error in the resimulation, which is approximately 20% RMS.

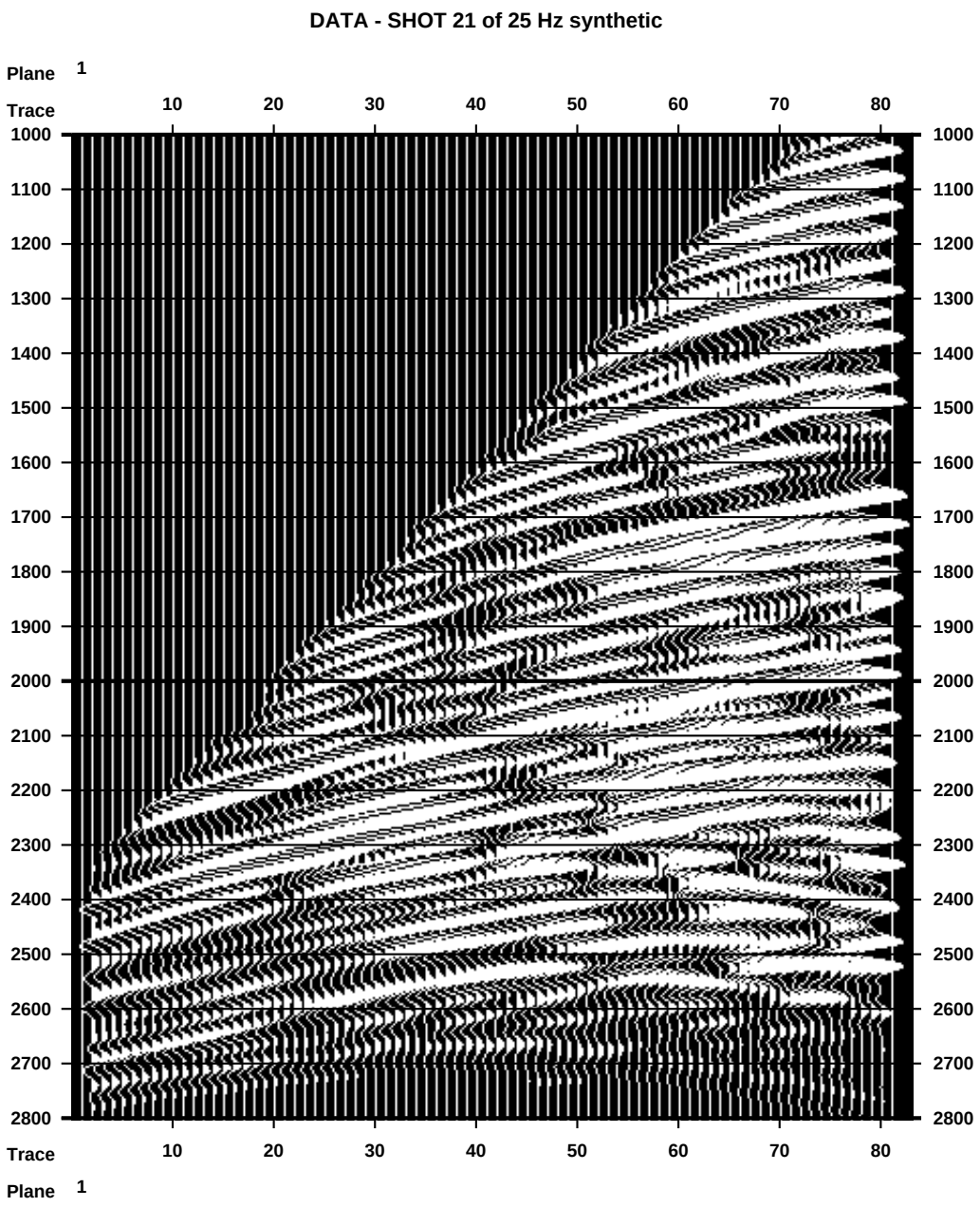

FIGURE 9(A): Synthetic data set derived from least squares inversion of 41 common source gathers from the survey described in Figure 1. Source is a bandpass filter. Long scale velocity obtained by smooting sonic log of nearby well. Least squares inversion estimate of short scale velocity perturbation displayed in Figure 9(c).

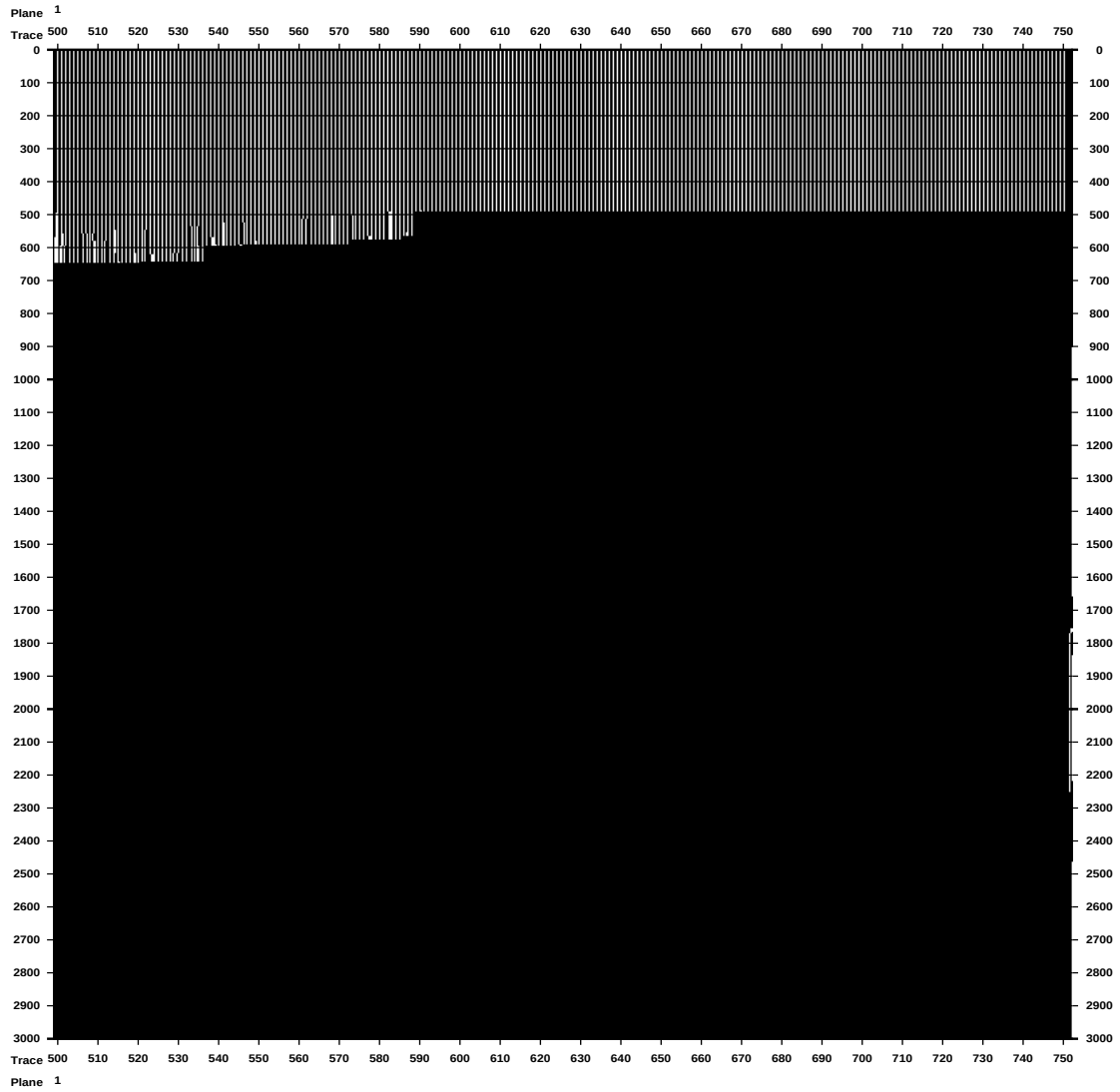

FIGURE 9(B): High frequency asymptotic inversion of data in Figure 9(a). Velocity model is that used to synthesize the data.

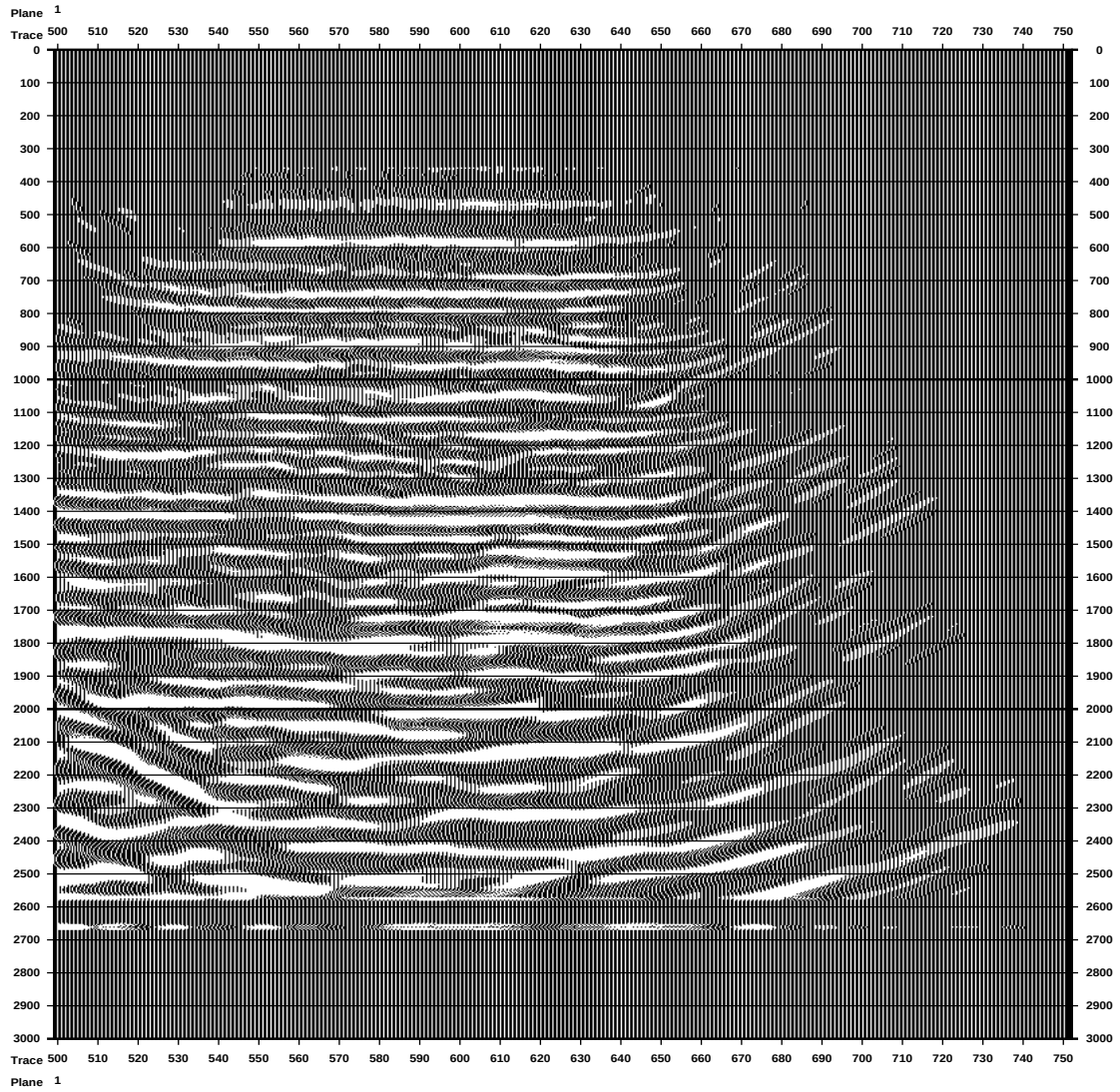

FIGURE 9(C): Short scale velocity perturbation field, used to generate data of Figure 9(a). To be compared with inversion output (Figure 9(b) - plotted on same scale). Note the aperture-limited nature of this result, from inverting a single shot record.

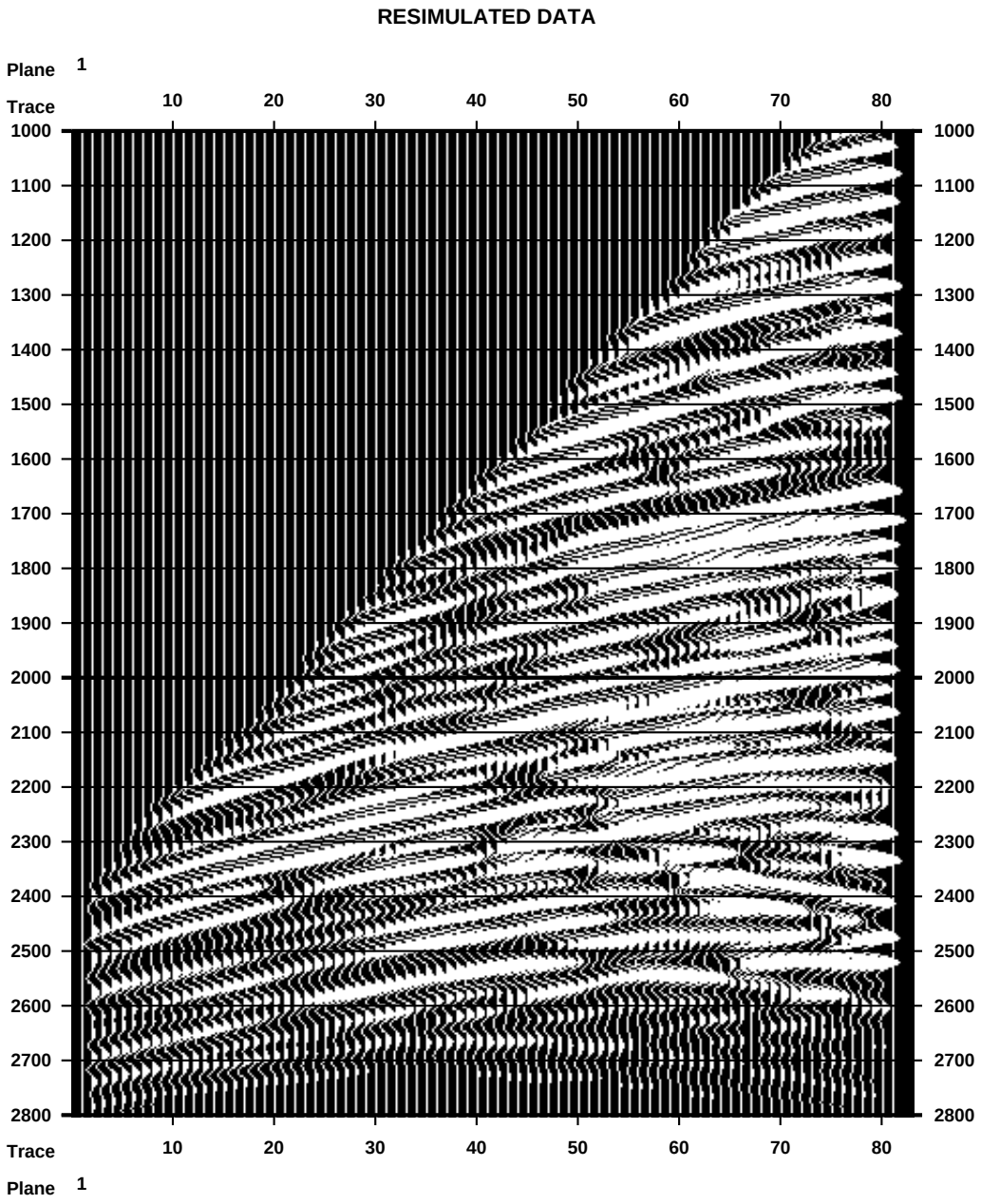

FIGURE 9(D): Resimulation of data. Compare to Figure 9(a) - plotted on same scale.

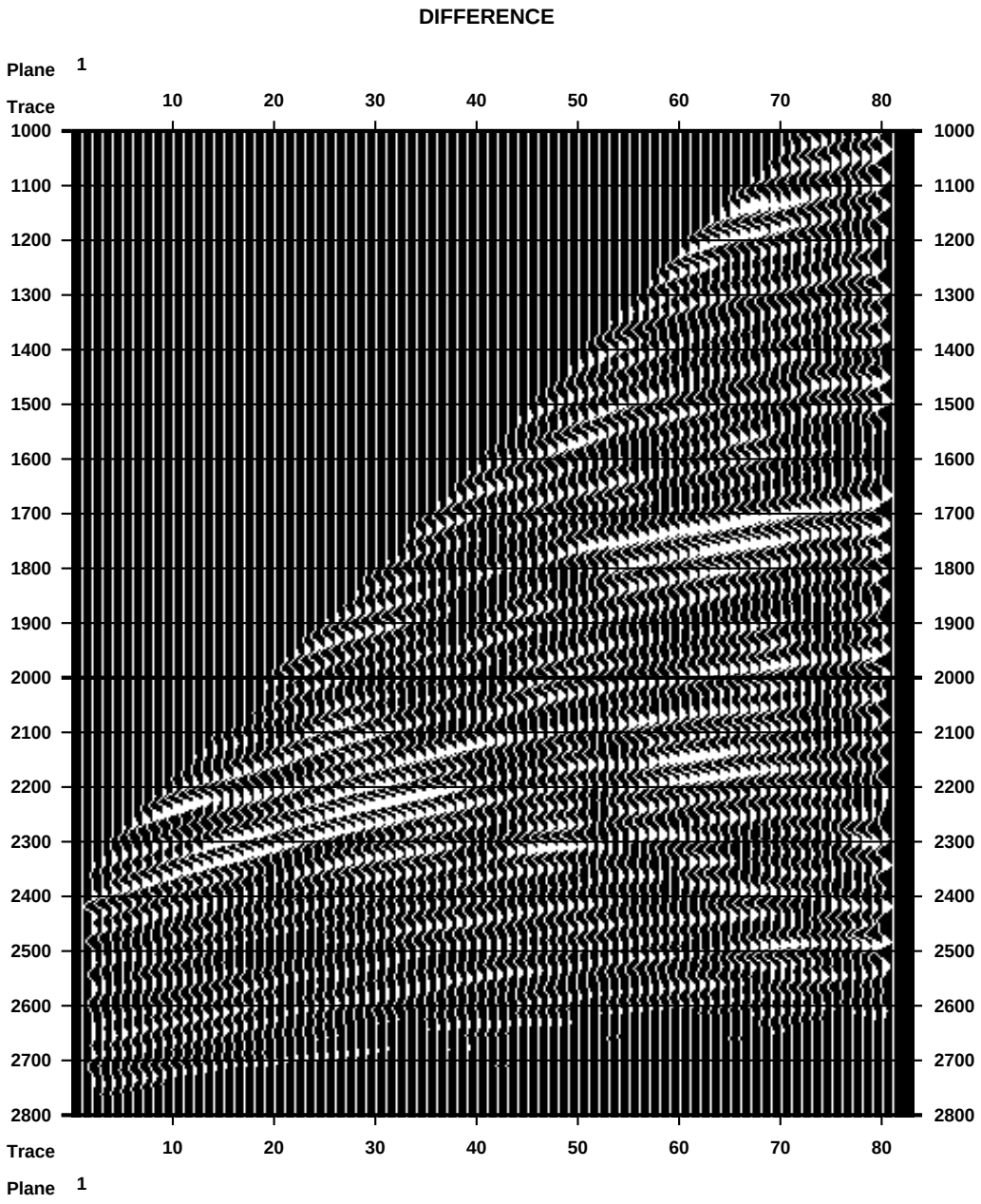

FIGURE 9(E): Difference of Figures 9(a), 9(d), plotted on same scale.

Aperture-limitation is intrinsic to the inversion problem (and, implicitly, to the migration problem as well). The bandlimited nature of f, on the other hand, adversely affects the accuracy of the inversion formulas just described. An alternate approach is the minimization of the error between predicted and observed linearized seismograms, say in the least-squares sense:

$$\underset{\text{over } \delta\sigma/\sigma, \delta\rho/\rho}{\text{minimize}} \quad \int dx_s \int dx_r \int dt_r \left[L_f[\rho, c] \left[\delta\sigma/\sigma, \delta\rho/\rho \right] - S_{\text{data}} \right]^2 .$$

Such (very large) linear least squares problems can be solved with some efficiency by iterative techniques of the conjugate gradient family (GOLUB and LOAN, 1983), Ch. 10). The aperture- and band-limited nature of the solution remains, but the solution obtained in this way solves a definite problem, in contrast to the high frequency asymptotic inversion formulas described above. See for example IKELLE et al., 1986 for an application of this methodology.

On the other hand high frequency asymptotic inversion can provide a reasonably accurate approximate right inverse to the scattering operator, as we saw above (Figure 9 and surrounding discussion). It is natural to think that this approximate inverse might be used to accelerate the progress of iterative methods, thus combining the two approaches. In the conjugate gradient literature, the use of approximate inverses to accelerate convergence is known as (pre- or post-) conditioning. See GOLUB and LOAN, 1983), Ch. 10 for a basic discussion and references. This combination of high frequency asymptotic and iterative least squares inversion has proven to be quite a bit more effective than either separately: see VIRIEUX et al., 1992, JIN and MADARIGA, 1994, MADARIAGA et al., 1992, SEVINK and HERMAN, 1993, and SEVINK and HERMAN, 1994 for accounts of very interesting work along these lines.

We end with a discussion of matters beyond the limits of wave imaging, as defined in these notes.

First, it was noted already in Section 2 that, in common with the literature on wave imaging without exception, we have assumed that no caustics occur in the incident ray family. This assumption amounts to a severe restriction on the degree of heterogeneity in the reference velocity field (WHITE, 1982). A robust modification of the techniques presented here must drop this assumption. Some progress in this direction:

> RAKESH, 1988: showed that the kinematic relation between high-frequency parameter perturbations and field perturbations persists, regardless of caustics (in fact that this relation is always a Fourier Integral Operator);
>
> PERCELL, 1989: established that reflected field amplitude anomalies may be caused by incident field caustics.
>
> NOLAN and SYMES, 1995: gave a rigorous interpretation of Percell's asymptotic expansions, showing that the normal operator for the single point source problem as studied above is not pseudodifferential in any open set containing caustic points.
>
> SMIT et al., 1995: showed that when source and receiver points occupy an *open set* on the surface, the integration over source and receiver point implicit in appli-

cation of the adjoint (see above!) renders the normal operator pseudodifferential, by smearing out the more singular parts.

Second, in order to apply any of the methodology based on perturbation of the wave field, it is necessary to determine the reference fields $\rho(x), c(x)$. Accurate estimation of $c(x)$ is especially critical for before-stack migration, as noted in Section 6, and *a fortiori* for the inversion methods of this section. At present velocity estimation for before-stack migration is regarded as a frontier research topic in reflection seismology.

Third, the mathematical basis of linearization is only poorly understood at present. Rather complete results for dimension 1 were obtained in SYMES, 1986b, LEWIS, 1989, and SUZUKI, 1988. These contrast with the much murkier situation in dimension > 1, where only partial results are available — see SUN, 1988, SYMES, 1986a, BOURGEOIS et al., 1989, BAO, 1990, FERNANDEZ-BERDAGUER et al., 1993. Estimates for the error between the response to finite model perturbations and their linear approximations are necessary for

(i) design of effective inversion algorithms

(ii) analysis of model/data of sensitivity by (linear) spectral techniques.

These estimates are of more than academic interest. See Santosa and Symes (1989) for an account of the consequences of the structural peculiarities of these estimates for velocity estimation.

Finally, we mention that the *significance* of the parameter estimates obtained by any of these techniques — integral or iterative linearized inversion, nonlinear inversion — is far from clear, because of the aperture- and band-limitations already mentioned. The discussion at the beginning of this section suggests that accurate point parameter values are not to be expected. At best, heavily filtered versions of the causative perturbations are accessible. For an interesting recent discussion of the obstacles to be overcome in interpreting inverted data, see BEYDOUN et al., 1990.

References

BAMBERGER, A., CHAVENT, G., HEMON, and LAILLY, P. (1982). Inversion of normal incidence seismograms. *Geophysics*, pages 757–770.

BAMBERGER, A., CHAVENT, G., and LAILLY, P. (1979). About the stability of the inverse problem in 1-d wave equation — application to the interpretation of seismic profiles. *Appl. Math. Opt.*, 5:1–47.

BAO, G. (1990). *Microlocal Regularity of an Inverse Problem for the Multidimensional Wave Equation.* PhD thesis, Department of Mathematical Sciences, Rice University, Houston, Texas, U.S.A.

BEYDOUN, W., MENDES, M., BLANCO, J., and TARANTOLA, A. (1990). North sea reservoir description: benefits of an elastic migration/inversion applied to multicomponent vertical seismic profile data. *Geophysics*, 55:209–217.

BEYLKIN, G. (1985). Imaging of discontinuities in the inverse scattering problem by inversion of a causal generalized radon transform. *J. Math. Phys.*, 26:99–108.

BEYLKIN, G. and BURRIDGE, R. (1990). Linearized inverse scattering problem of acoustics and elasticity. *Wave Motion*, 12:15–22.

BLEISTEIN, N. (1987). On the imaging of reflectors in the earth. *Geophysics*, 52:931–942.

BOURGEOIS, A., JIANG, B., and LAILLY, P. (1989). Linearized inversion: A significant step beyond pre-stack migration. *Geophysics J. Int.*, 99:435–445.

COURANT, R. and HILBERT, D. (1962). *Methods of Mathematical Physics*, volume II. Wiley-Interscience, New York.

FERNANDEZ-BERDAGUER, E. M., SANTOS, J. E., and SHEEN, D. (1993). An iterative procedure for estimation of variable coefficients in a hyperbolic system. Technical report, Purdue University.

FRIEDLANDER, F. (1958). *Sound Pulses*. Cambridge University Press.

GARDNER, G., editor (1985). *Migration of Seismic data*. Geophysics Reprint Series No. 4. Society of Exploration Geophysicists,, Tulsa.

GEL'FAND, I. and SHILOV, G. (1958). *Generalized Functions*, volume I. Academic Press, New York.

GOLUB, G. and LOAN, C. V. (1983). *Matrix Computations*. The Johns Hopkins University Press, Baltimore.

GUILLEMIN, V. and STERNBERG, S. (1979). *Geometric Asymptotics*. American Mathematical Society, Providence.

IKELLE, L., DIET, J., and TARANTOLA, A. (1986). Linearized inversion of multioffset seismic data in the omega-k domain. *Geophysics*, 51:1266–1276.

JIN, S. and MADARIGA (1994). Nonlinear velocity inversion by a two-step Monte-Carlo method. *Geophysics*, 59:577–590.

KOLB, P., COLLINO, F., and LAILLY, P. (1986). Prestack inversion of a 1D medium. *Proceedings of IEEE 74*, pages 498–506.

KRAVTSOV, Y. (1968). Two new asymptotic methods in the theory of wave propagation in inhomogeneous media. *Soviet Physics–Acoustics*, 14:1–17.

LAILLY, P. (1983). The seismic inverse problem as a sequence of before-stack migrations. In Bednar, J. et al., editors, *Conference on Inverse Scattering: Theory and Applications*, pages 206–220. SIAM, Philadelphia.

LEWIS, M. and SYMES, W. (1991). On the relation between the velocity coefficient and boundary value for solutions of the one-dimensional wave equation. *Inverse Problems*, 7:597–632.

LEWIS, R. (1989). *Source-Velocity Identification for a Layered Model of Reflection Seismology*. PhD thesis, Department of Mathematical Sciences, Rice University, Houston, Texas, U.S.A.

LIONS, J. (1972). *Nonhomogeneous Boundary Value Problems and Applications*. Springer Verlag, Berlin.

LUDWIG, D. (1966). Uniform asymptotic expansions at a caustic. *Comm. Pure Appl. Math.*, 29:215–250.

MADARIAGA, R., LAMBARÉ, G., VIRIEUX, J., and JIN, S. (1992). Iterative asymptotic inversin of seismic profiles in the acoustic approximation. *Geophysics*, 57:1138–1154.

NOLAN, C. and SYMES, W. W. (1995). Scattering from caustics. *Wave Motion*, in press.

PERCELL, C. (1989). The effect of caustics in acoustics inverse scattering experiments. Technical Report 89-3, Department of Mathematical Sciences, Rice University, Houston, Texas, U.S.A.

RAKESH (1988). A linearized inverse problem for the wave equation. *Comm. on P.D.E.*, 13(5):573–601.

SANTOSA, F. and SYMES, W. (1989). *An Analysis of Least-Squares Velocity Inversion*, volume 4 of *Geophysical Monographs*. Soc. of Expl. Geophys., Tulsa.

SEVINK, A. and HERMAN, G. (1993). Fast iterative solution of sparsely sampled seismic inverse problems. In Kleinman, R., Angell, T., Colton, D., Santosa, F., and Stakgold, I., editors, *Mathematical and Numerical Aspects of Wave Propagation*. SIAM, Philadelphia.

SEVINK, A. and HERMAN, G. (1994). Fast iterative solution of sparsely sampled seismic inverse problems. *Inverse Problems*, 10:937–948.

SMIT, D., VERDEL, A., and TEN KROODE, F. (1995). Linearized asymptotic inversion in the presence of caustics. *Wave Motion*, in press.

STICKLER, D., AHLUWALIA, D., and TING, L. (1981). Application of ludwigs's uniform progressing wave ansatz to a smooth caustic. *J. Acoust. Soc. Amer.*, 69:1673–1681.

SUN, Z. (1988). On the uniqueness of a multidimensional hyperbolic inverse problem. *Comm. on P.D.E.*, 13:1189–1208.

SUZUKI, T. (1988). Stability of an inverse hyperbolic problem. *Inverse Problems*, 4:273–290.

SYMES, W. (1986a). Linearization stability for an inverse problem in several-dimensional wave propagation. *SIAM J. Math. Analysis*, 17:132–151.

SYMES, W. (1986b). On the relation between coefficient and boundary values for solutions of webster's horn equation. *SIAM J. Math. Anal.*, 17:1400–1420.

TARANTOLA, A. (1984). Inversion of seismic reflection data in the acoustic approximation. *Geophysics*, 49:1259–1266.

TARANTOLA, A. (1986). A strategy for nonlinear elastic inversion of seismic reflection data. *Geophysics*, 51:1893–1903.

TAYLOR, M. (1981). *Pseudodifferential Operators*. Princeton University Press, Princeton, New Jersey.

VANTRIER, J. and SYMES, W. (1991). Upwind finite-difference calculation of travel-times. *Geophysics*, 56:812–821.

VIDALE, J. (1988). Finite-difference calculation of travel times. *Bull., Seis. Soc. Am.*, 78:2062–2076.

VIRIEUX, J., JIN, S., MADARIAGA, R., and LAMBARÉ, G. (1992). Two dimensional asymptotic iterative elastic inversion. *Geophys. J. Int.*, 108:575–588.

WHITE, B. (1982). The stochastic caustic. *SIAM J. Appl. Math.*, 44:127–149.

YILMAZ, O. (1987). Seismic data processing. In *Investigations in Geophysics No. 2*. Society of Exploration Geophysicists, Tulsa.